FH Salzburg
MultiMediaTechnology

Identifying the Ideal Length of Time to Aggregate Smartphone Data, in Order to Obtain Distinct Clusters to Predict Eating Crises

Bachelor Thesis 2

Author: Natasha Lauren Troth
Advisor: FH-Prof. DI Dr. Simon Ginzinger, MSc.

Salzburg, Austria, 29.06.2020

Affidavit

I herewith declare on oath that I wrote the present thesis without the help of third persons and without using any other sources and means listed herein; I further declare that I observed the guidelines for scientific work in the quotation of all unprinted sources, printed literature and phrases and concepts taken either word for word or according to meaning from the Internet and that I referenced all sources accordingly.

This thesis has not been submitted as an exam paper of identical or similar form, either in Austria or abroad and corresponds to the paper graded by the assessors.

Date *Signature*

First Name *Last Name*

Kurzfassung

SmartEater ist eine bevorstehende mHealth-Smartphone-App (Mobile Health) mit dem Ziel, dem Benutzer inhaltsabhängiges Feedback zu geben, um eine Episode mit Verlangen nach Essen abzuwenden. Mithilfe von Machine Learning und Smartphone Sensor- und Nutzungsdaten können Stress und bevorstehendes Verlangen vorhergesagt werden. Das Ziel dieser Arbeit ist es, Unsupervised Machine Learning zu verwenden, noch genauer Clusteranalyse, um das beste Zeit Delta zu finden, um aus diesen Daten qualitativ hochwertige Cluster zu erstellen. Die aufgezeichneten Smartphone Sensor- und Nutzungsdaten umfassen den Beschleunigungsmesser, die Lautstärke des Audios, den Prozentsatz der Einschaltdauer des Bildschirms, die Anzahl der Benachrichtigungen, die Lichtsensorwerte und die App-Nutzung in den Kategorien „Kommunikation“, „Videoplayer“ und „Sonstige“. Die von Testpersonen aufgezeichneten Daten werden in zwei Datensätzen (1 Stunde und 3 Stunden) mit jeweils mehreren Zeitlängen aggregiert. Nach dem Bereinigen und Normalisieren dieser Datensätze, wird die Anzahl der Dimensionen, mithilfe von t-SNE, von acht auf zwei reduziert. Geeignete t-SNE-Parameter werden abgestimmt, um die bestmögliche t-SNE-Visualisierung zu erzielen. Die dichtebasierten Clustering-Methoden DBSCAN und OPTICS werden verwendet, um Datenpunkte für jede der insgesamt zehn Zeitlängen in Cluster zu gruppieren. Die Ergebnisse werden unter Verwendung der mathematischen Bewertungsmaße Silhouette Score, Davies-Bouldin Index und Caliński-Harabasz Index verglichen. Die Ergebnisse zeigen, dass die Zeit Deltas 2 Stunden, 1 Stunde (beide aus dem 3-Stunden Datensatz), 1 Stunde und 30 Minuten (beide aus dem 1-Stunden Datensatz) die deutlichsten und klarsten Cluster bilden.

Abstract

SmartEater is an upcoming mHealth (mobile health) smartphone app, with the goal to provide the user with content-dependent feedback, to avert a food craving episode. Using machine learning and smartphone sensor and usage data, stress and upcoming cravings can be predicted. The goal of this thesis is to use unsupervised machine learning, more specifically cluster analysis, to find the ideal time delta to construct high quality clusterings from this data. The smartphone sensor and usage data recorded, includes accelerometer, volume of the audio, percentage of screen-on-time, number of notifications, light sensor values, and app usages in the categories "communication", "video players", and "other". The data recorded from test subjects is aggregated into two datasets (1 hour and 3 hours), each with multiple time lengths. After cleaning and normalising these datasets, the number of dimensions is reduced from eight to two using t-SNE. Suitable t-SNE parameters are tuned to create the best possible t-SNE visualisation. The density-based clustering methods DBSCAN and OPTICS are used to group data points into clusters for each of the total ten time lengths. These results are compared using the mathematical evaluation scores Silhouette Score, Davies-Bouldin Index, and Caliński-Harabasz Index. The results indicate, that the time deltas 2 hours, 1 hour (both from the 3 hour dataset), 1 hour, and 30 minutes (both from the 1 hour dataset) create the most distinct and well-defined clusters.

Contents

List of Figures

Abbreviations

PCA	Principal Components Analysis
SNE	Stochastic Neighbor Embedding
t-SNE	t-Distributed Stochastic Neighbor Embedding
DBSCAN	Density Based Spatial Clustering of Applications with Noise
OPTICS	Ordering Points To Identify the Clustering Structure

1 Introduction

SmartEater [1] is an upcoming mHealth (mobile health) app, with the goal to provide the user with content-dependent feedback, to avert a food craving episode. The app will predict future eating crises based on the user's past behaviour. In order to reduce intense user input, the app records and uses various smartphone sensor and usage data. With the help of data mining, machine learning algorithms, and pattern recognition, this recorded situational context data will aid in predicting stress. The following data is recorded by the app:

1. Movement of the smartphone (accelerometer)
2. Volume of the audio
3. Percentage of screen-on-time
4. Number of notifications
5. Light sensor values
6. App usages in the categories communication, video players, and other

This sensor data was recorded for different lengths of time on different test subjects and aggregated to 1 hour and 3 hour files. It is necessary to establish which time period will be most fitting to make accurate predictions for the future. This thesis will use cluster analysis to determine which time period is most significant.

Han, Pei, and Kamber (2011)[18, 32, 362, 363] declare, that data mining is used to discover patterns and knowledge from data. Cluster Analysis is a type of machine learning algorithm known as unsupervised machine learning. It is used in data mining to divide data into clusters (groups). Each cluster contains data that is similar to each other, but dissimilar to the data allocated to other clusters. Cluster Analysis can be used to acquire knowledge on the distribution of the data, discover characteristics, detect outliers and reduce noise, or to preprocess data for other algorithms.

There are several different methods to create clustering. Han, Pei, and Kamber (2011)[364, 366-367, 374, 385, 392] explain, that objects are often arranged into clusters using distance measures (e.g. Euclidean or Manhattan distance measures). The authors divide the clustering algorithms into the following categories:

- Partitioning methods (examples: k-means, k-medoids)
- Hierarchical methods (examples: BIRCH, Chameleon)
- Density-based methods (examples: DBSCAN, OPTICS)

1. https://sites.google.com/site/eatingandanxietylab/resources/smarteater

- Grid-based methods (examples: STING, CLIQUE)

According to Han, Pei, and Kamber (2011)[414], the above-mentioned clustering methods work well with datasets that are not high-dimensional and have less than 10 attributes. Since the SmartEater dataset only has 8 unique dimensions (columns), it is not considered high-dimensional. This paper will therefore be able utilise and compare the results of these types of clustering methods.

To reduce the size and amount of data, dimensionality reduction will be used. Han, Pei, and Kamber (2011)[93] define dimensionality reduction as a type of data reduction, which removes random attributes and creates a smaller dataset with close to equal integrity. This thesis will compare principal component analysis (PCA) and t-Distributed Stochastic Neighbor Embedding (t-SNE) to reduce the dimensionality.

The clustering methods will be implemented using the Python machine learning platform (e.g. Anaconda[2]), with the library scikit-learn[3]. These will be implemented on all the time lengths. The resulting clusters of each time length will be compared to one another and evaluated. Rousseeuw (1987) reveals how silhouettes can be used to measure the separation between clusters and therefore evaluate the quality of the resulting clusters. Other mathematical evaluation scores used are Davies-Bouldin Index (Davies and Bouldin (1979)) and Caliński-Harabasz Index (Caliński and Harabasz (1974)).

The thesis will be structured as follows: Section 2 will briefly present existing work relating to this subject. The following chapter, section 3, will concentrate on the theory of data mining and cluster analysis. After covering these topics, section 4 will describe the conducted experiment and its results. In the final sections, the findings of the experiment will be discussed and summarised.

2 Related work

As introduced in section 1, SmartEater[4] will be a mHealth (mobile health) app, that predicts future eating crises based on the user's past behaviour. The predictions are made on smartphone sensor and usage data, therefore reducing strenuous user input. The app will give the user content-dependent feedback, to avert a food craving episode.

Rahman et al. (2016)[141-148] introduced a similar idea in their paper. Their goal was to predict "About-to-Eat" and "Time until the Next Eating Event" stages by using wearable sensing devices, in order to reduce serious health issues (e.g. obesity). The authors state, that detecting when a person is eating is not helpful. It is more beneficial to predict moments shortly before the user is about to eat ("About-To-Eat").

Rahman et al. investigated how people were currently tracking their meals by conducting a survey. Under half of the participants had previously used food tracking/journalling tools. 48.9%

2. https://www.anaconda.com/
3. https://scikit-learn.org/stable/
4. https://sites.google.com/site/eatingandanxietylab/resources/smarteater

of these stopped using them within the first month. Respondents also wished for the app to take action directly before a meal/snack (”About-to-Eat” moments), thus supporting the authors' previous assumptions.

The authors used a variety of different sensors to record the following data: physical movement (raw accelerometer, gyroscope, step count, speed), caloric expenditure, heart rate, skin temperature, electrodermal activity (good indicator for psychological arousal), chewing and swallowing sounds (for detection of current eating events), and GPS location. Furthermore, the test subjects recorded self-reports, such as when they started eating, emotional state when eating, intensity of desire/craving and hunger, and end of eating. Eight participants, aged 26-54, took part in this study for five days. The recorded data then underwent cleaning and preprocessing, feature extraction, feature selection, and machine learning. In the feature extraction step, two parameters were used on the processed sensor time series to create windows. Firstly, the feature extraction window size parameter regulated the time duration in a specific window. While a short window duration could catch immediate characteristics in the sensor time series, a coarse one could be used for long term trends. The authors used a variety of window sizes, varying from 5 to 120 minutes. The prediction model results would decide the best window. The second parameter, the window shift size, established the time duration between two neighbouring windows, for example meaning window *n* was shifted one minute compared to window *(n - 1)*. A constant shift of one minute was used for all window sizes.

In the feature selection step, the most relevant features were selected (e.g. the location features, as they were not beneficial and merely represented noise). Signal processing and machine learning were used on the sensor streams to train an ”About-to-Eat” moment classifier. The classifier's performance was further inspected, in order to see how the different feature extraction window sizes affected it. The small window sizes were vulnerable to noise and the coarse ones were unable to detect recent events, which were crucial in creating the classifier. As can be seen in figure 1, the smaller window sizes have a higher gap between precision and recall[5]. The performance with window sizes between 60 and 80 minutes is higher and more consistent.

The performance for the ”Time until Next Eating Event” model gained a correlation coefficient of 0.49. The most fitting feature extraction window size was assessed, the best performance was reached with a window size of 100 minutes. The authors further claim, that both models could be improved by incorporating person-dependent data from the target user to the models (e.g. person-specific eating pattern, lifestyle).

Stütz et al. (2015)[240, 242-248] research, whether data collected by a user's smartphone can be used to predict stress. In their study, they used an android smartphone app called ”TheStress-Collector” (TSC) to collect smartphone usage and sensor data in the background. Collected data included: activity, app usage, network traffic, reboot activity (power on and off events), calls (min, max and mean dB-values collected by the microphone), environment brightness, timestamps of received messages, noise exposure, and screen activity. Fifteen participants installed

5. According to Han, Pei, and Kamber (2011)[306-307], precision and recall are measures used in classification. Precision describes the exactness (how many of the as positive selected items are positive), recall defines the completeness (how many positive items have been correctly selected). The F-score is a measure that combines precision and recall (harmonic mean).

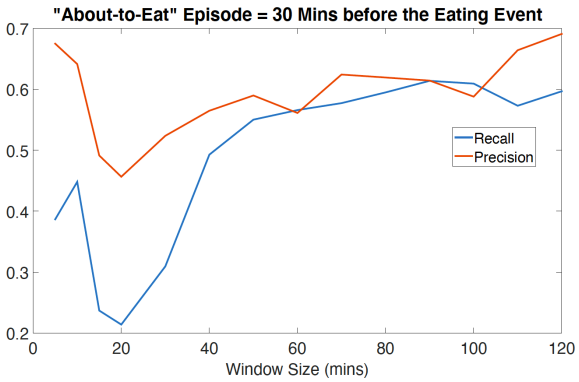

Figure 1: This graph depicts the F measure of the different feature extraction window sizes of the ”About-to-Eat” classifier (Rahman et al. 2016)[148]. The performance with window sizes between 60 and 80 minutes is higher and more consistent.

the app on their smartphone and took part in the conducted study for two weeks. Seven times a day they would fill out questionnaires (at set times), which included the perceived stress score (PSS) and their current stress status. The stress levels were predicted by WEKA's machine learning algorithms. The mean absolute error (MAE) and Pearson correlation were used for the evaluation. The results of this study presented compelling correlations between PSS and the data collected by the smartphone app. The weekly PSS average, as opposed to the daily one, included the highest correlation coefficient. Thus, it is expected, that it is easier to spot longer periods of high stress than shorter ones. This paper is also a team publication featured in the research project from which SmartEater was developed.

In their experiment, Ameko et al. (2018) intend to predict user's negative affect states, in order to provide targeted just-in-time mental health interventions. Sixty-five students participated in the study. Through a smartphone app, GPS location data, accelerometer (activity) data, phone calls, SMS, and ecological momentary assessments (EMA), data was collected and used to cluster participants according to their behavioural profiles. Grouping the participants this way seemed to improve the predictive model's performance.

Other related work: Dey and Chakraborty (2015)[1,2,6,7] give an example, where clustering was implemented to predict future weather. Air pollutant data was preprocessed and then arranged into clusters using (incremental) DBSCAN clustering. Finally, priority based protocol was used on them to predict weather conditions and a temperature range. The accuracy of the technique, based on hit and miss times, was calculated to approximately 74.5%. Sornbootnark and Khoenkaw (2019) use smartphone sensor data (e.g. accelerometer) to predict excessive alcohol consumption, in order to replace breathalysers. Their algorithm produced 100% accuracy, however with 15 minute lags.

3 Methods

3.1 Data mining

Larose and Larose (2015)[4] declare, that data mining is used to recognise patterns and trends in large amounts of data. Han, Pei, and Kamber (2011)[16-18] explain, that the term ”data mining” is a misnomer. A more suitable phrase would be ”knowledge mining from data”. The word ”mining” represents valuable nuggets found within large amounts of raw material. Other names used to describe the same process include: knowledge discovery from data (KDD), knowledge extraction, data/pattern analysis, data archaeology, and data dredging. The discovery of data is an iterative process represented in the following steps: data cleaning, data integration (combine multiple data sources), data selection (relevant data is extracted), data transformation (into applicable forms for data mining), data mining (discover patterns), pattern evaluation (determine if patterns have a meaning), and knowledge presentation.

As stated by Larose and Larose (2015)[9-13, 15-16], data mining requires continuous human supervision for quality monitoring and evaluation. Software alone will serve wrong results. Data mining is used for description of patterns and trends, estimation of numerical values, prediction of future results, classification of categorical variables, clustering of similar objects and association of attributes.

Larose and Larose (2015)[160] describe the two types of data mining methods: *supervised* and *unsupervised*. Han, Pei, and Kamber (2011)[363] interpret supervised learning as *learning by examples*, whereas unsupervised learning is *learning by observation*. Larose and Larose (2015)[160] continue, in supervised methods, there is a predefined target variable and the model learns which values of the target variable correspond to which values of the predictor variable. The goal of the unsupervised approach is to find patterns and structure in the inserted variables. Therefore, no target variable is established. Clustering is used in this thesis and further detailed in section 3.4.

3.2 Data preprocessing

In his book, McCue (2014)[53] mentions, that generally in data mining, the analysis itself requires 20% of the time. The other 80% is the preparation of the data.

To make data useful in data mining, Larose and Larose (2015)[20] point out, that datasets first need to undergo a data preprocessing step. Raw data extracted directly from databases can be incomplete (values are missing), noisy (contains outliers), or may contain out-dated or redundant data. García, Luengo, and Herrera (2015)[45] state, that dirty data can impact the produced model, making it less reliable. The significance of its effect depends on the implemented data mining method. Larose and Larose (2015)[20, 45] define, the goal is to decrease the irrelevant data that is fed into the model, thus reducing the amount of irrelevant data received out of the model. The authors also report, that ID fields should be removed from the dataset used in data mining algorithms, since the value is different for each record and not helpful. It could how-

ever prove harmful, since a relationship might be presumed that isn't there. Further information preparation steps are outlined in the next sections below.

3.2.1 Missing values

According to Pyle (1999)[83], it is good practice to differentiate "empty" values from "missing" ones. Empty values do not have a comparable real-world value. Missing values, however, do have underlying values, they simply weren't recorded. Removing the record with the missing value would mean wasting the data stored in the other fields of that record, that might contain relevant information. Substituting the value means, that the record can be used. A consideration is how to substitute the missing value, without adding bias to the dataset. An inadequately chosen replacement value could distort the dataset, by adding data which doesn't exist in the real world. Larose and Larose (2015)[23, 25] give an example, of how replacing missing values can lead to invalid results. The authors experimented with a database of cars. Substituting a missing brand with a random value (here "Japan") led to a car, that didn't exist. Larose and Larose suggest, that a missing value can be replaced, either with a constant determined by the data analyst, with a field mean (for numerical values) or mode (for categorical values), with a random value, or with imputed values based on the different features of the record.

3.2.2 Normalisation

Han, Pei, and Kamber (2011)[105] describe normalisation as giving the attributes of a dataset equal weight. For example, it can transform the data to fall in a smaller, common range (e.g. [-1, 1]). It therefore hinders variables with large ranges from outweighing ones with smaller ranges. People's income would, for instance, have a larger range than binary attributes.

García, Luengo, and Herrera (2015)[46-48] review the following normalisation methods: *min-max normalization*, *z-score normalization*, and *decimal scaling normalization*. For the following examples, A is a numerical attribute from a dataset, a single value of this attribute is represented with v:

- Min-max normalization scales the original numerical values to a newly defined range, with a new minimum ($newMin_A$) and maximum ($newMax_A$) (e.g. 0.0 and 1.0). The original minimum and maximum values found in A are presented as min_A and max_A respectively:
$$v' = \frac{v - min_A}{max_A - min_A}(newMax_A - newMin_A) + newMin_A$$
The intervals [0, 1] and [-1, 1] are common intervals for normalisation.

- Z-score (or zero-mean) normalization normalises the values using the mean ($\bar{A}$) and standard deviation σ_A of the values A.
$$v' = \frac{v - \bar{A}}{\sigma_A}$$

After this transformation, the mean equals zero and the standard deviation is one. The advantages of this normalisation method take effect, when the min and max values of A are not known, or when there are outliers that could bias the min-max method.

- Decimal scaling is another normalisation method.

3.3 Dimensionality reduction

Bellman (1957)[20-22] first introduces the *curse of dimensionality*. The curse effects a mathematical model, when there are a large number of variables. The real world is complex and by trying to incorporate as many real world features into a mathematical model as possible, it becomes complicated. A too simple model however, will not be suitable for prediction. Bellman (1961)[94] further details the results of *the curse of dimensionality*. Functions with one variable can be visualised as curve in a 2D space and a function with two variables in a 3D space. Depicting functions with more variables however, is more problematic (both for visualisation and tabulation). As stated by Han, Pei, and Kamber (2011)[93], dimensionality reduction is a data reduction method. Data reduction is utilised to attain a smaller, more concentrated dataset, whilst mostly keeping the integrity of the initial dataset. Principal components analysis and t-SNE are the dimensionality reduction techniques used to reduce the SmartEater dataset.

3.3.1 Principal Components Analysis (PCA)

Principal components analysis was first proposed by Pearson (1901) and Hotelling (1933). Pearson's approach is to identify a line or plane that best fits the collected variables plotted to a plane. In order to determine the best fitting line or plane, means, standard-deviations, and correlations are used (Pearson 1901)[559-560]. Hotelling (1933)[5] introduces his method as the method of principal components. Jolliffe (2002)[7] clarifies, that while these two papers used different methods, the standard algebraic derivation was announced by Hotelling (1933). According to Han, Pei, and Kamber (2011)[95-96], the general idea is to calculate k orthonormal vectors, the so called principal components. These unit vectors present a basis for the input data, which are a linear combination of the principal components. Larose and Larose (2015)[94] explain, that the principal components can be discovered, by rotating the initial coordinate system to the direction of maximum variability. These then create a new coordinate system. Hotelling (1933)[4, 5, 15] reveals, that the components are chosen with decreasing amount of variance. Therefore, the one with the highest variance is chosen first. The next highest is chosen orthogonal to the one before, and so on. Han, Pei, and Kamber (2011)[96] mention, that in data mining, the vectors with the lowest variance are removed, thus reducing the number of dimensions. Despite the loss of data, the components with higher variance can approximate the original data.

3.3.2 t-Distributed Stochastic Neighbor Embedding (t-SNE)

In their paper, Maaten and Hinton (2008)[2579-2580] introduce t-SNE, a method of dimensionality reduction and visualising high dimensional data on a two or three-dimensional plot.

The authors mention, that while linear methods like PCA concentrate on making sure low-dimensional representations of data points are apart from each other, they are typically unable to bring similar low-dimensional representations near.

The authors describe, that t-SNE is a variation of Stochastic Neighbor Embedding (SNE), introduced by Hinton and Roweis (2003). Maaten and Hinton (2008)[2581] explain, that the first step in SNE is to transform the Euclidean distances between points in high-dimensional space into the conditional similarity probabilities. According to Hinton and Roweis (2003)[858], such a probability $p_{i,j}$ would arise from the similarity between the two data points x_i and x_j. This is the probability of x_i picking the point x_j as its neighbour. Maaten and Hinton (2008)[2581] clarify, that this is the probability of x_i picking the point x_j as its neighbour under the circumstance, that the neighbours were chosen according to their probability density under a Gaussian, x_i being its centre. This results in the conditional probability being high for close data points and imperceptibly small for those further apart. In a similar way, the conditional probability between the low-dimensional data points y_i and y_j (counterparts to high-dimensional x_i and x_j), represented by $q_{i,j}$, is calculated. Maaten and Hinton (2008)[2581] state, that if the similarity of x_i and x_j has been correctly mapped by y_i and y_j, then $p_{i,j}$ will be equal to $q_{i,j}$.

Hinton and Roweis (2003)[858] further explain, that the goal is to reduce the difference between $p_{i,j}$ and $q_{i,j}$, thus finding a suitable low-dimensional representation of the high-dimensional data. This is accomplished by minimising a cost function, comprised of the sum of the Kullback-Leibler divergences between $\mathrm{p_{i,j}}$ and $q_{i,j}$. Maaten and Hinton (2008)[2583] reveal, that the advantages of t-SNE over SNE are, the improvement of its cost function (symmetrised version of SNE) and the use of Student-t distribution as opposed to Gaussian for the similarity calculation in the low-dimensional area.

To apply t-SNE to a dataset, Maaten and Hinton (2008)[2582] describe, the σ_i has to be chosen for variance of the Gaussian centred over x_i. Depending on the density, different values of σ_i provide better results. For example, in a denser region, a smaller σ_i is recommended, but not in less denser regions. This makes it unlikely to be able to find an overall optimal σ_i for the dataset. Hinton and Roweis (2003)[858] declare, that σ_i can be chosen by hand or is found using a binary search. This would equalise the distribution entropy to log$k$, k being the effective number of local neighbours or the so called *perplexity*. The *perplexity* is a parameter chosen by the user for the SNE by hand. Maaten and Hinton (2008)[2582] imply, that this parameter should be chosen between 5 and 50 and that SNE is quite robust to the chosen value. Another parameter to be set is the learning rate. Han, Pei, and Kamber (2011)[332] clarify, that the learning rate parameter is used to support the finding of global minimums, instead of being caught in a local minimum. A learning rate set too low will result in slow learning. In contrast, a learning rate set too high could lead to poor results.

3.4 Cluster analysis

Hartigan (1975)[1] describes clustering as a means to group similar objects together. For example, two planets are considered similar, if (given measurement error) it is probable they could be perceived as the same planet. Romesburg (2004)[2] gives the gathering of a variety of pebbles

and sorting them into piles of similar attributes (e.g. shape, size, colour) as an example of cluster analysis. Hartigan (1975)[1-3, 6] further explains, that it can be expected from similar objects for them to act and be treated the same. Clustering is also used to name, display, summarise, predict, and require explanation of the objects in the cluster. If some of the objects assigned to a cluster exhibit certain properties, it is expected that the other objects in this cluster will exhibit them as well. Real-world examples of clustering include classifications of animals, plants and diseases.

Han, Pei, and Kamber (2011)[361-363] state, that the objects placed into one cluster are dissimilar to the objects assigned to other clusters. The fact that cluster analysis can find groups by itself, gives it its unique advantage. Clustering is a type of unsupervised machine learning, since the class label for each group is unknown and needs to be discovered. In data mining, it is utilised to understand the distribution of the data and inspect the distinctions between clusters. Moreover, it can be used to preprocess data for other data mining methods, such as characterisation, attribute subset selection, and classification. Cluster analysis is used in various fields, including: biology, security, business intelligence, image pattern recognition, and web search. It can be used to place customers into groups, organise projects into categories in project management, and to sort web search results into concise groups. Furthermore, it can be used to detect outliers, since these are located outside of clusters.

3.5 Overview of clustering algorithms

Han, Pei, and Kamber (2011)[363-365] list the following requirements clustering methods must meet:

- Scalability
- Ability to work with different attribute types
- Recognising clusters with arbitrary shapes
- Requirements for domain knowledge (for parameter selection)
- Ability to handle noise
- Incremental clustering (integrate updates without recomputation)
- Insensitivity to the order of the input
- Ability to cluster high-dimensional data
- Capability to cluster under certain constraints
- Interpretability and usability of the results

Han, Pei, and Kamber (2011)[366-367] present different clustering algorithms. The general categories are partitioning methods, hierarchical methods, density-based methods, and grid-based methods.

3.5.1 Partitioning methods

Partitioning methods are the easiest and most significant types of clustering methods. The data is divided into k (generally pre-defined) number of groups (clusters). Many of the partitioning methods use distance measures to calculate their clusters. If the number of clusters (k) is pre-defined, then the clustering algorithm will create an initial segregation into k clusters. Objects are then relocated to improve the partitioning. Examples: k-means, k-medoids (Han, Pei, and Kamber 2011)[366, 368].

3.5.2 Hierarchical methods

The data is grouped into a hierarchy (”tree”) of clusters. There are two different approaches: *agglomerative* or *divisive*. In the *agglomerative* or *bottom-up* approach, each object creates its own cluster. Step by step, it is then merged into its closest neighbours until all objects belong to one cluster, or a condition for termination comes true. In the *divisive* or *top-down* approach, all objects initially form one cluster together and are divided until each object is contained in its own cluster, or a condition is met to terminate the process. Each merge or split decision influences the quality of the resulting clusters and must therefore be well chosen since it cannot be undone. Examples: BIRCH, Chameleon (Han, Pei, and Kamber 2011)[366, 367, 373, 374].

3.5.3 Density-Based methods

The majority of clustering methods (e.g. partitioning and hierarchical methods) use distance-based approaches, which results in only finding clusters with spherical shapes. Density-based methods have the ability to find clusters with various shapes. In these methods, objects are continuously added to the cluster, so long as the number of objects/data points (density) close by is larger than a given threshold. The clusters are comprised of high-density areas of objects. These are separated by spaces with low-density. Accordingly, this method is also useful for removing noise and outliers. The following two density-based clustering algorithms were used in the experiment: DBSCAN and OPTICS (Han, Pei, and Kamber 2011)[367, 385].

3.5.3.1 DBSCAN

Ester et al. (1996)[226-229] introduce a density-based clustering algorithm, the Density Based Spatial Clustering of Applications with Noise. This method is able to find clusters with different shapes and work efficiently on large spatial datasets. The algorithm searches in a given radius (Eps = epsilon parameter) around a data point. If within this radius a minimum number of points (MinPts parameter) exists, then this point is added to the cluster (core point). A data point (p) is considered a border point, if inside of its Eps neighbourhood there is a core point (q). A data point is labelled as noise, if it does not belong to any clusters (has no core points within the given radius).

According to Han, Pei, and Kamber (2011)[388], a weakness of DBSCAN is the fact that the results rely on the chosen parameters. If these are selected differently, the clustering results can differ. These parameters can often be challenging to select.

Ester et al. (1996)[230] supports the selection of the Eps and MinPts parameters. The idea is to select the ideal parameters for the "thinnest" cluster. The first step is to construct a sorted *k*-dist graph. For a specific *k*, the distance *d* of every point *p* to its *k*th nearest neighbour is calculated. These distances are then sorted in descending order and depicted on a graph. Such a graph can be seen in figure 2. The goal is to locate the *threshold* of the highest distance to the *k*th nearest neighbour in the "thinnest" cluster. The first point in the "valley", as can be seen at the tip of the arrow in figure 2, is this threshold point. The points to the left of it with higher distances are likely to be noise and the points to the right belong to clusters. The authors suggest selecting 4 for *k*. Experiments have shown that the results for higher values for *k* do not vary greatly. They therefore recommend defining MinPts as 4 and using a 4-dist graph to estimate the Eps parameter.

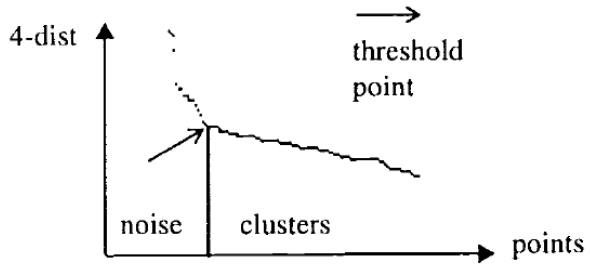

Figure 2: Sorted 4-dist graph (distance for each point to its fourth nearest neighbour) to calculate DBSCAN Eps parameter. The first point in the "valley" is supposedly the ideal value. The points to the left with higher distances are likely to be noise and the points to the right are part of clusters (Ester et al. 1996)[230].

3.5.3.2 OPTICS

Han, Pei, and Kamber (2011)[388] mention, that OPTICS was created to improve the selection of global parameters problem in DBSCAN. Ankerst et al. (1999)[49, 51-54, 57, 60] present the density base clustering algorithm OPTICS (Ordering Points To Identify the Clustering Structure). This method in itself does not specifically create clusters. Instead, it orders the dataset according to its density-based clustering structure. For each object, the values *core-distance* and *reachability-distance* are calculated. The *core-distance* of an arbitrary data point (object) *o* is the distance to the nearest point within Eps that completes the MinPts rule and therefore labels point *o* as a core point. If there is not the number of MinPts in the Eps neighbourhood, then the *core-distance* of that point is undefined. The *reachability-distance* of an object *p* to core object *o*, is defined as the max value of the core-distance and the distance from object *o* to object *p*. Likewise, if *o* is not a core object, then the *reachability-distance* of *p* is undefined.

The data points are ordered by the OPTICS algorithm (using their reachability-distance) to create a reachability plot. This plot is relatively stable towards the input parameters. In figure 3,

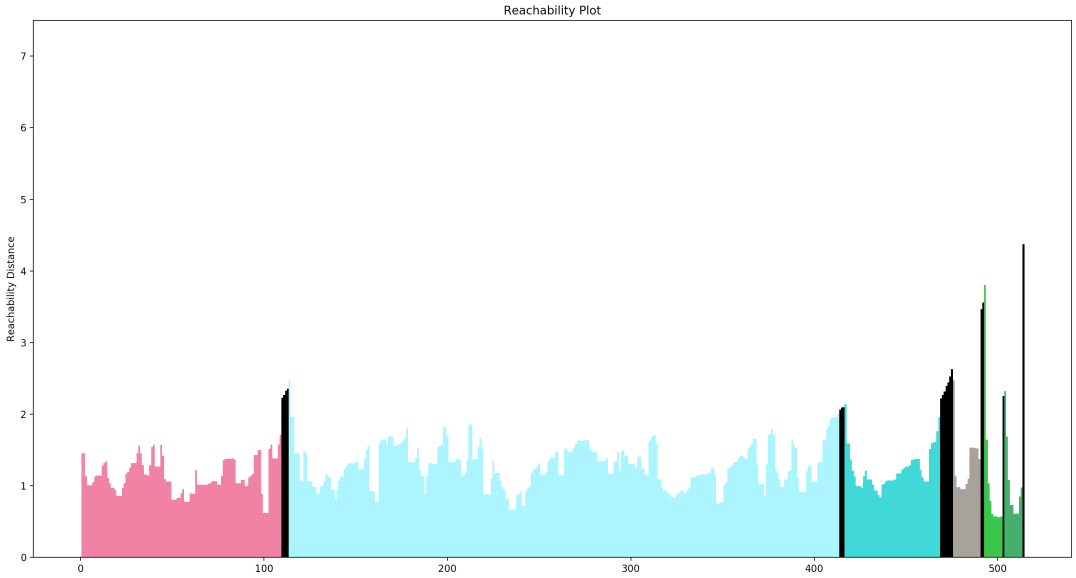

Figure 3: OPTICS reachability plot constructed from a portion of the SmartEater dataset (reduced through t-SNE). Dips can be seen, where clusters (bars that are not black) have been highlighted. The black bars indicate noise.

a reachability plot calculated from a portion of the SmartEater dataset (reduced through t-SNE) is depicted.

Clusters can be automatically constructed from the reachability plot by pinpointing the start-of-cluster and end-of-cluster regions and combining regions that match into clusters (or nested clusters). Since the reachability-distance of a point is the distance from the set of its predecessors and through OPTICS' specific ordering, the clusters are the dips in the reachability plots. Figure 4 depicts a scatter plot with OPTICS clustering. The coloured points indicated clusters, whilst the black points highlight noise. The corresponding reachability plot (figure 3) shows that the clusters were formed from the dips.

3.5.4 Grid-Based methods

The previously mentioned clustering methods are data-driven (they accommodate the distribution of the data objects). Grid-based methods are space-driven (they do not rely on the distribution of the data objects). The data objects are quantised into grid cells on a multiresolution grid. The actions required for clustering are executed on the grid structure. The grid size (number of cells) determines the processing time. Grid-based methods perform faster than other clustering methods. Examples: STING, CLIQUE (Han, Pei, and Kamber 2011)[367, 392].

Han, Pei, and Kamber (2011)[414, 416] clarify, that the clustering methods mentioned above have a good functionality when used on a dataset with fewer than 10 attributes.

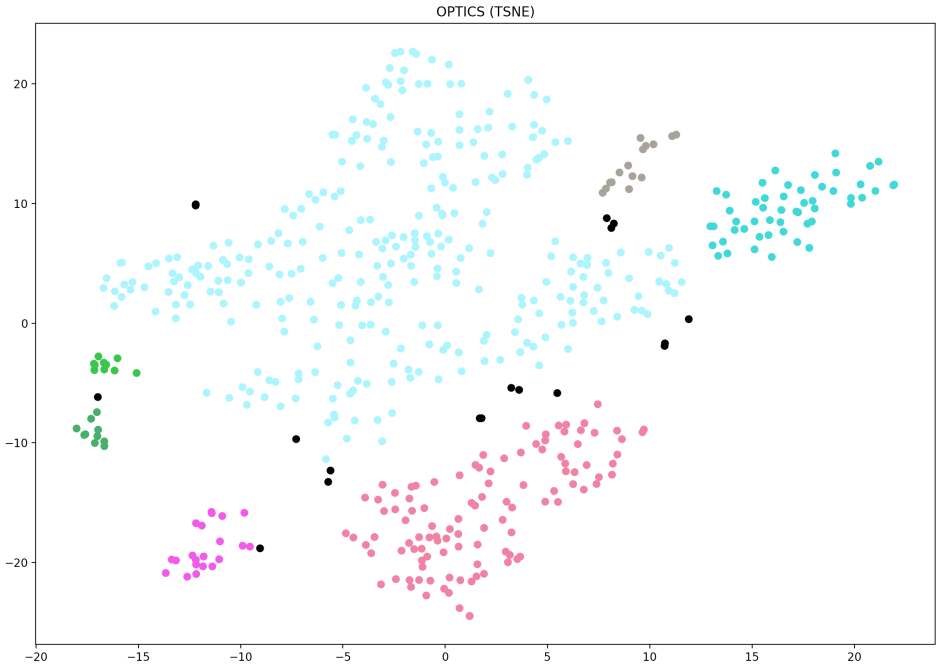

Figure 4: OPTICS clustering, extracted from the reachability plot in figure 3. The cluster colours can be compared to the colours in the dips of the reachability plot. The black points indicate noise.

3.6 Evaluating clustering results

Han, Pei, and Kamber (2011)[396, 399, 401] point out, that the cluster quality needs to be evaluated. Generally, there are two ways to measure the quality of clustering: extrinsic methods and intrinsic methods. In extrinsic methods (or supervised methods), there is a ground truth available. This ground truth is usually produced by experts (humans). Intrinsic methods are used, when there is no ground truth available. In intrinsic methods, the clusters are evaluated by how well they are separated from one another and how compact they are (e.g. *silhouette coefficient*). The experiment conducted in this paper uses intrinsic methods, since there is no ground truth for comparison.

3.6.1 Silhouette Coefficient

In his paper, Rousseeuw (1987)[55-56, 59] proposes a new graphical display using silhouettes, to help determine how well objects belong to their assigned clusters. It can be used to interpret and validate the results of clustering. It is also utilised to compare clusters created by different algorithms, the input data being the same.

The formula is as follows: With the use of silhouettes, the author's goal is to find out, if the quality of the clusters is high. Hence, the dissimilarities of the objects within a cluster are small, and the dissimilarities are large compared to the objects in other clusters. For each object

i in cluster *A*, the value *s(i)* is calculated. The variable *a(i)* contains the average dissimilarity of the object *i* to each other object in the same cluster. If there are no other objects in the cluster, *s(i)* is set to zero (most neutral value). The variable *b(i)* is determined by firstly calculating the average dissimilarity for each neighbouring cluster that isn't *A*. The shortest of these values, therefore the next closest cluster to *A*, is then assigned to *b(i)*. This cluster may be seen as the next best choice for *i*. *b(i)* can only be calculated, if there are other clusters besides *A*. The formula for *s(i)* is as follows:

$$s(i) = \frac{b(i) - a(i)}{max\{a(i), b(i)\}}$$

The resulting value *s(i)* is a number in the range of *-1* $\leq$ *s(i)* $\leq$ *1*:

$$s(i) = \begin{cases} 1 - a(i)/b(i) & \text{if } a(i) < b(i) \\ 0 & \text{if } a(i) = b(i) \\ b(i)/a(i) - 1 & \text{if } a(i) > b(i) \end{cases}$$

A *s(i)* value close to 1 reveals, that the dissimilarity within a cluster is smaller than the dissimilarity to the neighbouring cluster. Therefore it suggests, that the assignment of that object is good, since it is most likely the most suitable cluster for *i* (well-classified). A *s(i)* value close to 0 means, that *a(i)* and *b(i)* are almost equal and it is uncertain whether cluster *A* or its neighbour is a more suitable fit. If *s(i)* is near -1, then the dissimilarity within a cluster is larger than the dissimilarity to the next closest cluster. Thus, it would have been more natural to assign *i* to the neighbouring cluster, since it is closer to it (misclassified).

The *average silhouette width* can be calculated for single clusters. It is established by calculating the average of all objects that belong to said cluster. An average score can also be calculated from each object *i* for the whole chart (dataset), the so called *overall average silhouette width*.

3.6.2 Davies-Bouldin Index

A second cluster evaluation method is the Davies-Bouldin Index, which was proposed by Davies and Bouldin (1979)[224-227]. The succeeding formula describes the average similarity of a cluster with the cluster that is most similar to it (R_{ij}). *i* and *j* represent the determined clusters, S_i and S_j stand for the dispersions of the clusters, and M_{ij} is the distance between the two cluster centroids.

$$R_{ij} = \frac{S_i + S_j}{M_{ij}}$$

The Davies-Bouldin Index equals:

$$\overline{R} = \frac{1}{N} \sum_{i=1}^{N} R_i$$

This metric can be used to compare clustering results. The lower of the two $\bar{R}$ values indicates the better partitioning.

3.6.3 Caliński-Harabasz Index

As a third evaluation score, Caliński and Harabasz (1974)[3, 7, 10-12, 25] is used to evaluate and compare the resulting clusters in the experiment. The Caliński-Harabasz Index or Variance Ratio Criterion (VRC) is calculated as follows, where n is the number of points, k is the number of clusters, $WGSS$ is the within-group (cluster) sum of squares, and $BGSS$ is the between-group (cluster) sum of squares.

$$VRC = \frac{BGSS}{k-1} / \frac{WGSS}{n-k}$$

If k is not known, it is set to 2, then 3, and so on. The density of the clusters can be calculated with the sums of the squared distances from the cluster centroids to the points. The more natural the clusterings are, the higher VRC will be, since the variation within the cluster is lower.

4 Results

The goal of this paper is to identify, which time delta for aggregation is ideal to construct distinct clusters from smartphone sensor and usage data. The data for this experiment was collected for the upcoming SmartEater [6] mobile health app. The goal of this app is to present the user with content-dependent feedback, with the hope to prevent food craving episodes. By evaluating the user's behaviour (through smartphone sensor and usage data), the app predicts eating crises through stress, therefore eliminating the need of intense user input.

Various sensor and usage data was recorded for the SmartEater project, by the 46 testers' smartphones (for different periods of time). The columns of the data were organised as follows (N is the number of times the data was recorded in the time period and app usage is in percent of lag-interval minutes):

- TIME: timestamp, when the data was aggregated (format: YYYY-DD-MM hh:mm:ss)
- ACC (1-N): values received from the accelerometer (average jerk). According to the Android developers documentation[7], the accelerometer (acceleration sensor) records the acceleration (including the force of gravity) enforced onto the smartphone.
- AUDIO (1-N): volume of the audio
- SCRN (1-N): percentage of screen-on-time
- NOTIF (1-N): number of notifications
- LIGHT (1-N): (environment) light sensor values

6. https://sites.google.com/site/eatingandanxietylab/resources/smarteater
7. https://developer.android.com/guide/topics/sensors/sensors_motion

- APP_COM (1-N): app usage in the category *communication*
- APP_VID (1-N): app usage in the category *video players*
- APP_OTHER (1-N): app usage of all other categories (excluding *video players* and *communication*)

The recorded smartphone sensor and usage data was aggregated into multiple .csv (Comma-Separated Values[8]) files. Furthermore, these files were distinguished into folders, according to their time delta. Two different time lengths were used:

- 1h: The data was aggregated in 2.5 hour intervals, whereby each row contained data from an aggregation of 1 hour, in four 15 minute lags.
- 3h: The data was aggregated in 1.5 hour intervals, whereby each row contained data from an aggregation of 3 hours, in six 30 minute lags.

Each row contains the data value of a specific test user for one of the time periods (e.g. 1h or 3h).

Python was used to conduct the experiment, more specifically using the Anaconda[9] Python distribution platform for data science. The scikit-learn[10] (short sklearn) Python package provides simple tools for predictive data analysis and was used for data preparation, dimensionality reduction, and clustering. The plots were rendered using the Python Matplotlib[11] library.

4.1 Preparation of the dataset

Initially, the raw data was distributed into multiple .csv files (one file per user, per time interval). The files were read and processed by the Python Pandas[12] tool. This programming library offers fast and flexible functionalities for data analysis. It utilises DataFrames which are fast and efficient 2D data structures, used to store tabular data. Using the Pandas *read_csv*[13] and *concat*[14] methods, the files with identical time periods were transformed and concatenated to one collective DataFrame.

8. https://tools.ietf.org/html/rfc4180
9. https://www.anaconda.com/
10. https://scikit-learn.org/stable
11. https://matplotlib.org
12. https://pandas.pydata.org,https://pandas.pydata.org/about/
13. https://pandas.pydata.org/pandas-docs/stable/reference/api/pandas.read_csv.html
14. https://pandas.pydata.org/pandas-docs/stable/reference/api/pandas.concat.html

4.1.1 Missing values

The raw data contained several rows with empty cells. Section 3.2.1 mentions substitution of missing data, thus preserving rows which could otherwise contain important information. In doing so however, the existing patterns could be disrupted. In order to maintain the data's patterns, rows with missing values were removed. Using the Pandas' *dropna*[15] function (deletes rows with missing values), all rows containing empty cells were dropped. Of the original 8283 rows from the 1 hour time period files, only 3279 (39.59%) rows were complete and remained. In the 3 hour files, only 6218 from 14091 (44.13%) persisted.

4.1.2 Normalisation

The recorded values from the different smartphone sensors were spread over different number ranges. For example, whilst the values that describe the screen-on-time ranged between -20 and 2.0, the light sensor values could reach from 0 to over 60,000. As explained in 3.2.2, values with higher ranges can inadvertently outweigh smaller values. To be sure that the values are weighted the same, the sklearn *StandardScaler*[16](z-score normalization) was used to normalize the data. As mentioned in section 3.2.2, z-score normalization is more robust to outliers, that could otherwise bias min-max normalization. Therefore, z-score normalization was used instead of min-max normalization.

4.1.3 Selection of columns (attributes)

In order to only use meaningful data to receive significant results, it was important to remove columns that did not contain any predictive content. The TIME column was removed for this reason. Since the TIME column only showed the time and date when the data was recorded periodically (in fixed intervals), it was different for each row (per user), like an index. It could have however bias the results if left in.

Depending on what time length was being assessed, a different number of columns per feature was extracted. For example, if in the 1h dataset a time length of 30 minutes was requested, the first two columns (first two 15 minutes) would be extracted for each feature (ACC, SCRN, etc.).

To reduce the number of dimensions (number of columns), columns that had recorded the same feature but at different time lags (e.g. ACC1-N), were compressed to one column, by calculating their mean. Each unique feature only required one column. This step therefore reduced the number of columns to only 8 instead (of the total 32 in the 1h dataset and 48 in the 3h dataset, when using all the columns).

15. `https://pandas.pydata.org/pandas-docs/stable/reference/api/pandas.DataFrame.dropna.html`
16. `http://scikit-learn.org/stable/modules/generated/sklearn.preprocessing.StandardScaler.html`

4.1.4 Chain shaped data

Initial visualisations of the dataset (with t-SNE dimensionality reduction) showed a chain formalisation of the data across various t-SNE parameters. This chain can be seen in figure 5 (light blue data points, almost swirl shaped). A similar accumulation of the same data points, though this time shaped as a line, can further also be seen in the PCA dimensionality reduced dataset (see figure 6).

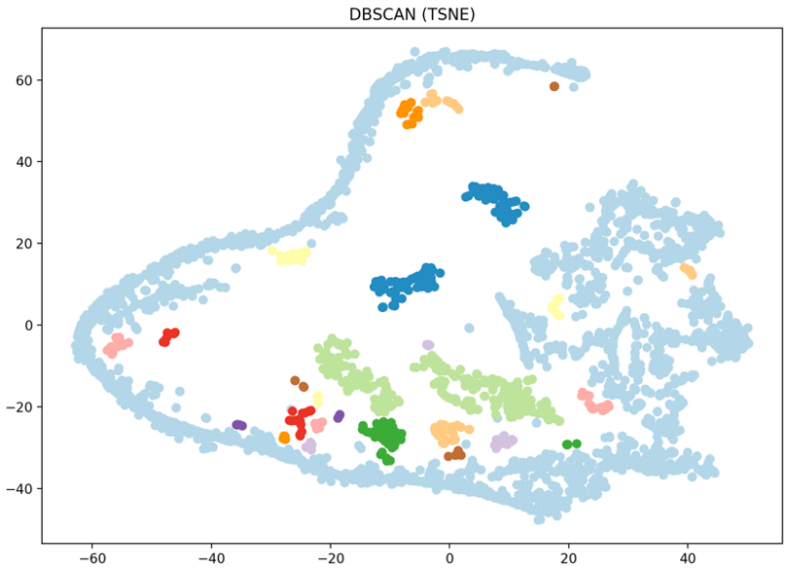

Figure 5: 1h dataset with DBSCAN clustering. A chain of data points (light blue points) can be seen in the dataset.

An initial thought, was that the chain was a consequence of dependencies within the data or columns. For example, the three APP columns indicate the percentage of time in a lag-interval a certain type of app was used. Therefore, if say a communication app was used 100% of this time, the APP_COM cell for this time would be 1. Using this app for 100% of the time would mean, that the values in the other APP columns for this time would have to be 0 (0%), since they would not have been able to be used. To test this theory, the APP columns were removed from the dataset and the 2D scatter plot was recalculated. The chain however was still visible. Step by step, each column was removed, to see if it was the cause of the chain. The chain did not disappear though, which indicated, that the problem was not due to the columns, but rather the rows. The chain also became less dense and less visible when reducing the number of inserted .csv files (lower number of records). This supported the notion, that the rows could be the cause.

The next theory, was that points from a same test subject might exhibit similarities and were therefore causing the chain. To see which data points were contained in the chain, the row index number was added as a label to each data point in the scatter plot. Furthermore, each test user data file was assigned a different random colour, so that it became visible in the plot, which

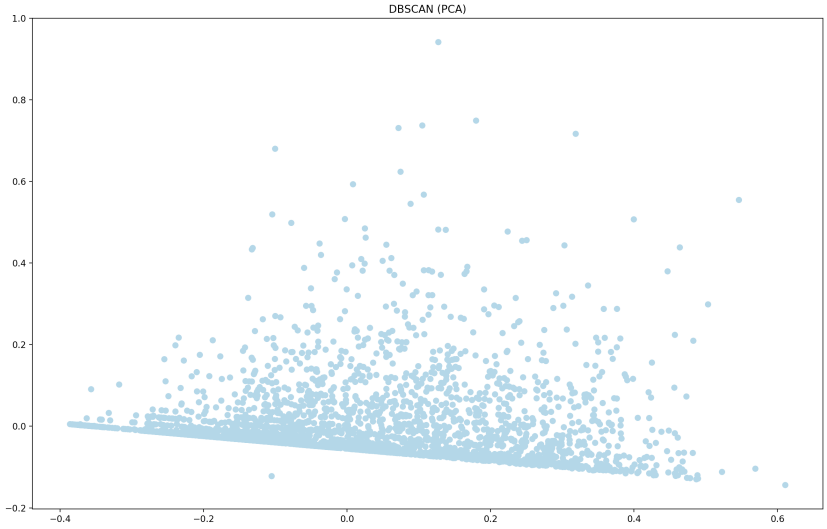

Figure 6: There is a collection of points along a line. This same accumulation can also be visualised as a chain in the t-SNE reduced dataset in figure 5.

data points belonged to the same user. The resulting scatter plot is visualised in figure 7. From this plot it can be seen, that several data points from the same test subject cluster together in the chain, indicating similarity. There are however points from each user in different locations of the chart, not only in the chain. This implied, that the chain was not being caused by the test subjects, but rather by certain rows.

The ensuing step was to use the data point indices to look for similarities in the row values. By comparing the rows in the chain, it became evident, that multiple rows shared a lot of the same feature values. Rows not in the chain however, had different values. Looking at the same rows in the unclean dataset (after concatenation of the .csv data files and removal of rows with missing values), rows found in the chain had several columns all with the value 0. Further inspection showed, that when the SCRN value was 0, LIGHT, NOTIF and the APP columns where also 0. When a smartphone screen is off, the apps are not being used (apart from, for example, notifications), which explains why the APP columns were mostly 0. The NOTIF values were often 0, presumably because the user was not constantly receiving notifications. The environment light was also often 0 when SCRN was 0, maybe because it was in a pocket or bag. To test whether these rows were causing the chain to occur, rows that didn't have at least 50% of non-zero values were removed. As can be seen in figure 8, the chain is much less prevalent. The colours belonging to the test users also appear to be more distributed. Naturally, this reduced the total number of rows left. The average number of rows left for the 1h data files, depending on the chosen time length, was 1654 from initial 8283 (19.97%). In the 3h dataset, only an average of 3976.5 from the original 14091 rows remained (28.22%).

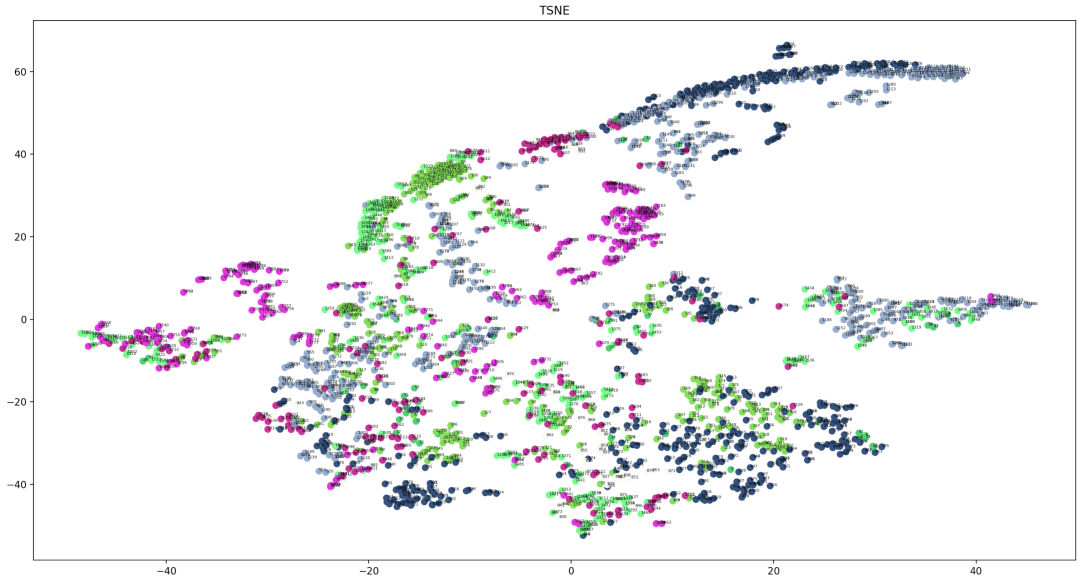

Figure 7: t-SNE results in a scatter plot, the chain is visible. Each colour indicates one test subject. The test subjects have clustered together slightly in the chain. The index of each data point is also displayed.

4.2 Dimensionality reduction

The dimensionality reduction methods PCA and t-SNE were used to reduce the number of dimensions (number of attributes, so in this case number of columns).

4.2.1 PCA

PCA was the initial approach used in the experiment. The sklearn *PCA*[17] function was used to reduce the number of dimensions to 2, which simplified visualisation in 2D scatterplots. Before the removal of the chain (section 4.1.4), the PCA allowed 65%-95% (depending on data preparation type and aggreation files) of the data's important structures to be accounted for in only the first two or three principle components. After the removal of the chain, the first three components only contained almost 50% of the important structures. Of the 8 components, 7 would have been needed to account for over 90% of these formations (for both the 1h and 3h datasets). As figure 9a shows, the resulting data from these components did not show any significant clusters, in comparison to the t-SNE results. The principle components were further depicted in a 3D scatter plot, to evaluate whether the extra dimension revealed more structure. However, as can be seen in 9b, only very little more structure was revealed. It is considered, that as PCA is a linear dimensionality reduction method, it might not be suitable to transform the SmartEater dataset.

17. `https://scikit-learn.org/stable/modules/generated/sklearn.decomposition.PCA.html`

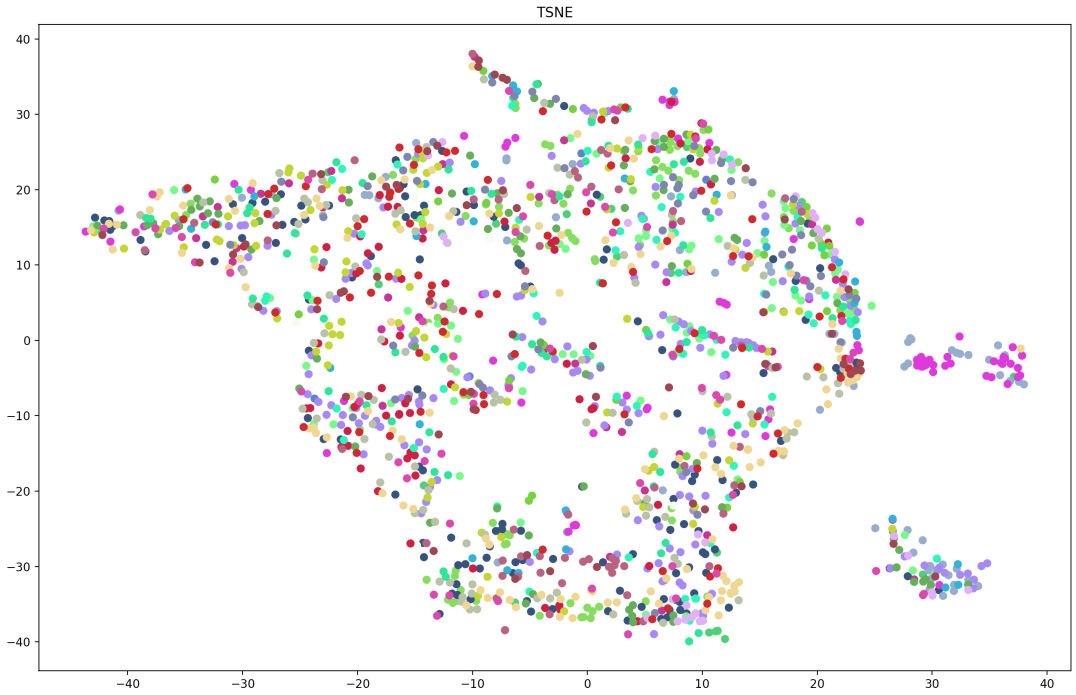

Figure 8: t-SNE calculated after the removal of rows with less than 50% of values that weren't 0. The chain is less visible and less dominant.

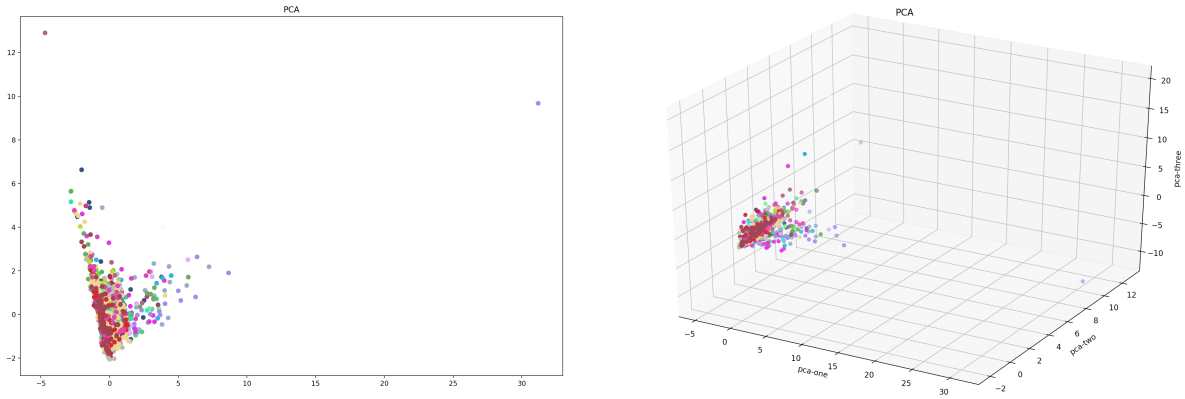

Figure 9: 2D (a) and 3D (b) scatter plots of the PCA results. The data points only appear to form one cluster with little visible structure.

4.2.2 t-SNE

The t-SNE results proved to be more significant than the PCA ones. The t-SNE algorithm was implemented using the sklearn *t-SNE*[18] implementation. To effectively apply the t-SNE algorithm, it was important to identify the parameters (perplexity, learning, and number of iterations) most suitable to the SmartEater dataset, as described in section 3.3.2. The number of iterations was originally set to the default value 1000, but was later raised to 5000, to avoid receiving significantly different results each time t-SNE was run. Raising the number of iterations provided more consistent results. The overall structure of these were the same, though usually rotated differently. Wattenberg, Viégas, and Johnson (2016) also used 5000 iterations in their experiments and stated that their t-SNE plots had reached a stable point by then.

To find suitable perplexity and learning rate t-SNE parameters to create the most distinct clusters possible, multiple 2D t-SNE scatter plots were created using different perplexity and learning rate values. The to determine the perplexity parameter[19], multiple values between the recommended 5 and 50, in steps of 10 (except for the first step which was 5) were tested. A perplexity of 45 was further added, since it had shown good results in tests performed before the chain described in section 4.1.4 was removed. The resulting scatter plots are listed in the appendix A.1. When visually comparing the different perplexities, the data points in the lower perplexity graphs (e.g. 5 and 10) appear to be randomly scattered and have no structure. The higher the perplexity gets, the more the data points take on structure and more distinct and well defined clusters appear. From a perplexity of 20, the 1h data files appear to start forming such clusters. When scanning the higher perplexities, it can be seen, that clusters become more separated. The scatter plots from perplexity 30 to 50 appear to have formed well defined clusters.

To assist in selecting the perplexity parameter, the three mathematical evaluation scores, mentioned in section 3.6, were compared. Figure 10 displays the Silhouette Coefficient, Davies-Bouldin Index, and Caliński-Harabasz Index, calculated for the DBSCAN and OPTICS clusterings from different perplexities. As explained in section 3.6, the Silhouette Score indicates better, denser clustering, when it is closer to 1, and incorrect clustering if the value is close to -1. The lower of two Davies-Bouldin Index and the higher of the Caliński-Harabasz Index scores suggests better clustering. The green highlighted values indicate the best achieving evaluation score values (1h or 3h files), for the corresponding clustering method. Furthermore, the dark green highlighted values also accentuate the overall best scoring values over all datasets (1h and 3h files). The number of these best scoring fields will henceforth be referred to as number of ”wins”. With 4 wins, a perplexity of 20 has the highest number of best achieving score values. The perplexities of 10, 40, and 45 tied in second place with 2 wins. While according to the scores, perplexity 20 creates the best clusters, visually the clusters appear better defined with a perplexity between 30 and 50. For this reason, the focus of the comparison of the scores was moved to the scores that were highest, whose perplexity was between 30 and 50. Perplexity 40 had the most wins in figure 11 and was chosen as the final parameter. These tests were conducted a second time (see appendix A.1.8), using the average of two different t-SNE results for

18. `https://scikit-learn.org/stable/modules/generated/sklearn.manifold.TSNE.html`

19. Wattenberg, Viégas, and Johnson (2016) proved to be a helpful source in tuning this parameter.

1h Files

	Perplexity: 5	Perplexity: 10	Perplexity: 20	Perplexity: 30	Perplexity: 40	Perplexity: 45	Perplexity: 50
DBSCAN (TSNE)							
Silhouette	0.012301321	0.17785606	0.23409332	0.13068332	0.020629907	-0.001459693	-0.13791381
Davies Bouldin	1.332029385	1.502340712	1.236333265	1.396269294	1.765516415	2.312260633	2.06274638
Calinski Harabasz	11.79207398	24.68251028	100.4317614	337.5606908	527.1113507	555.0973937	381.4331244
OPTICS							
Silhouette	-0.56731904	-0.2652787	0.0904175	0.12797767	0.028060276	-0.053797465	-0.13770019
Davies Bouldin	1.173244861	1.624939639	1.271594621	1.423696525	1.627679428	2.927482693	2.039984915
Calinski Harabasz	5.865016692	11.64971005	34.93509218	165.8283109	427.7636283	420.6156948	343.8819753

3h Files

	Perplexity: 5	Perplexity: 10	Perplexity: 20	Perplexity: 30	Perplexity: 40	Perplexity: 45	Perplexity: 50
DBSCAN (TSNE)							
Silhouette	0.19653113	0.30535686	0.28253406	0.162854	0.005408226	-0.056066718	-0.11255615
Davies Bouldin	1.357905465	1.454077361	1.295397242	1.345344464	1.595251196	1.633439218	1.568908348
Calinski Harabasz	18.52401582	43.48411771	149.8457962	454.3884285	821.6969448	418.2231883	427.8332514
OPTICS							
Silhouette	-0.33854422	0.003906393	0.16133659	0.14873675	0.06374386	0.052369475	-0.045151174
Davies Bouldin	1.302466526	1.276339339	1.338689898	1.522294895	1.600873186	1.72163966	1.598151632
Calinski Harabasz	7.909086677	18.77438054	56.32308984	214.1240169	538.5429769	547.9833581	480.4260331

best values in files (1h or 3h)

best values total (1h and 3h)

Figure 10: Comparison of Silhouette Coefficient, Davies-Bouldin Index, and Caliński-Harabasz Index for different t-SNE **perplexities** in **steps of 5 and 10**. The green highlighted values indicate the best achieving evaluation score values (1h or 3h files), for the corresponding clustering method. Furthermore, the dark green highlighted values also accentuate the overall best scoring values over all datasets (1h and 3h files).

each of the datasets. While the scores are slightly different, a perplexity of 40 was again the overall best achieving value.

The same principle was used to determine the ideal value for the learning rate parameter. The sklearn t-SNE documentation [20] states, that the learning rate is normally set between 10 and 1000, hence the learning rate in the scatter plots was chosen in this interval. The various resulting scatter plots can be seen in the appendix A.2. The differences in the arrangement of the data points over the plots is not as substantial as it was when testing for the perplexity. The results, listed in figure 12 revealed, that the learning rate 10 scores highest with a learning rate of 800 coming in second. Since roughly 200 steps were taken between the learning rate values, smaller steps were taken (i.e. 50) around the winning value, to see if an even better performance could be accomplished (figure 55, in appendix A.2.7). While 10 still achieved best in the one hour time length files, 800 came top in the three hour files, indicating that 10 might not be the best rate for these. Consequently, the values 20 and 30 were also evaluated (figure 56, in appendix A.2.7). While a learning rate of 10 still came top in the one hour files, 30 came top in the three hour files. With the hope of finding a value in between 10 and 30 that satisfied both time lengths, the learning rates 10, 15, 20, 25, and 30 were ultimately compared exclusively. The results in figure 13 exposed, that this final comparison lead to the learning rate 20 being the most suitable.

20. `https://scikit-learn.org/stable/modules/generated/sklearn.manifold.TSNE.html`

1h Files			
	Perplexity: 40	Perplexity: 45	Perplexity: 50
DBSCAN (TSNE)			
Silhouette	0.020629907	-0.001459693	-0.13791381
Davies Bouldin	1.765516415	2.312260633	2.06274638
Calinski Harabasz	527.1113507	555.0973937	381.4331244
OPTICS			
Silhouette	0.028060276	-0.053797465	-0.13770019
Davies Bouldin	1.627679428	2.927482693	2.039984915
Calinski Harabasz	427.7636283	420.6156948	343.8819753

3h Files			
	Perplexity: 40	Perplexity: 45	Perplexity: 50
DBSCAN (TSNE)			
Silhouette	0.005408226	-0.056066718	-0.11255615
Davies Bouldin	1.595251196	1.633439218	1.568908348
Calinski Harabasz	821.6969448	418.2231883	427.8332514
OPTICS			
Silhouette	0.06374386	0.052369475	-0.045151174
Davies Bouldin	1.600873186	1.72163966	1.598151632
Calinski Harabasz	538.5429769	547.9833581	480.4260331

	best values in files (1h or 3h)
	best values total (1h and 3h)

Figure 11: Comparison of the evaluation scores of the top three **perplexity candidates 40, 45, and 50**. The green highlighted values indicate the best achieving evaluation score values (1h or 3h files), for the corresponding clustering method. Furthermore, the dark green highlighted values also accentuate the overall best scoring values over all datasets (1h and 3h files).

As with the perplexity, the learning rate tests were also reproduced, averaging two different t-SNE outcomes. The results are illustrated in appendix A.2.8. The value 800 appears to be more dominant than the lower parameter values (e.g. 10 and the favourite 20). To further compare 20 and 800, appendix A.2.9 contains a table (figure 61) comparing 4 different runs of scores from average t-SNE results. With 2 wins more than 20, 800 has the overall better score results. Figures 62 and 63 (in appendix A.2.8) visually compare the scatter plots created with a learning rate of 20 and 800. The plots and clusters appear very similar. The clusters from perplexity 20 however seem slightly more compact (less smaller clusters). A learning rate of 20 was thus selected for the final learning rate parameter. However, 800 was also used in the final results.

The final t-SNE parameters, from which the results were then used by the DBSCAN and OPTICS clustering methods in the next section, were as follows: perplexity = 40, learning_rate = 20, and n_iter = 5000. A run of the resulting graphs are depicted in figures 14 and 15.

4.3 Clustering

The clustering algorithms used for the SmartEater dataset, were DBSCAN and OPTICS. One of the advantages of these density-based clustering methods (as mentioned in section 3.5.3) are that there are less parameters to configure. There is also no need to define a fixed number of k clusters to find, since the cluster boundaries are regulated by density. This technique also allows arbitrary-shaped clusters to be correctly identified. The t-SNE dimensionality reduction

1h Files						
	Learning Rate: 10	Learning Rate: 200	Learning Rate: 400	Learning Rate: 600	Learning Rate: 800	Learning Rate: 1000
DBSCAN (TSNE)						
Silhouette	0.050185006	-0.042344864	-0.017635347	-0.010426269	0.037798844	-0.000416309
Davies Bouldin	1.813219735	2.676732504	2.890704798	2.026635472	1.537629516	1.546143153
Calinski Harabasz	619.5024641	419.1989183	460.313768	415.8237768	412.8616309	372.21986
OPTICS						
Silhouette	0.04723522	-0.035783995	-0.034918476	0.045697644	0.036134463	-0.03027331
Davies Bouldin	2.644154104	1.968641447	2.381197506	1.641226189	1.512853515	1.787453062
Calinski Harabasz	545.2578195	280.3873883	348.4819534	313.0720379	243.8295466	271.4756449

3h Files						
	Learning Rate: 10	Learning Rate: 200	Learning Rate: 400	Learning Rate: 600	Learning Rate: 800	Learning Rate: 1000
DBSCAN (TSNE)						
Silhouette	-0.053747308	0.0587465	0.061668195	0.07413952	0.08301577	0.109837286
Davies Bouldin	2.315636084	1.592984772	1.480249005	1.649978246	1.40672888	1.435522581
Calinski Harabasz	495.6689234	451.0644601	370.6595195	339.2929074	325.3370665	371.3897933
OPTICS						
Silhouette	-0.002017022	0.049122266	0.058030702	0.07046428	0.08165444	0.10488015
Davies Bouldin	2.196366077	1.671782196	1.557507298	1.684883853	1.485960484	1.538449188
Calinski Harabasz	607.8271457	215.1723563	160.6469519	151.0756862	130.86284	159.6005369

best values in files (1h or 3h)

best values total (1h and 3h)

Figure 12: Comparison of Silhouette Coefficient, Davies-Bouldin Index, and Caliński-Harabasz Index for different t-SNE **learning rate** values, in **steps of 200** (except the first step of 190). The green highlighted values indicate the best achieving evaluation score values (1h or 3h files), for the corresponding clustering method. Furthermore, the dark green highlighted values also accentuate the overall best scoring values over all datasets (1h and 3h files).

approach provided more significant results than PCA. Thus, the cleaned data and t-SNE modified data (with two components) was fed into the clustering algorithms DBSCAN and OPTICS.

4.3.1 DBSCAN

The DBSCAN algorithm was applied on the SmartEater dataset using the sklearn *DBSCAN*[21] function. Section 3.5.3.1 describes the functionality of the DBSCAN clustering method. As mentioned, one of the disadvantages of DBSCAN is the need to specify parameters, which can change the outcome of the results. In order to establish suitable parameters, *k*-dist graphs were generated for the 1h and 3h datasets. The graphs contained the distances kth nearest neighbors. As recommended by Ester et al. (1996)[230], *MinPts* and *k* were set to 4 and the graphs were used to determine *Eps*. The idea was to select *Eps* suitable for the ”thinnest” cluster, however being careful to avoid noise. As can be seen in figures 16a and 16b, the ”valley” starts at roughly a 4th nearest neighbor distance (threshold) of 2.

21. `https://scikit-learn.org/stable/modules/generated/sklearn.cluster.DBSCAN.html`

1h Files					
	Learning Rate: 10	Learning Rate: 15	Learning Rate: 20	Learning Rate: 25	Learning Rate: 30
DBSCAN (TSNE)					
Silhouette	0.050185006	0.07569929	-0.06679525	0.020656068	0.038768608
Davies Bouldin	1.813219735	2.061975606	1.525274298	1.85890212	1.939580286
Calinski Harabasz	619.5024641	445.2348946	248.4124961	580.7423117	577.4117352
OPTICS					
Silhouette	0.04723522	0.11635833	-0.01730663	0.03974744	0.07930727
Davies Bouldin	2.644154104	2.912734806	1.375044564	1.838551904	1.521993726
Calinski Harabasz	545.2578195	451.6774344	253.4888154	482.5849166	453.56707

3h Files					
	Learning Rate: 10	Learning Rate: 15	Learning Rate: 20	Learning Rate: 25	Learning Rate: 30
DBSCAN (TSNE)					
Silhouette	-0.053747308	-0.001016365	-0.014693906	0.008068903	0.09359318
Davies Bouldin	2.315636084	2.025401879	1.624380463	1.828098116	1.698168632
Calinski Harabasz	495.6689234	749.4941048	441.8649747	631.5502642	819.1717685
OPTICS					
Silhouette	-0.002017022	0.056000855	0.08187237	0.0838738	0.0860974
Davies Bouldin	2.196366077	1.979177605	1.767960982	1.928988022	1.85835621
Calinski Harabasz	607.8271457	511.9817211	677.3212302	666.0735705	455.2848506

best values in files (1h or 3h)

best values total (1h and 3h)

Figure 13: Comparison of Silhouette Coefficient, Davies-Bouldin Index, and Caliński-Harabasz Index for different t-SNE **learning rate** values. The goal is to find a **learning rate value between 10 and 30**, that satisfies both the 1h and 3h datasets. The green highlighted values indicate the best achieving evaluation score values (1h or 3h files), for the corresponding clustering method. Furthermore, the dark green highlighted values also accentuate the overall best scoring values over all datasets (1h and 3h files).

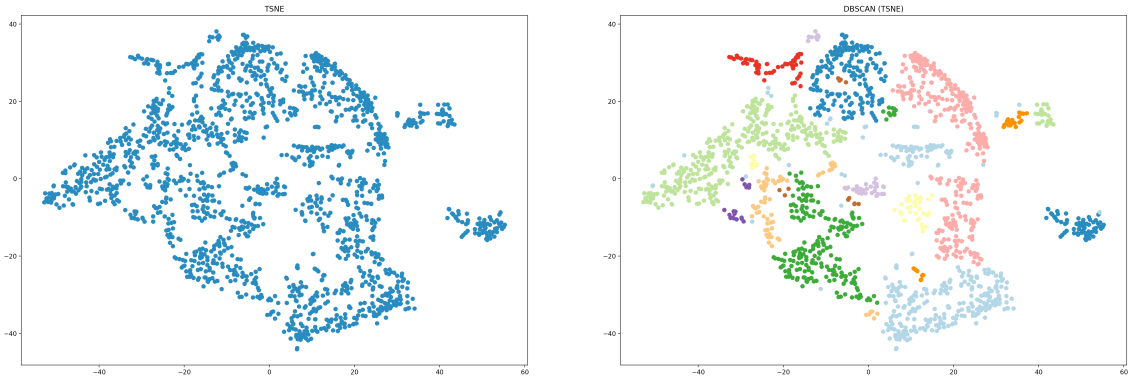

Figure 14: Final t-SNE parameters (1h data files): perplexity=40, learning_rate=20, n_iter=5000

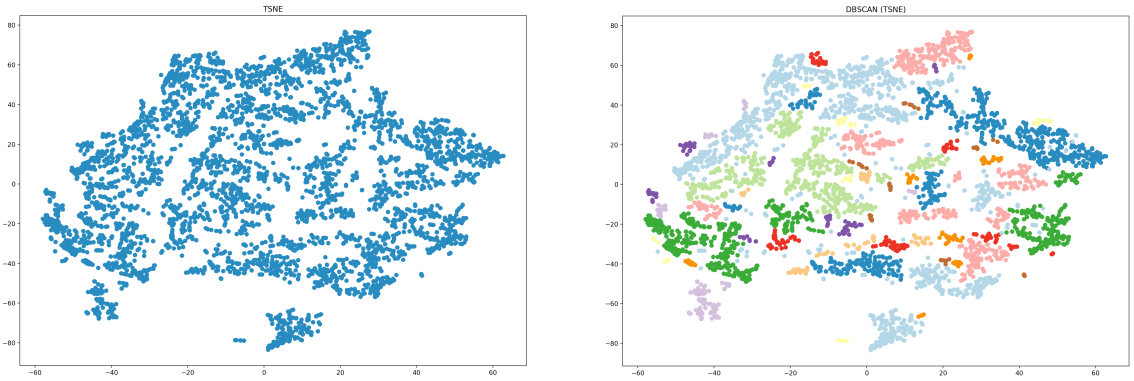

Figure 15: Final t-SNE parameters (3h data files): perplexity=40, learning_rate=20, n_iter=5000

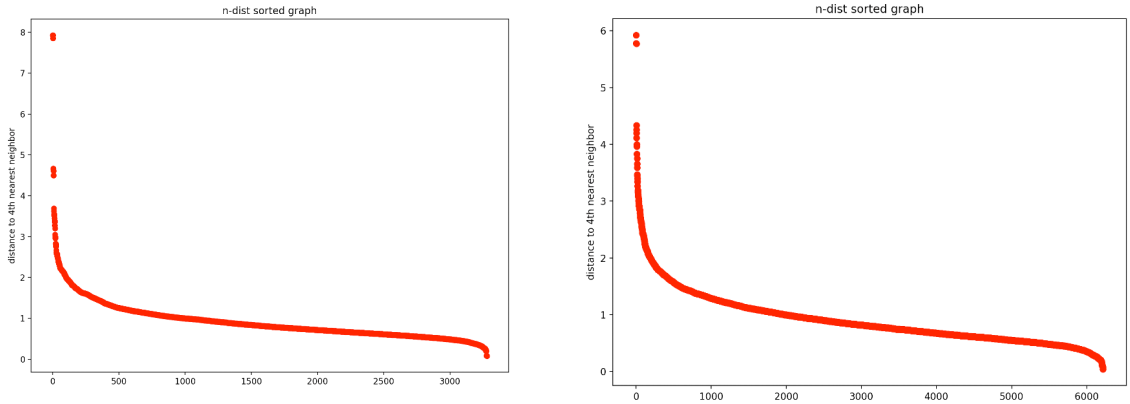

(a) 1h dataset

(b) 3h dataset

Figure 16: Sorted 4-dist graphs (distance for each point to its fourth nearest neighbor), used to determine a suitable *Eps* parameter for the DBSCAN algorithm. The ”valley” starts at roughly the 4th nearest neighbor distance of 2, therefore *Eps* should be 2.

The DBSCAN algorithm was applied, with the parameters eps = 2 and min_samples (MinPts) = 4. The results of this clustering method can be seen in figure 17. Black coloured data points were labelled as noise.

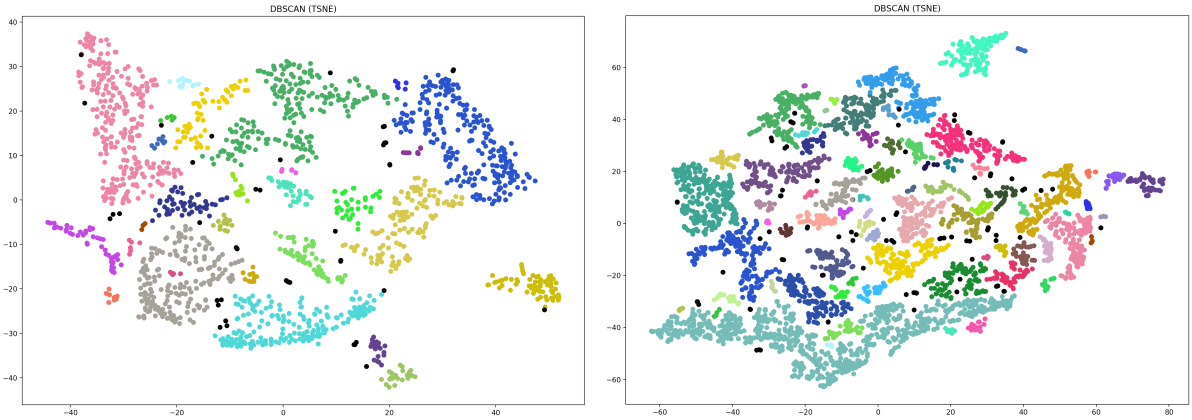

(a) 1h dataset DBSCAN clustering (first column - 15 min).

(b) 3h dataset DBSCAN clustering (first column - 30 min).

Figure 17: DBSCAN clustering results.

4.3.2 OPTICS

The OPTICS algorithm was also implemented with its sklearn implementation[22]. As stated in section 3.5.3.2, the OPTICS algorithm creates a reachability plot for the data points. Initially, the clusters were extracted using the clustering method ”xi”. This is the automatic cluster extraction method, as introduced by Ankerst et al. (1999). The visual results of these clusterings appeared to contain many points that were not assigned to clusters (noise, black coloured data points), as can be seen in figure 18. Moreover, the corresponding reachability plots (figure 19) showed many points that were not assigned to a cluster (also coloured black). This resulted in the DBSCAN method being used to cluster the OPTICS results instead. The *Eps* parameter was set to 2, as determined before for the DBSCAN clustering algorithm. The resulting clusters are depicted in figure 20. The corresponding reachability plots are illustrated in figure 21. As can be seen, the DBSCAN clustering contains much less noise (less black data points and less black bars in the reachability plot). The clusters appear larger and more well defined.

22. `https://scikit-learn.org/stable/modules/generated/sklearn.cluster.OPTICS.html`

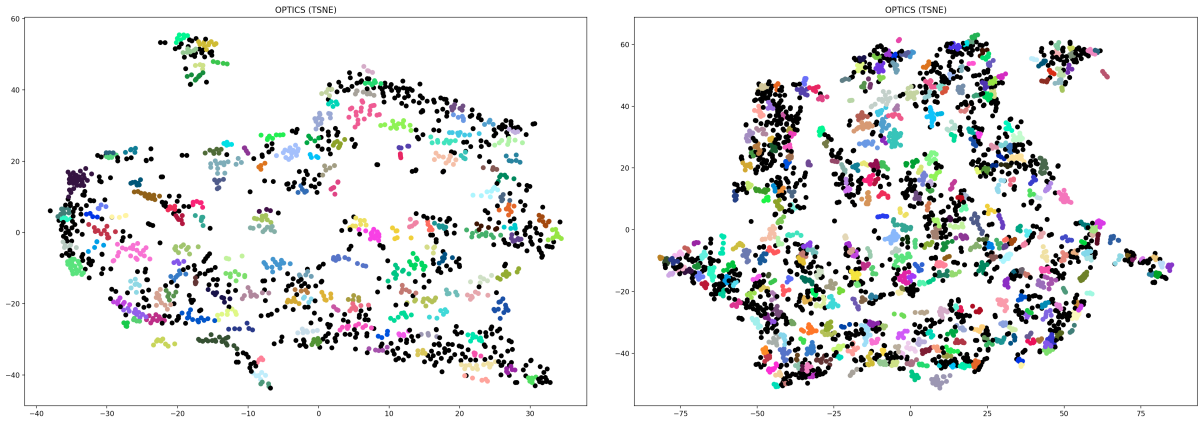

(a) 1h dataset (first column - 15 min). (b) 3h dataset (first column - 30 min)

Figure 18: OPTICS automatic cluster extraction (xi) results. The coloured data points highlight clusters, whilst the black data points indicate noise. The corresponding reachability plots are depicted in figure 19.

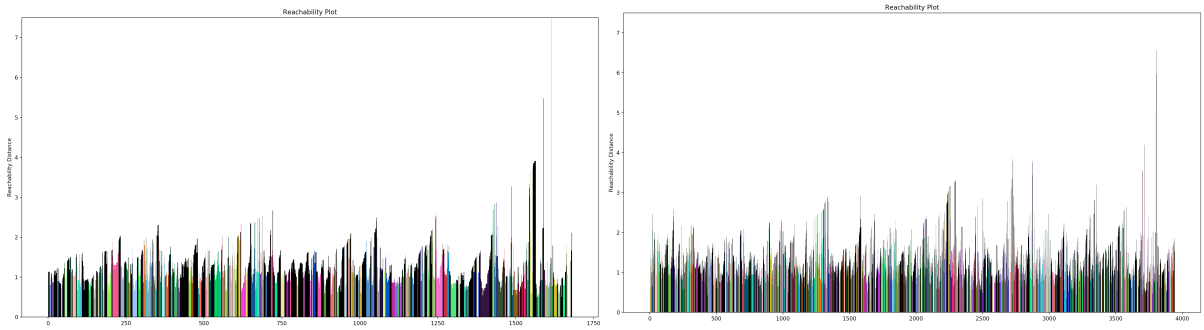

(a) 1h dataset (first column - 15 min) (b) 3h dataset (first column - 30 min)

Figure 19: OPTICS reachability plot using OPTICS automatic cluster extraction (xi). The coloured bars highlight clusters, whilst the black ones indicate noise. The full sized plots are illustrated in appendix B, figures 64 and 65.

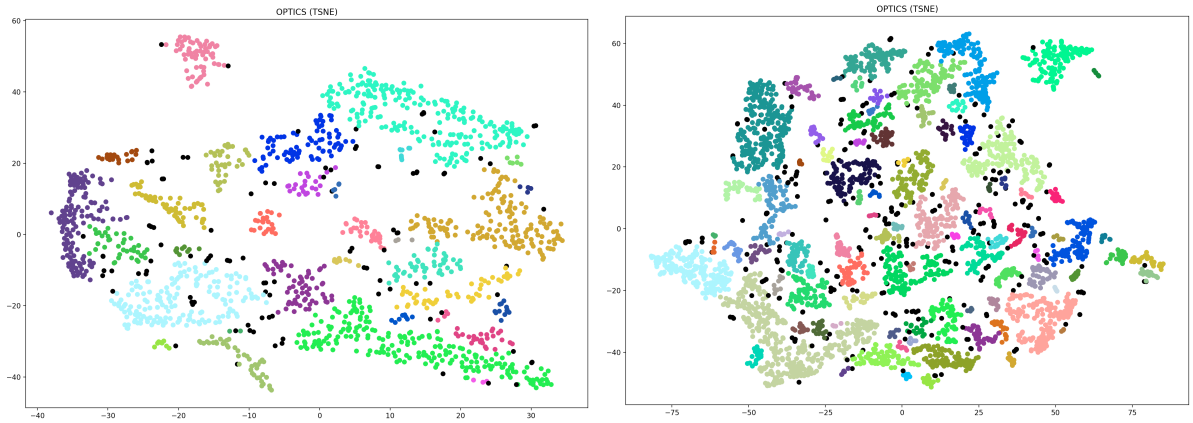

(a) 1h dataset (first column - 15 min) (b) 3h dataset (first column - 30 min)

Figure 20: OPTICS clustering results using DBSCAN clustering. The coloured data points highlight clusters, whilst the black data points indicate noise. The corresponding reachability plots are depicted in figure 21.

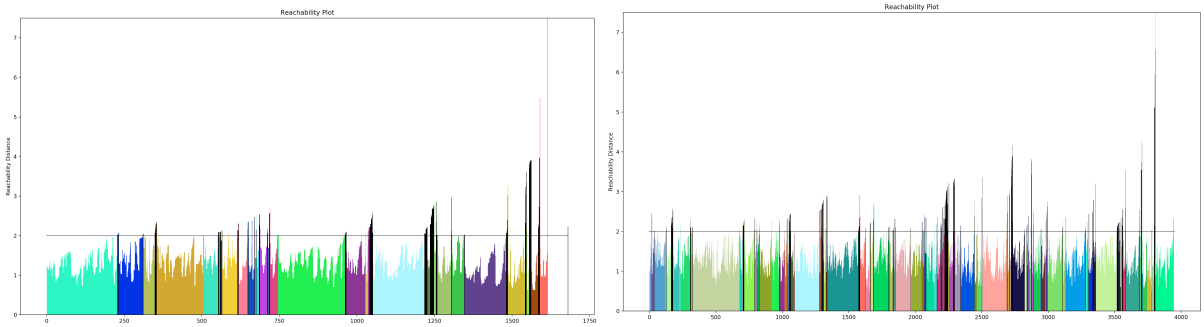

(a) 1h dataset (first column - 15 min) (b) 3h dataset (first column - 30 min)

Figure 21: OPTICS reachability plot using DBSCAN clustering. The coloured bars highlight clusters, whilst the black ones indicate noise. The eps parameter, set at 2, his highlighted with a horizontal line. The full sized plots are illustrated in appendix B, figures 66 and 67.

The final DBSCAN and OPTICS clusterings scatter plots for each time delta are compared in appendix C.1.

4.4 Comparison and evaluation of cluster results from different time lengths

The three mathematical evaluation scores mentioned in section 3.6, i.e. Silhouette Coefficient, Davies-Bouldin Index, and Caliński-Harabasz Index, were used to compare the resulting clusters. They were each implemented using the sklearn library, the same way as in section 4.2.2. These three scores were calculated and stored for each DataFrame, after each clustering algorithm was applied (DBSCAN and OPTICS) for each time length. The resulting values were then compared and are detailed in this section.

The experiment was run on each time length (*1h files:* 15 min, 30 min, 45 min, 1h; *3h files:* 30 min, 1h, 1 h 30 min, 2h, 2h 30 min, 3h). The numbers were different for each time the results were calculated, since t-SNE produces slightly different results. Therefore, the t-SNE and clustering was run multiple times and the results were compared. In figures 78 and 79, two individual t-SNE and clusterings were run, figure 80 depicts the average scores of these two. Figure 81 depicts an average of a different two runs. These mentioned runs all held the learning rate parameter 20. Since a learning rate of 800 also proved to be a viable choice, the t-SNE and clustering was also run twice and averaged with this learning rate (figure 82). These figures (78 to 82) are located in appendix C.2. The mean was taken from all these results, thus creating figure 22. From these, there is no clear winner, although there are some stronger candidates, i.e. 15 min (1h), 1h (1h), and 2h (3h).

Like in section 4.2.2, when comparing the t-SNE results, the green fields from all the above mentioned results, or number of wins, were summed to see which time length had the best number of scores the most times. These wins per dataset (1h or 3h - all green fields) for the 1h data files are pictured in figure 23a and in figure 23b for the 3 hour data files. The two top winners for the 1h data files and the 3h data files, were: 15 min (1h), 30 min (1h), 2h (3h), and 1h (3h). Figure 24 shows the comparison of the dark green wins (1h and 3h). The top four results were: 30 min (1h), 1h (3h), 2h (3h), and 30 min (3h). The number of wins is to some extent reliable on the resulting scores from other time lengths it happened to be compared with. It also does not fully factor in the full extent by how far this time length was better. For this reason, time lengths that were among the mentioned stronger candidates at least once (either in figures 22, 23a and 23b, or 24) were compared solely to each other. The results are detailed in figure 25. The 2h time delta achieved the majority of best scores (wins) in this final comparison.

1h Files						
	15 min	30 min	45 min	1h		
DBSCAN (TSNE)						
Silhouette	0.053476365	0.013788914	-0.038610232	-0.052956536		
Davies Bouldin	2.04244793	1.597171222	1.755245051	1.577807591		
Calinski Harabasz	494.5009903	349.3147449	344.8215987	364.2258626		
OPTICS						
Silhouette	0.078437062	0.12075056	-0.017926106	0.05120006		
Davies Bouldin	1.844121062	1.596800429	1.828162369	1.461980828		
Calinski Harabasz	398.3315599	347.2439435	268.4922909	303.9834533		
3h Files						
	30 min	1h	1h 30 min	2h	2h 30 min	3h
DBSCAN (TSNE)						
Silhouette	0.011948289	0.045027432	0.029207257	0.084418905	0.058235747	0.066334556
Davies Bouldin	1.702623809	1.581150429	1.713516524	1.523790147	1.590690427	1.608006213
Calinski Harabasz	513.226822	639.5570987	496.3219016	525.4316832	525.3219704	523.1398047
OPTICS						
Silhouette	0.052804309	0.077179238	0.105263528	0.08859444	0.077369563	0.083093493
Davies Bouldin	1.774005053	1.649207334	1.621448729	1.4901967	1.45541583	1.653579405
Calinski Harabasz	442.9552584	408.6641751	325.6016964	320.8891861	325.764943	298.096556
	best values in files (1h or 3h)					
	best values total (1h and 3h)					

Figure 22: **Evaluation scores** comparison averaged from **figures 78, 79, 80, 81, and 82** (located in appendix C.2). The green highlighted values indicate the best achieving evaluation score values (1h or 3h files), for the corresponding clustering method. Furthermore, the dark green highlighted values also accentuate the overall best scoring values over all datasets (1h and 3h files).

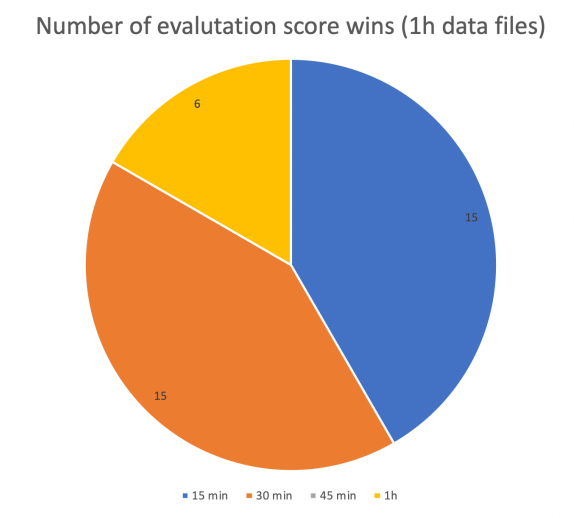

(a) Number of evaluation score wins (1h or 3h dataset) for the 1h data files.

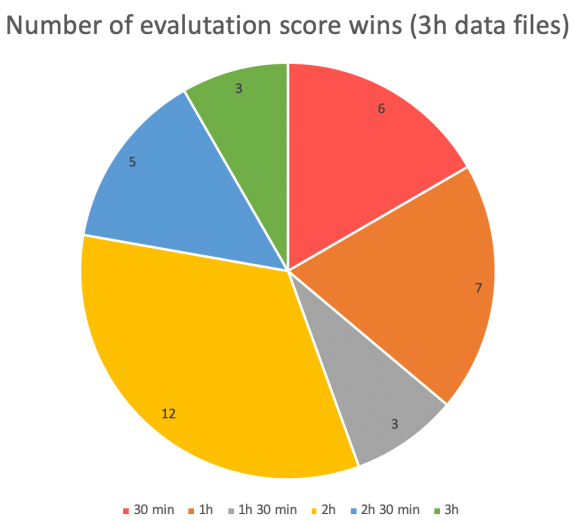

(b) Number of evaluation score wins (1h or 3h dataset) for the 3h data files.

Figure 23: Comparison of number of evaluation score wins (1h or 3h dataset).

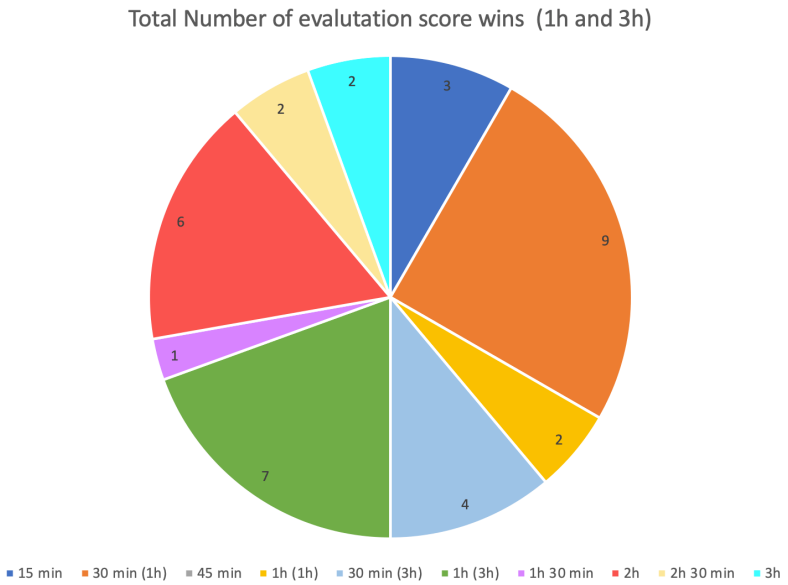

Figure 24: Number of dark green evaluation score wins (overall wins in 1h and 3h dataset).

	15 min (1h)	30 min (1h)	1h	30 min (3h)	1h (3h)	2h (3h)
DBSCAN (TSNE)						
Silhouette	0.053476365	0.013788914	-0.052956536	0.011948289	0.045027432	0.084418905
Davies Bouldin	2.04244793	1.597171222	1.577807591	1.702623809	1.581150429	1.523790147
Calinski Harabasz	494.5009903	349.3147449	364.2258626	513.226822	639.5570987	525.4316832
OPTICS						
Silhouette	0.078437062	0.12075056	0.05120006	0.052804309	0.077179238	0.08859444
Davies Bouldin	1.844121062	1.596800429	1.461980828	1.774005053	1.649207334	1.4901967
Calinski Harabasz	398.3315599	347.2439435	303.9834533	442.9552584	408.6641751	320.8891861
	best values in files (1h or 3h)					

Figure 25: Comparison of **top evaluation score performers** (of clusterings) from figures 22, 23a, 23b, and 24. The light green highlighted cells indicate the best value across the different time lengths for that score.

1h vs 3h Files		
	1h	3h
DBSCAN (TSNE)		
Silhouette	-0.052956536	0.066334556
Davies Bouldin	1.577807591	1.608006213
Calinski Harabasz	364.2258626	523.1398047
OPTICS		
Silhouette	0.05120006	0.083093493
Davies Bouldin	1.461980828	1.653579405
Calinski Harabasz	303.9834533	298.096556
	best values in files (1h or 3h)	

Figure 26: Evaluation scores comparison from **averaged 1h and 3h dataset** runs of t-SNE and clustering.

5 Discussion

Section 4.4 revealed, that the 2h time length (from the 3h dataset) produced the most distinct and well defined clusters, according to the evaluation scores. The order of the other top performing time lengths was further assessed. By eliminating the winning column from figure 25 iteratively and comparing the resulting time lengths (see figure 83 in appendix C.2), the following order can be assumed: 2h (3h), 1h (1h), 1h (3h), 30 min (1h), 30 min (3h), and 15 min (1h). 1h (3h) out performs when compared directly to 30 min (1h). The direct comparison, for example, of 30 min (1h), 1h (1h), and 1h (3h) (figure 84 in appendix C.2) however, results in 1h (3h) placing first, 1h (1h) placing second and 30 min (1h) placing third. When considering the highest number of evaluation score ”wins” over different t-SNE and clustering results, the 30 min time delta (from the 1h dataset) came top, followed by the 1h time length and then the 2h time length (both from the 3h dataset) (see figure 24). These final results show, that the exact placing of these time lengths is hard to determine, since it depends on how they were compared. However, 2h (3h), 1h (3h), 1h (1h), and 30 min (1h) proved to be the best performers across the different comparison methods used. The 45 minute time delta in the 1 hour data files appeared to perform the lowest, with 0 wins. The fact that 45 never out performed the other time lengths shows consistency, despite the different results.

The results from Rahman et al. (2016) (as mentioned in section 2) showed, that higher time lengths (e.g. 100 minutes) performed better than shorter ones. They deducted, that smaller window sizes were susceptible to noise and had a higher gap between precision (exactness) and recall (completeness). This discovery could also apply to the results of this experiment, considering that the 2h and 1h time lengths placed in the top three results.

To determine whether the 1 hour or 3 hour aggregation files led to better clusters, the average results of both time files are compared in figure 26. Both the 1h and 3h datasets have the same

number of wins. When scanning other comparisons of the evaluation scores (also the ones utilised for finding the t-SNE parameters), it is noticeable, that the 1h and 3h datasets either have the same number of wins, or the 3h dataset has more. This indicates that overall, the three hour aggregation files produce more superior clusters. Of the 36 number of wins across all time deltas (the 1h and 3h aggregation files combined), 14 of these were achieved by the 1h data file time lengths (38.9%), the other 22 by the 3 hour dataset (61.1%). A possible explanation, as to why the 3h dataset might have created better clusters, was that the cleaned dataset had more rows (as revealed in section 4.1.4). The use of more data could have resulted in more similar rows and more improved clusters. Another aspect to consider, is that sensor data recorded for shorter time lengths might not be long enough to detect underlying stress patterns. There were also shorter intervals in between the recordings of the 3h dataset (1.5h instead of 2.5 for the 1h dataset). Therefore, less time was missed, where important patterns might have occurred.

Moreover, the higher the number of rows, the more robust the clusters could be towards potential outliers. As explained in section 3.6.1, the Silhouette Score compares the within cluster distances to the distance of a neighbouring cluster. If many points are well placed within a cluster, an outlier will have little impact against the many short distances. However, if the cluster is not very dense and only contains a few ”good” assigned data points, an outlier could have a larger impact on the result.

In order to provide Just-in-Time Intervention, the SmartEater app would need to predict upcoming stress. There are different types of stress. The Canadian Centre for Studies on Human Stress (CSHS) [23] differentiate acute and chronic stress. Acute stress is caused by a particular event or setting, when something is new and feels out of control (e.g. presentations). Chronic stress is longer term and caused by repeated situations that cause stress. The data points would need to account for and recognise these different types of stress patterns. For example, if stress is short, then a longer time delta will likely make it seem less relevant, compared to all the unstressed data. However, if it is long, a shorter time delta might miss it or only perceive a small part of it. This could be a reason why middle time lengths, such as 2h, 1h (3h data files) and 30 min (1h) created more distinct clusters, since they may have been more likely to recognise these differences. The fact that there was not one specific time length that always performed higher than the others shows, that a single time length may not be enough to be able to create clear clusters. Different time lengths might be needed to detect different patterns. Since the 3h data files appeared to perform better, this could point to the fact that stress requires a longer time period to predict. The 3h files also appear to have more, but smaller clusters. This variety could indicate, that more various types of stress were able to be found.

For future work, it might be beneficial to collect more data from users for a longer period of time, in attempt to further narrow down the resulting time lengths found in this thesis. It would also be necessary to confirm that the clusters were created for stress levels and not for each user (since a user's behaviour could exhibit similarities). As implemented in this thesis, this could be observed by highlighting each user's results with a unique colour. It might also be beneficial to support the mathematical evaluations with hand drawn clusters found by test users in user

23. https://humanstress.ca/stress/understand-your-stress/acute-vs-chronic-stress/

studies. Especially since the scores are different each time t-SNE is computed, sometimes leading to different results. As mentioned in section 3.1 by Larose and Larose (2015)[9], data mining requires continuous human supervision for quality monitoring and evaluation.

6 Conclusion

This thesis compared different time deltas for aggregation, to determine which one is ideal to construct high quality clusterings from smartphone sensor and usage data. The data was recorded from different test subjects for the SmartEater mobile health app. The datasets aggregated into 1h and 3h files were preprocessed, in which missing values, unnecessary columns and rows with more than 50% zeros were removed. The resulting rows were normalised using z-score normalization. Using t-SNE, the 8 existing dimensions (attributes) were reduced to 2 and visualised in scatter plots. Such plots were created for each of the total 10 time lengths (1h and 3h files combined). DBSCAN and OPTICS clustering algorithms were used to group the data points together into clusters. The Silhouette Score, Davies-Bouldin Index, and Caliński-Harabasz Index were used to mathematically evaluate the resulting clusters for each time length. The comparison of these scores suggests, that the following time lengths produce the most distinct and well defined clusters: 2h, 1h (both from the 3h dataset), 1h, and 30 min (both from the 1h dataset). The results of this study suggest, that various time lengths might be necessary to receive the clearest clusters. User studies to evaluate hand drawn clusters would be a further step to identify appropriate time lengths to generate more distinct clusters and therefore be used to predict eating crises.

References

Ameko, M. K., L. Cai, M. Boukhechba, A. Daros, P. I. Chow, B. A. Teachman, M. S. Gerber, and L. E. Barnes. 2018. "Cluster-based Approach to Improve Affect Recognition from Passively Sensed Data." In *2018 IEEE EMBS International Conference on Biomedical Health Informatics (BHI)*, 434–437. Las Vegas, NV, USA, March. doi:10.1109/BHI.2018.8333461.

Ankerst, Mihael, Markus M. Breunig, Hans-Peter Kriegel, and Jörg Sander. 1999. "OPTICS: Ordering Points to Identify the Clustering Structure." *SIGMOD Rec.* (Philadelphia, Pennsylvania, USA), SIGMOD '99, 28, no. 2 (June): 49–60. doi:10.1145/304181.304187.

Bellman, R. E. 1957. *Dynamic Programming*. Rand Corporation research study. Princeton, New Jersey: Princeton University Press. ISBN: 9780691079516.

———. 1961. *Adaptive Control Processes: A Guided Tour*. Princeton Legacy Library. Princeton, New Jersey: Princeton University Press. ISBN: 9781400874668.

Caliński, T., and J. Harabasz. 1974. "A Dendrite Method for Cluster Analysis." *Communications in Statistics - Theory and Methods* 3 (January): 1–27. doi:10.1080/03610927408827101.

Davies, D. L., and D. W. Bouldin. 1979. "A Cluster Separation Measure." *IEEE Transactions on Pattern Analysis and Machine Intelligence* PAMI-1, no. 2 (April): 224–227. doi:10.1109/TPAMI.1979.4766909.

Dey, R., and S. Chakraborty. 2015. "Convex-hull DBSCAN clustering to predict future weather." In *2015 International Conference and Workshop on Computing and Communication (IEMCON)*, 1–8. Vancouver, BC, Canada, October. doi:10.1109/IEMCON.2015.7344438.

Ester, M., H. Kriegel, J. Sander, and X. Xu. 1996. "A density-based algorithm for discovering clusters in large spatial databases with noise." In *Proc. 2nd Int. Conf. Knowledge Discovery and Data Mining (KDD'96)*, 96:226–231. 34. Portland, Oregon: AAAI Press, August.

García, Salvador, Julián Luengo, and Francisco Herrera. 2015. *Data Preprocessing in Data Mining*. Switzerland: Springer International Publishing. ISBN: 978-3-319-10246-7. doi:10.1007/978-3-319-10247-4.

Han, J., J. Pei, and M. Kamber. 2011. *Data Mining: Concepts and Techniques*. 3rd Edition. Burlington, Massachusetts: Elsevier. ISBN: 978-0-12-381479-1.

Hartigan, John A. 1975. *Clustering Algorithms*. New York, NY, USA: John Wiley & Sons, Inc. ISBN: 978-0-471-35645-5.

Hinton, Geoffrey E, and Sam T. Roweis. 2003. "Stochastic Neighbor Embedding." In *Advances in Neural Information Processing Systems*, 15:857–864. http://papers.nips.cc/paper/2276-stochastic-neighbor-embedding.pdf.

Hotelling, Harold. 1933. *Analysis of a complex of statistical variables into principal components.* Baltimore: Warwick & York.

Jolliffe, I.T. 2002. *Principal Component Analysis: Second Edition.* Springer Series in Statistics. New York, USA: Springer-Verlag New York. ISBN: 0-387-95442-2. doi:10.1007/b98835.

Larose, Daniel T, and Chantal D Larose. 2015. *Data Mining and Predictive Analytics.* 2nd Edition. Wiley Series on Methods and Applications in Data Mining. Hoboken, New Jersey: John Wiley & Sons. ISBN: 9781118116197.

Maaten, Laurens van der, and Geoffrey Hinton. 2008. "Visualizing Data using t-SNE." *Journal of Machine Learning research* 9 (Nov): 2579–2605.

McCue, C. 2014. *Data Mining and Predictive Analysis: Intelligence Gathering and Crime Analysis.* Oxford: Butterworth-Heinemann (Elsevier). ISBN: 9780128004081.

Pearson, Karl. 1901. "LIII. On lines and planes of closest fit to systems of points in space." *The London, Edinburgh, and Dublin Philosophical Magazine and Journal of Science* 2 (11): 559–572. doi:10.1080/14786440109462720.

Pyle, D. 1999. *Data Preparation for Data Mining.* Burlington, Massachusetts: Morgan Kaufmann. ISBN: 9781558605299.

Rahman, Tauhidur, Mary Czerwinski, Ran Gilad-Bachrach, and Paul Johns. 2016. "Predicting "About-to-Eat" Moments for Just-in-Time Eating Intervention." In *Proceedings of the 6th International Conference on Digital Health Conference,* 141–150. Montréal, Québec, Canada: Association for Computing Machinery, April. ISBN: 9781450342247. doi:10.1145/2896338.2896359.

Romesburg, H. Charles. 2004. *Cluster Analysis for Researchers.* Morrisville, North Carolina: Lulu Press. ISBN: 9781411606173.

Rousseeuw, Peter J. 1987. "Silhouettes: a graphical aid to the interpretation and validation of cluster analysis." *Journal of computational and applied mathematics* 20:53–65. doi:10.1016/0377-0427(87)90125-7.

Sornbootnark, P., and P. Khoenkaw. 2019. "Excessive Alcohol Craving Prediction Algorithm Using Smartphone Accelerometer Sensor." In *2019 Joint International Conference on Digital Arts, Media and Technology with ECTI Northern Section Conference on Electrical, Electronics, Computer and Telecommunications Engineering (ECTI DAMT-NCON),* 335–338. Nan, Thailand, January. doi:10.1109/ECTI-NCON.2019.8692267.

Stütz, Thomas, Thomas Kowar, Michael Kager, Martin Tiefengrabner, Markus Stuppner, Jens Blechert, Frank H. Wilhelm, and Simon Ginzinger. 2015. "Smartphone Based Stress Prediction." In *User Modeling, Adaptation and Personalization,* edited by Francesco Ricci, Kalina Bontcheva, Owen Conlan, and Séamus Lawless, 240–251. Cham: Springer International Publishing. doi:10.1007/978-3-319-20267-9_20.

Wattenberg, Martin, Fernanda Viégas, and Ian Johnson. 2016. "How to Use t-SNE Effectively." *Distill* (October). doi:10.23915/distill.00002. http://distill.pub/2016/misread-tsne.

Appendices

A t-SNE parameters comparison figures

In the following figures, the t-SNE results of different perplexity and learning rate parameters are compared, for the different time length files (1h and 3h), using the first columns of each feature (1h: first 15 minutes, 3h: fist 30 minutes). The left scatter plots depict t-SNE results, the right scatter plots visualise DBSCAN clusterings of t-SNE results). The DBSCAN cluster colourings were placed here to support in perceiving the differences between the t-SNE structured data and to see when the most distinct and well defined clusters were formed.

A.1 Perplexity

A.1.1 Perplexity = 5

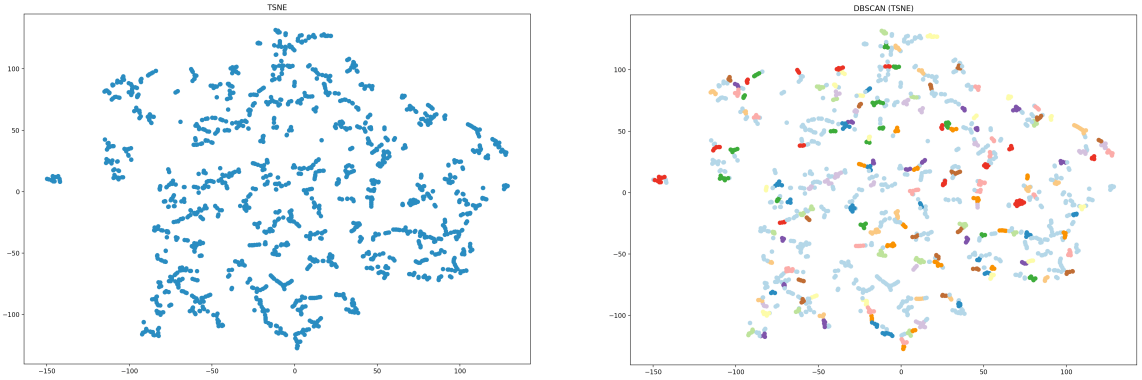

Figure 27: **1h** data files, t-SNE calculated with the following parameters: **perplexity=5**, n_iter=5000, learning_rate=50

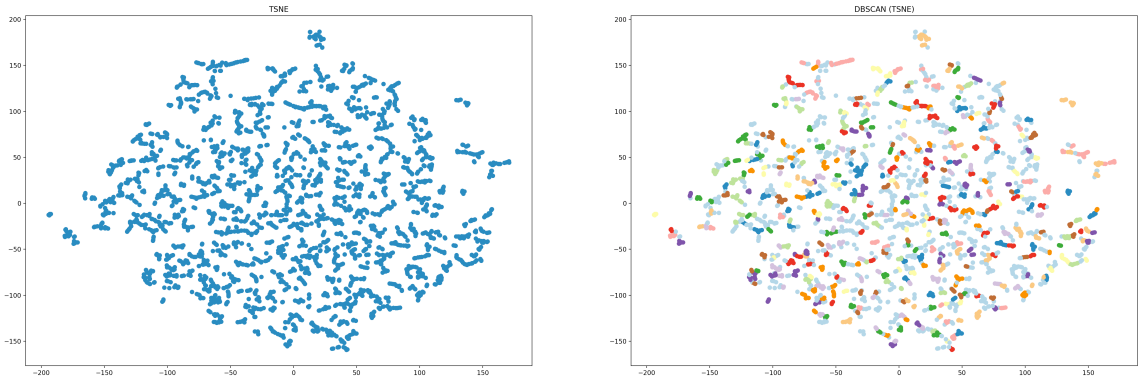

Figure 28: **3h** data files, t-SNE calculated with the following parameters: **perplexity=5**, n_iter=5000, learning_rate=50

A.1.2 Perplexity = 10

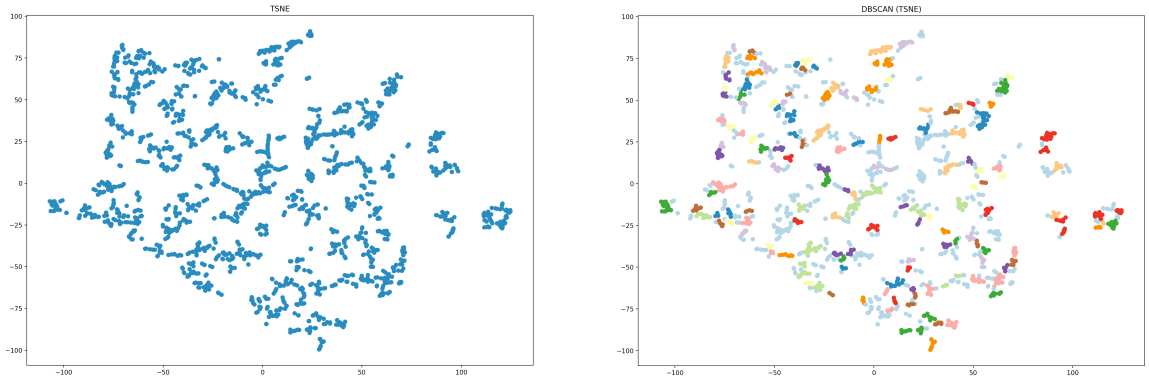

Figure 29: **1h** data files, t-SNE calculated with the following parameters: **perplexity=10**, n_iter=5000, learning_rate=50

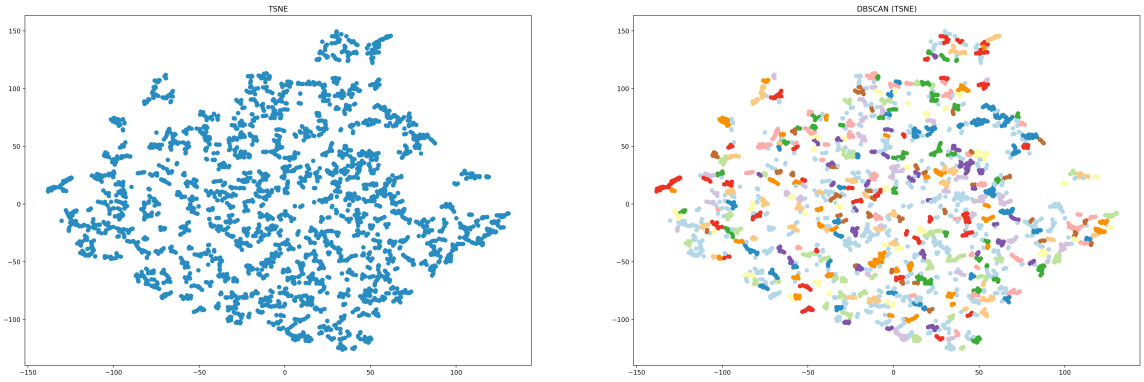

Figure 30: **3h** data files, t-SNE calculated with the following parameters: **perplexity=10**, n_iter=5000, learning_rate=50

A.1.3 Perplexity = 20

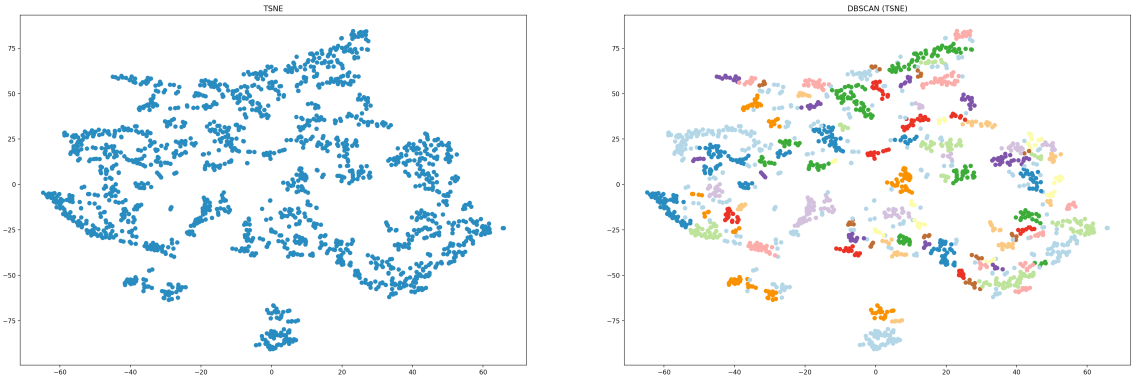

Figure 31: **1h** data files, t-SNE calculated with the following parameters: **perplexity=20**, n_iter=5000, learning_rate=50

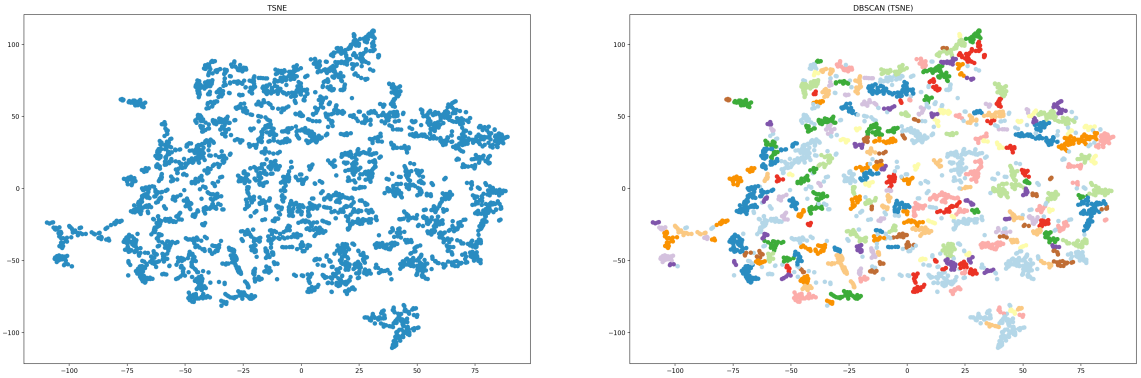

Figure 32: **3h** data files, t-SNE calculated with the following parameters: **perplexity=20**, n_iter=5000, learning_rate=50

A.1.4 Perplexity = 30

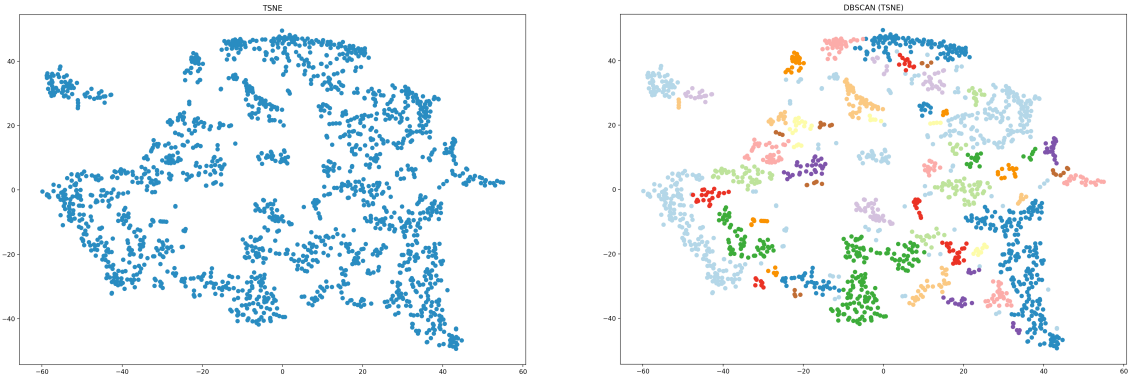

Figure 33: **1h** data files, t-SNE calculated with the following parameters: **perplexity=30**, n_iter=5000, learning_rate=50

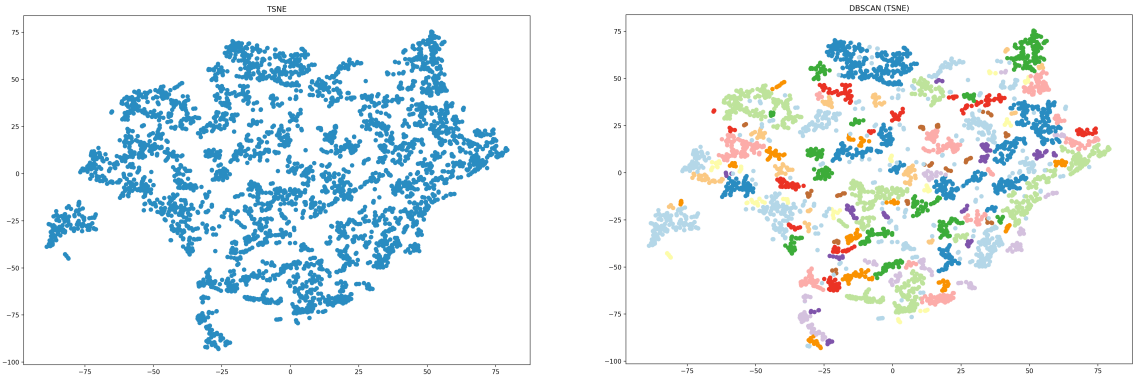

Figure 34: **3h** data files, t-SNE calculated with the following parameters: **perplexity=30**, n_iter=5000, learning_rate=50

A.1.5 Perplexity = 40

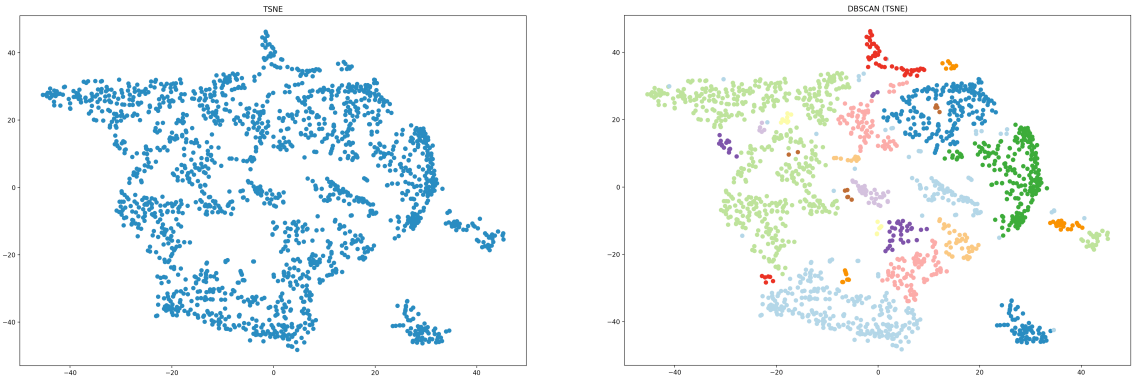

Figure 35: **1h** data files, t-SNE calculated with the following parameters: **perplexity=40**, n_iter=5000, learning_rate=50

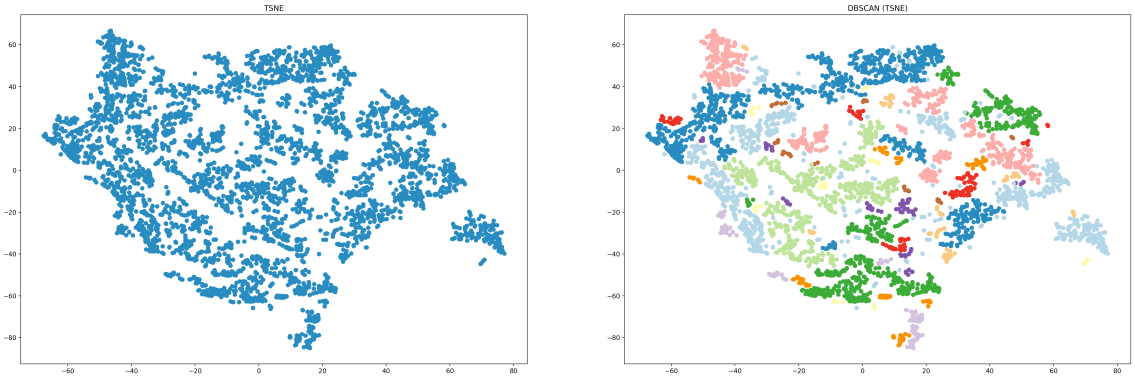

Figure 36: **3h** data files, t-SNE calculated with the following parameters: **perplexity=40**, n_iter=5000, learning_rate=50

A.1.6 Perplexity = 45

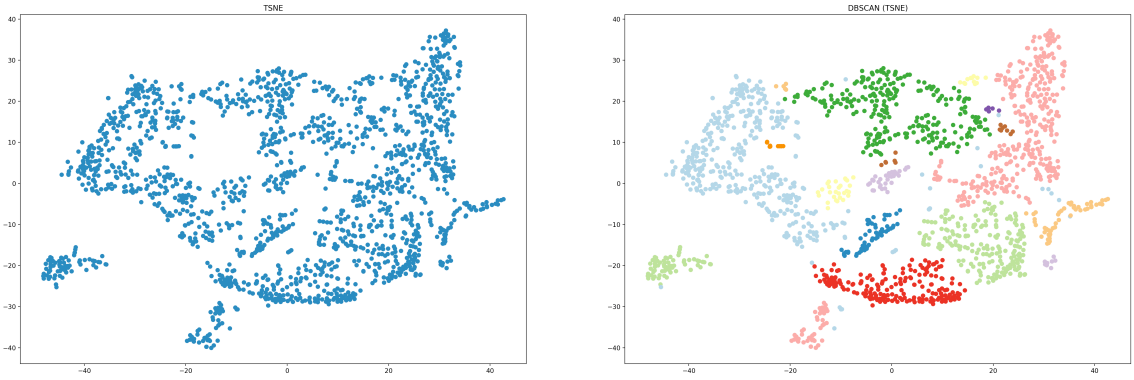

Figure 37: **1h** data files, t-SNE calculated with the following parameters: **perplexity=45**, n_iter=5000, learning_rate=50

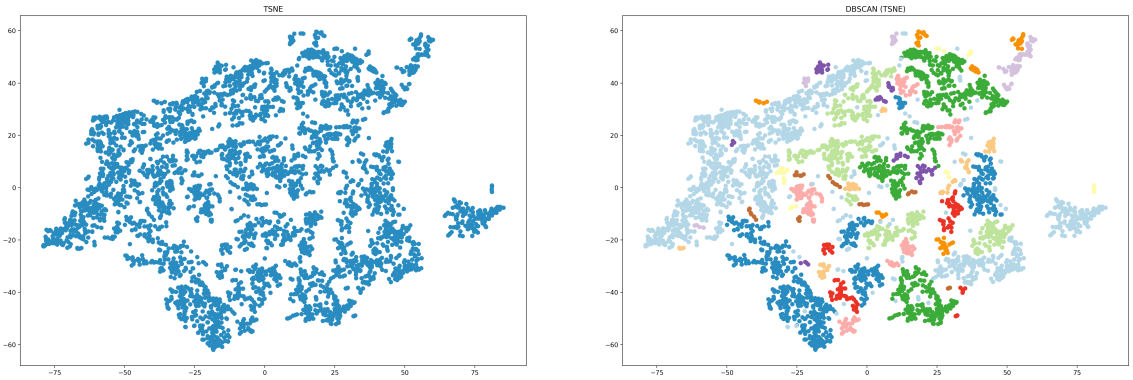

Figure 38: **3h** data files, t-SNE calculated with the following parameters: **perplexity=45**, n_iter=5000, learning_rate=50

A.1.7 Perplexity = 50

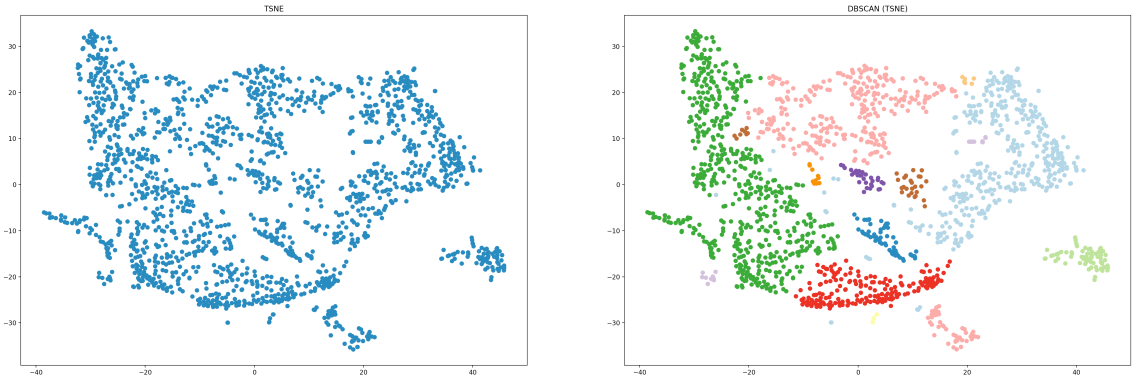

Figure 39: **1h** data files, t-SNE calculated with the following parameters: **perplexity=50**, n_iter=5000, learning_rate=50

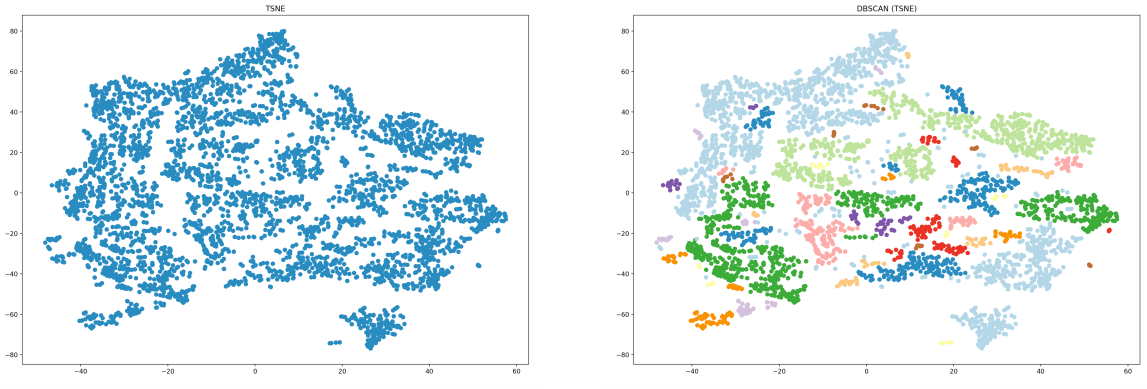

Figure 40: **3h** data files, t-SNE calculated with the following parameters: **perplexity=50**, n_iter=5000, learning_rate=50

A.1.8 Perplexity Comparison Results (Average of two different t-SNE runs)

In the following figures, the green highlighted values indicate the best achieving evaluation score values (1h or 3h files), for the corresponding clustering method. Furthermore, the dark green highlighted values also accentuate the overall best scoring values over all datasets (1h and 3h files).

1h Files							
	Perplexity: 5	Perplexity: 10	Perplexity: 20	Perplexity: 30	Perplexity: 40	Perplexity: 45	Perplexity: 50
DBSCAN (TSNE)							
Silhouette	0.017019369	0.19126232	0.257092565	0.17063424	0.054603353	-0.074523993	-0.171010017
Davies Bouldin	1.403668307	1.446398049	1.239208781	1.767317317	1.84461589	2.479778037	1.825281178
Calinski Harabasz	12.15170592	24.79178797	100.0146068	241.9789113	563.5035835	437.3758651	329.6007263
OPTICS							
Silhouette	-0.561546922	-0.246936843	0.072907798	0.110969819	0.034138191	-0.048403323	-0.168361336
Davies Bouldin	1.206983736	1.477320921	1.379751733	2.01127775	1.841140623	2.805988833	2.087488648
Calinski Harabasz	6.242372565	11.29904904	34.8081723	121.1196102	390.1107083	443.3149674	288.6146754
3h Files							
	Perplexity: 5	Perplexity: 10	Perplexity: 20	Perplexity: 30	Perplexity: 40	Perplexity: 45	Perplexity: 50
DBSCAN (TSNE)							
Silhouette	0.187188387	0.292015851	0.285667479	0.193456471	0.031343713	-0.053399093	-0.181974486
Davies Bouldin	1.378079722	1.360209014	1.297094447	1.442256841	1.735051282	1.795796982	1.483932052
Calinski Harabasz	18.05272734	41.40515662	125.5679156	324.4924046	603.9489233	431.4155601	294.2764864
OPTICS							
Silhouette	-0.345607281	-0.027698424	0.14453043	0.16002439	0.060340196	-0.001508603	-0.110961363
Davies Bouldin	1.322159387	1.378912049	1.286376249	1.525305635	1.862524881	1.703454207	2.190983827
Calinski Harabasz	8.067148543	16.79004273	49.04119384	134.4265238	431.4900781	510.0124077	454.230048
	best values in files (1h or 3h)						
	best values total (1h and 3h)						

Figure 41: Comparison of the average of two Silhouette Coefficients, Davies-Bouldin Indices, and Caliński-Harabasz Indices for different t-SNE **perplexities** in **steps of 5 and 10**.

1h Files			
	Perplexity: 40	Perplexity: 45	Perplexity: 50
DBSCAN (TSNE)			
Silhouette	0.054603353	-0.074523993	-0.171010017
Davies Bouldin	1.84461589	2.479778037	1.825281178
Calinski Harabasz	563.5035835	437.3758651	329.6007263
OPTICS			
Silhouette	0.034138191	-0.048403323	-0.168361336
Davies Bouldin	1.841140623	2.805988833	2.087488648
Calinski Harabasz	390.1107083	443.3149674	288.6146754
3h Files			
	Perplexity: 40	Perplexity: 45	Perplexity: 50
DBSCAN (TSNE)			
Silhouette	0.031343713	-0.053399093	-0.181974486
Davies Bouldin	1.735051282	1.795796982	1.483932052
Calinski Harabasz	603.9489233	431.4155601	294.2764864
OPTICS			
Silhouette	0.060340196	-0.001508603	-0.110961363
Davies Bouldin	1.862524881	1.703454207	2.190983827
Calinski Harabasz	431.4900781	510.0124077	454.230048
	best values in files (1h or 3h)		
	best values total (1h and 3h)		

Figure 42: Comparison of the average of two evaluation scores of the top three perplexity candidates **40, 45, and 50**.

A.2 Learning Rate

A.2.1 Learning Rate = 10

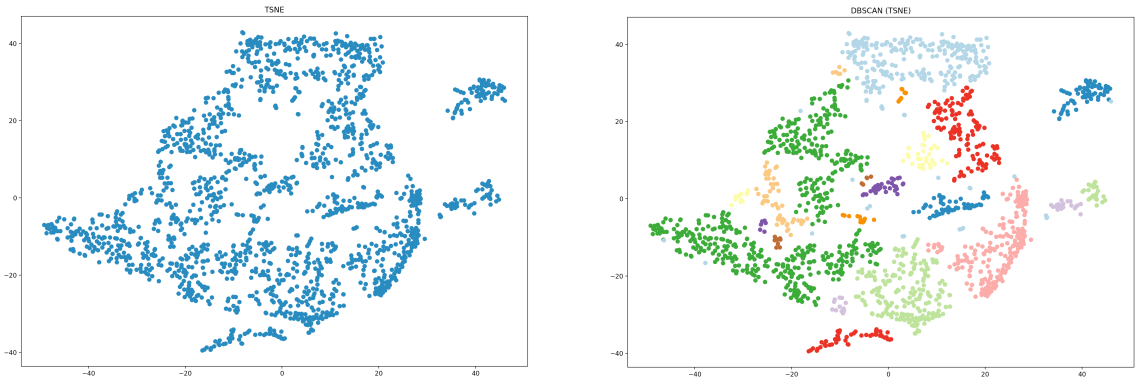

Figure 43: **1h** data files, t-SNE calculated with the following parameters: perplexity=40, n_iter=5000, **learning_rate=10**

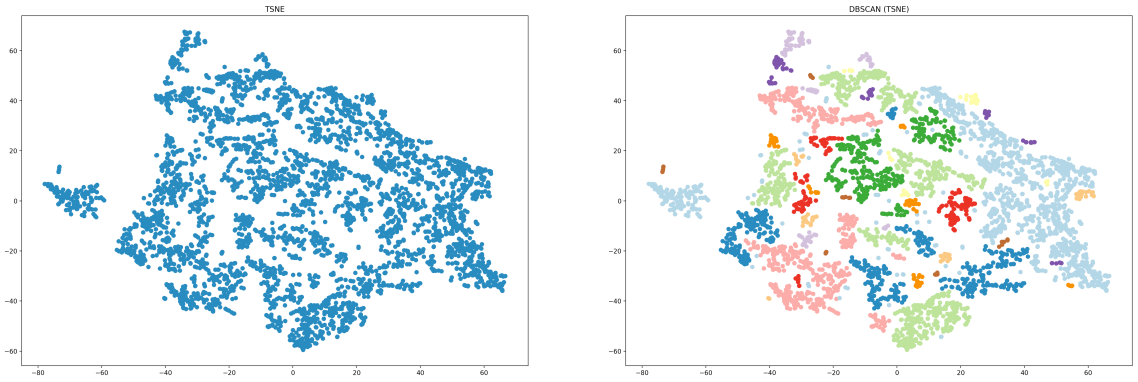

Figure 44: **3h** data files, t-SNE calculated with the following parameters: perplexity=40, n_iter=5000, **learning_rate=10**

A.2.2 Learning Rate = 200

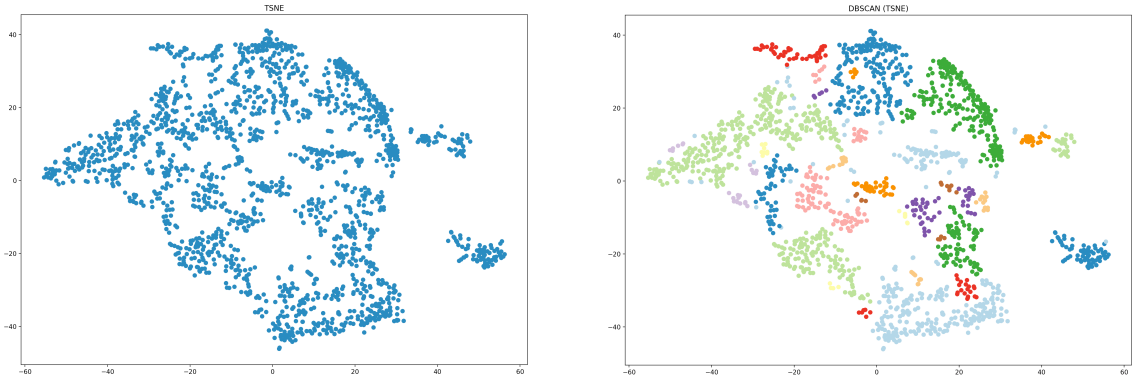

Figure 45: **1h** data files, t-SNE calculated with the following parameters: perplexity=40, n_iter=5000, **learning_rate=200**

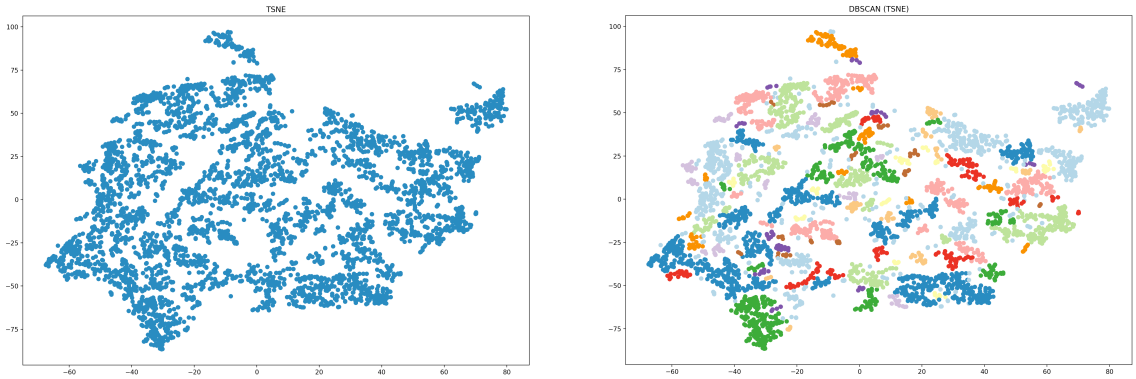

Figure 46: **3h** data files, t-SNE calculated with the following parameters: perplexity=40, n_iter=5000, **learning_rate=200**

A.2.3 Learning Rate = 400

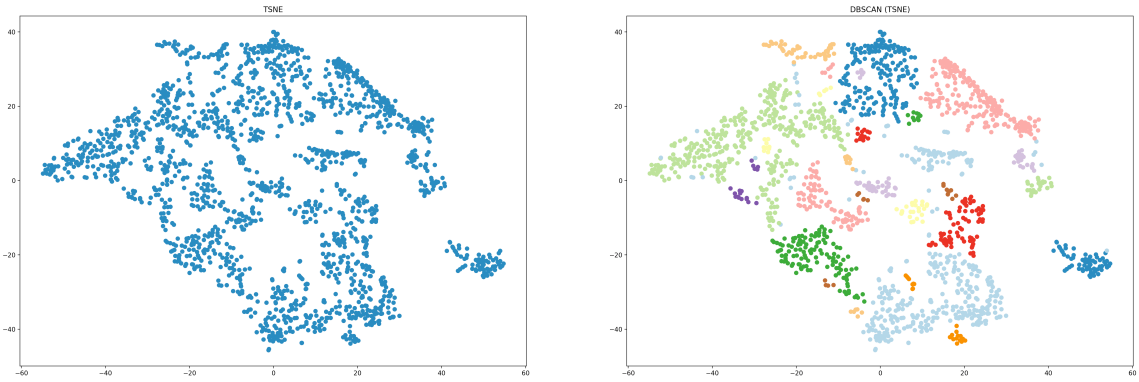

Figure 47: **1h** data files, t-SNE calculated with the following parameters: perplexity=40, n_iter=5000, **learning_rate=400**

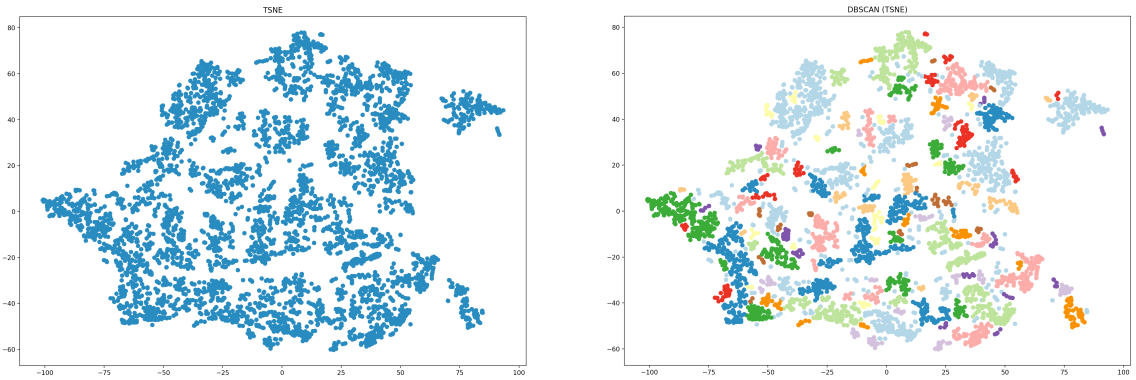

Figure 48: **3h** data files, t-SNE calculated with the following parameters: perplexity=40, n_iter=5000, **learning_rate=400**

A.2.4 Learning Rate = 600

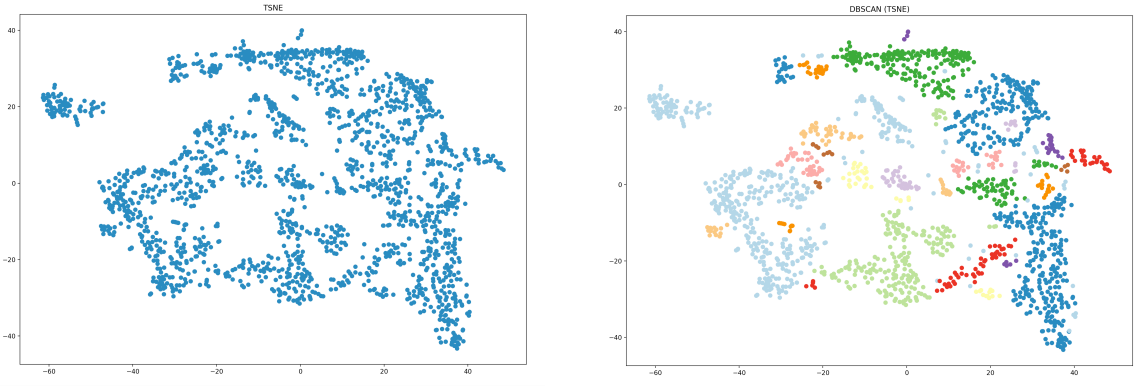

Figure 49: **1h** data files, t-SNE calculated with the following parameters: perplexity=40, n_iter=5000, **learning_rate=600**

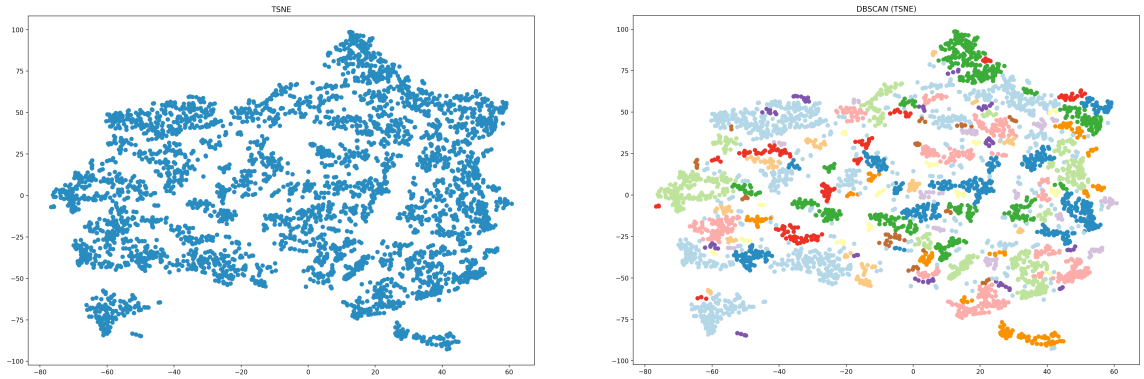

Figure 50: **3h** data files, t-SNE calculated with the following parameters: perplexity=40, n_iter=5000, **learning_rate=600**

A.2.5 Learning Rate = 800

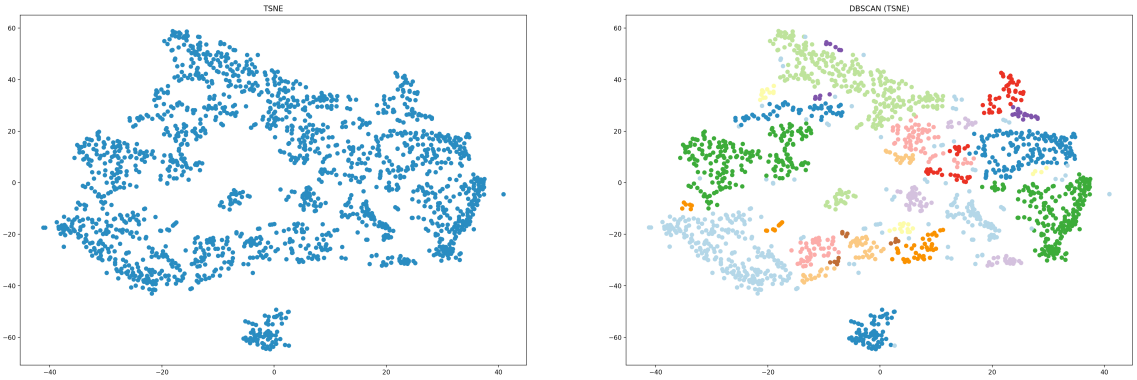

Figure 51: **1h** data files, t-SNE calculated with the following parameters: perplexity=40, n_iter=5000, **learning_rate=800**

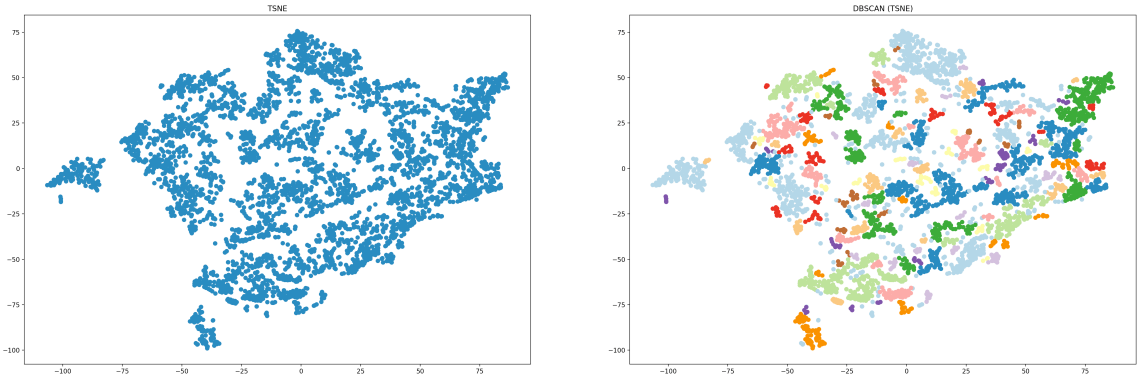

Figure 52: **3h** data files, t-SNE calculated with the following parameters: perplexity=40, n_iter=5000, **learning_rate=800**

A.2.6 Learning Rate = 1000

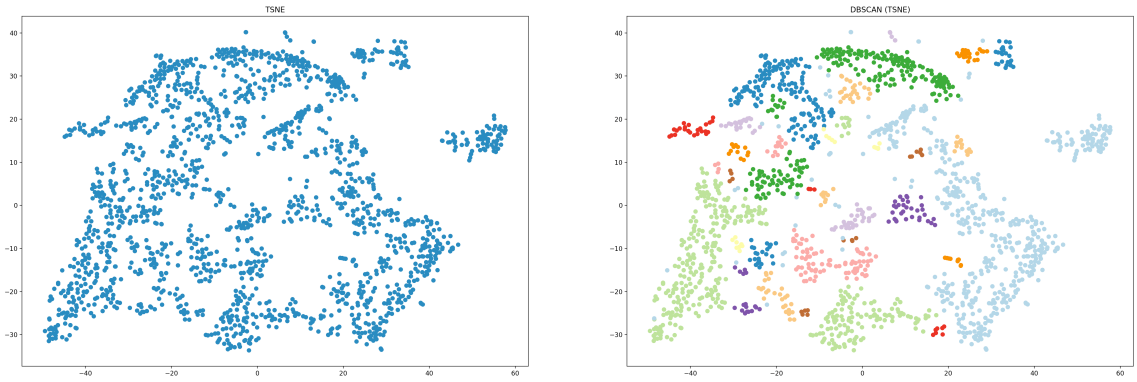

Figure 53: **1h** data files, t-SNE calculated with the following parameters: perplexity=40, n_iter=5000, **learning_rate=1000**

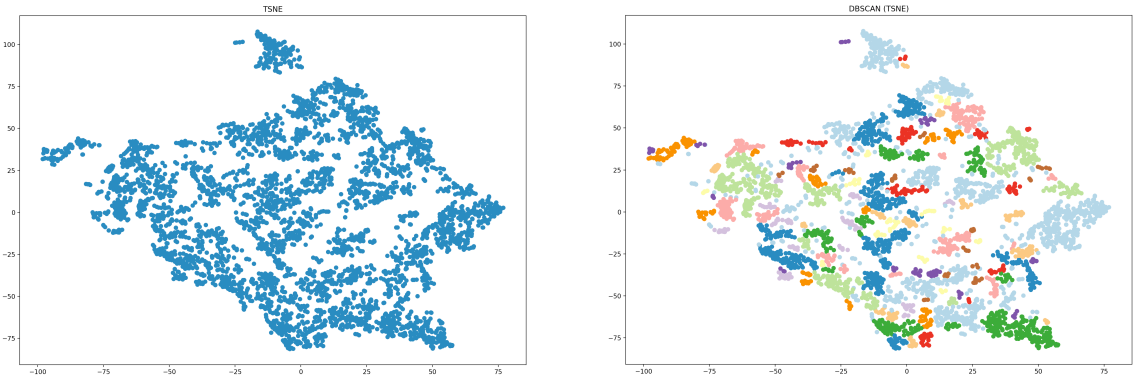

Figure 54: **3h** data files, t-SNE calculated with the following parameters: perplexity=40, n_iter=5000, **learning_rate=1000**

A.2.7 Learning Rate Detailed Comparison Results

In the following figures, the green highlighted values indicate the best achieving evaluation score values (1h or 3h files), for the corresponding clustering method. Furthermore, the dark green highlighted values also accentuate the overall best scoring values over all datasets (1h and 3h files).

1h Files

	Learning Rate: 10	Learning Rate: 50	Learning Rate: 100	Learning Rate: 150	Learning Rate: 800
DBSCAN (TSNE)					
Silhouette	0.050185006	0.020629907	0.043174922	0.00881206	0.037798844
Davies Bouldin	1.813219735	1.765516415	1.792311036	1.84207799	1.537629516
Calinski Harabasz	619.5024641	527.1113507	508.9986796	477.6877339	412.8616309
OPTICS					
Silhouette	0.04723522	0.028060276	0.014973388	-0.010167263	0.036134463
Davies Bouldin	2.644154104	1.627679428	1.943985252	2.038386818	1.512853515
Calinski Harabasz	545.2578195	427.7636283	384.5284878	321.2113347	243.8295466

3h Files

	Learning Rate: 10	Learning Rate: 50	Learning Rate: 100	Learning Rate: 150	Learning Rate: 800
DBSCAN (TSNE)					
Silhouette	-0.053747308	0.005408226	0.08698505	0.056991242	0.08301577
Davies Bouldin	2.315636084	1.595251196	1.65346247	1.51375092	1.40672888
Calinski Harabasz	495.6689234	821.6969448	632.2392584	519.0302785	325.3370665
OPTICS					
Silhouette	-0.002017022	0.06374386	0.08698636	0.091826566	0.08165444
Davies Bouldin	2.196366077	1.600873186	1.609330153	1.509671627	1.485960484
Calinski Harabasz	607.8271457	538.5429769	275.9978949	245.4457569	130.86284

best values in files (1h or 3h)

best values total (1h and 3h)

Figure 55: Comparison of Silhouette Coefficient, Davies-Bouldin Index, and Caliński-Harabasz Index for different t-SNE **learning rate** values. Smaller learning rate value **steps of 50** were taken (except for the first step which is 40 and the last step to 800) between each test.

1h Files					
	Learning Rate: 10	Learning Rate: 20	Learning Rate: 30	Learning Rate: 40	Learning Rate: 800
DBSCAN (TSNE)					
Silhouette	0.050185006	-0.06679525	0.038768608	0.01700433	0.037798844
Davies Bouldin	1.813219735	1.525274298	1.939580286	1.772676736	1.537629516
Calinski Harabasz	619.5024641	248.4124961	577.4117352	551.6767392	412.8616309
OPTICS					
Silhouette	0.04723522	-0.01730663	0.07930727	0.047520984	0.036134463
Davies Bouldin	2.644154104	1.375044564	1.521993726	1.630649614	1.512853515
Calinski Harabasz	545.2578195	253.4888154	453.56707	436.5401766	243.8295466
3h Files					
	Learning Rate: 10	Learning Rate: 20	Learning Rate: 30	Learning Rate: 40	Learning Rate: 800
DBSCAN (TSNE)					
Silhouette	-0.053747308	-0.014693906	0.09359318	0.028022699	0.08301577
Davies Bouldin	2.315636084	1.624380463	1.698168632	1.619440691	1.40672888
Calinski Harabasz	495.6689234	441.8649747	819.1717685	741.2875739	325.3370665
OPTICS					
Silhouette	-0.002017022	0.08187237	0.0860974	0.06130342	0.08165444
Davies Bouldin	2.196366077	1.767960982	1.85835621	1.767468795	1.485960484
Calinski Harabasz	607.8271457	677.3212302	455.2848506	429.6428288	130.86284
	best values in files (1h or 3h)				
	best values total (1h and 3h)				

Figure 56: Comparison of Silhouette Coefficient, Davies-Bouldin Index, and Caliński-Harabasz Index for different t-SNE **learning rate** values. Smaller learning rate value **steps of 10** were taken (except for the last step to 800) between each test.

A.2.8 Learning Rate Comparison Results (Average of two different t-SNE runs)

In the following figures, the green highlighted values indicate the best achieving evaluation score values (1h or 3h files), for the corresponding clustering method. Furthermore, the dark green highlighted values also accentuate the overall best scoring values over all datasets (1h and 3h files).

1h Files						
	Learning Rate: 10	Learning Rate: 200	Learning Rate: 400	Learning Rate: 600	Learning Rate: 800	Learning Rate: 1000
DBSCAN (TSNE)						
Silhouette	-0.003757648	0.010789386	-0.018090254	-0.053359557	0.056309521	0.036684237
Davies Bouldin	2.196037766	1.802399748	2.290698136	1.896887987	1.77401152	1.703924631
Calinski Harabasz	543.0662147	461.4313593	427.1877972	384.7281333	432.2476651	485.0086521
OPTICS						
Silhouette	0.031175781	-0.000287511	0.017186441	0.036526404	0.075913355	0.088797659
Davies Bouldin	1.632716286	1.595774028	1.72943669	1.788465571	1.626137502	1.559785165
Calinski Harabasz	499.5216878	297.430407	297.1071965	347.6386925	298.9557343	325.8533935

3h Files						
	Learning Rate: 10	Learning Rate: 200	Learning Rate: 400	Learning Rate: 600	Learning Rate: 800	Learning Rate: 1000
DBSCAN (TSNE)						
Silhouette	-0.047304191	0.059058443	0.052361935	0.055812217	0.067903891	0.092090182
Davies Bouldin	1.958708445	1.509463728	1.486604812	1.485684064	1.476445909	1.401655093
Calinski Harabasz	478.6291387	445.8470406	454.0323481	368.3546676	369.9180331	339.4951441
OPTICS						
Silhouette	0.063918628	0.070420966	0.067922488	0.084858529	0.078014418	0.081889041
Davies Bouldin	1.908380671	1.563361642	1.739927567	1.535153239	1.521979543	1.456861854
Calinski Harabasz	649.3951529	203.4380081	208.4273457	157.9961534	150.9460601	137.0631837

	best values in files (1h or 3h)
	best values total (1h and 3h)

Figure 57: Comparison of Silhouette Coefficient, Davies-Bouldin Index, and Caliński-Harabasz Index for different t-SNE **learning rate** values, in **steps of 200** (except the first step of 190).

1h Files					
	Learning Rate: 10	Learning Rate: 50	Learning Rate: 100	Learning Rate: 150	Learning Rate: 800
DBSCAN (TSNE)					
Silhouette	-0.003757648	0.034104612	0.023020575	0.021991953	0.056309521
Davies Bouldin	2.196037766	1.839113174	1.918253028	2.077872768	1.77401152
Calinski Harabasz	543.0662147	487.2372447	408.9806962	495.7494691	432.2476651
OPTICS					
Silhouette	0.031175781	0.016049685	0.030655831	0.006348168	0.075913355
Davies Bouldin	1.632716286	1.703277523	1.917903749	1.702313578	1.626137502
Calinski Harabasz	499.5216878	360.6840936	308.6386538	307.6976429	298.9557343

3h Files					
	Learning Rate: 10	Learning Rate: 50	Learning Rate: 100	Learning Rate: 150	Learning Rate: 800
DBSCAN (TSNE)					
Silhouette	-0.047304191	0.046594031	0.047196072	0.046747934	0.067903891
Davies Bouldin	1.958708445	1.47995198	1.561185204	1.463983483	1.476445909
Calinski Harabasz	478.6291387	679.3870954	557.5937578	611.2247497	369.9180331
OPTICS					
Silhouette	0.063918628	0.075235315	0.067135818	0.066724166	0.078014418
Davies Bouldin	1.908380671	1.625187367	1.58668401	1.589883483	1.521979543
Calinski Harabasz	649.3951529	379.5759629	290.1587463	324.4484223	150.9460601

	best values in files (1h or 3h)
	best values total (1h and 3h)

Figure 58: Comparison of Silhouette Coefficient, Davies-Bouldin Index, and Caliński-Harabasz Index for different t-SNE **learning rate** values. Smaller learning rate value **steps of 50** were taken (except for the first step which is 40 and the last step to 800) between each test.

1h Files

	Learning Rate: 10	Learning Rate: 20	Learning Rate: 30	Learning Rate: 40	Learning Rate: 800
DBSCAN (TSNE)					
Silhouette	-0.003757648	0.051418006	0.037215631	0.024115672	0.056309521
Davies Bouldin	2.196037766	1.830794508	2.060517734	2.123406309	1.77401152
Calinski Harabasz	543.0662147	609.8260254	564.2559305	569.1097081	432.2476651
OPTICS					
Silhouette	0.031175781	0.085824259	0.050168812	0.042932201	0.075913355
Davies Bouldin	1.632716286	1.562171815	1.75508086	1.576809691	1.626137502
Calinski Harabasz	499.5216878	518.8980998	440.7310544	459.9814168	298.9557343

3h Files

	Learning Rate: 10	Learning Rate: 20	Learning Rate: 30	Learning Rate: 40	Learning Rate: 800
DBSCAN (TSNE)					
Silhouette	-0.047304191	-0.006364155	0.044669248	0.046343155	0.067903891
Davies Bouldin	1.958708445	1.881712505	2.12244492	1.749100916	1.476445909
Calinski Harabasz	478.6291387	540.0932863	774.4791625	658.1757762	369.9180331
OPTICS					
Silhouette	0.063918628	0.050251506	0.076243207	0.049795788	0.078014418
Davies Bouldin	1.908380671	1.931390827	2.018979173	1.789714946	1.521979543
Calinski Harabasz	649.3951529	463.7734489	481.6214212	389.1751855	150.9460601

best values in files (1h or 3h)

best values total (1h and 3h)

Figure 59: Comparison of Silhouette Coefficient, Davies-Bouldin Index, and Caliński-Harabasz Index for different t-SNE **learning rate** values. Smaller learning rate value **steps of 10** were taken (except for the last step to 800) between each test.

1h Files

	Learning Rate: 10	Learning Rate: 15	Learning Rate: 20	Learning Rate: 25	Learning Rate: 30
DBSCAN (TSNE)					
Silhouette	-0.003757648	0.040198717	0.051418006	0.032236848	0.037215631
Davies Bouldin	2.196037766	1.814792808	1.830794508	1.936491197	2.060517734
Calinski Harabasz	543.0662147	591.6592988	609.8260254	511.6861804	564.2559305
OPTICS					
Silhouette	0.031175781	0.067535594	0.085824259	0.038215108	0.050168812
Davies Bouldin	1.632716286	1.659834614	1.562171815	1.758027983	1.75508086
Calinski Harabasz	499.5216878	504.9991816	518.8980998	389.5913488	440.7310544

3h Files

	Learning Rate: 10	Learning Rate: 15	Learning Rate: 20	Learning Rate: 25	Learning Rate: 30
DBSCAN (TSNE)					
Silhouette	-0.047304191	0.010419452	0.008094903	-0.012381725	0.044669248
Davies Bouldin	1.958708445	1.875585513	1.897687221	1.75000284	2.12244492
Calinski Harabasz	478.6291387	656.9170813	704.0852625	639.2657184	774.4791625
OPTICS					
Silhouette	0.063918628	0.056145657	0.06045679	0.061573535	0.076243207
Davies Bouldin	1.908380671	1.880787198	1.796566584	1.860657595	2.018979173
Calinski Harabasz	649.3951529	648.5003401	590.1095848	661.0214236	481.6214212

best values in files (1h or 3h)

best values total (1h and 3h)

Figure 60: Comparison of Silhouette Coefficient, Davies-Bouldin Index, and Caliński-Harabasz Index for different t-SNE **learning rate** values, in **steps of 5**.

A.2.9 Learning Rate Comparison of 20 and 800

1h Files								
	Learning Rate: 20	Learning Rate: 800	Learning Rate: 20	Learning Rate: 800	Learning Rate: 20	Learning Rate: 800	Learning Rate: 20	Learning Rate: 800
DBSCAN (TSNE)								
Silhouette	0.051418006	0.056309521	0.047943175	-0.033673551	0.010282498	0.044229511	0.024733488	0.13869074
Davies Bouldin	1.830794508	1.77401152	1.874245766	3.045774889	2.077463481	1.680621133	1.844101414	1.659377639
Calinski Harabasz	609.8260254	432.2476651	628.4310062	284.5810113	555.3438459	457.8654554	543.4246332	561.299456
OPTICS								
Silhouette	0.085824259	0.075913355	0.076782033	0.023241794	0.06412942	0.06140846	0.057013668	0.145829111
Davies Bouldin	1.562171815	1.626137502	1.661925846	3.121565966	1.616248147	1.618311235	1.652082936	1.913545308
Calinski Harabasz	518.8980998	298.9557343	509.1943472	298.6138012	486.7785298	329.8427659	464.8406325	402.876503

3h Files								
	Learning Rate: 20	Learning Rate: 800	Learning Rate: 20	Learning Rate: 800	Learning Rate: 20	Learning Rate: 800	Learning Rate: 20	Learning Rate: 800
DBSCAN (TSNE)								
Silhouette	-0.006364155	0.067903891	0.016517494	0.08418332	0.003429756	0.054691602	0.003097915	0.083377987
Davies Bouldin	1.881712505	1.476445909	2.090600357	1.534382164	1.923601101	1.437163727	2.006669308	1.516726218
Calinski Harabasz	540.0932863	369.9180331	696.4164007	349.0248311	650.4633185	359.6352328	763.8873521	304.9316986
OPTICS								
Silhouette	0.050251506	0.078014418	0.058208089	0.098020062	0.07693895	0.076097637	0.030158926	0.069448814
Davies Bouldin	1.931390827	1.521979543	1.918330176	1.493803848	1.693677609	1.505156616	1.956116792	1.578533436
Calinski Harabasz	463.7734489	150.9460601	453.7829979	138.1019652	568.1096084	149.4634161	488.459881	128.4181964

best values in files (1h or 3h)

best values total (1h and 3h)

Figure 61: Comparison of Silhouette Coefficient, Davies-Bouldin Index, and Caliński-Harabasz Index for the t-SNE **learning rate values 20 and 80**. The green highlighted values indicate the best achieving evaluation score values (1h or 3h files), for the corresponding clustering method. Furthermore, the dark green highlighted values also accentuate the overall best scoring values over all datasets (1h and 3h files).

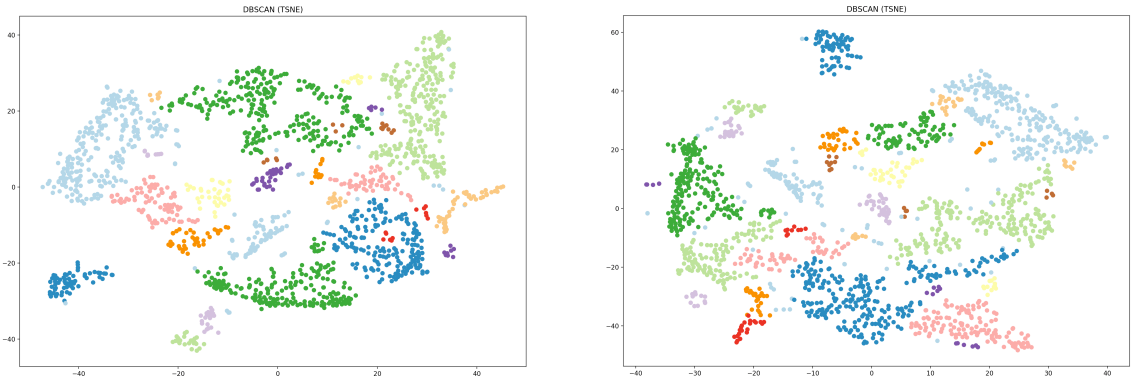

Figure 62: **1h** data files comparison of learning rate: a) 20, b) 800

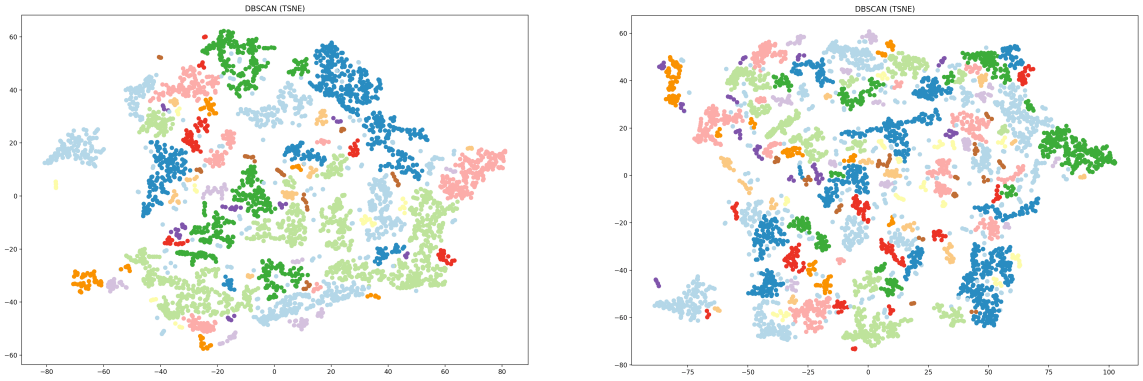

Figure 63: **3h** data files comparison of learning rate: a) 20, b) 800

B Optics reachability plots

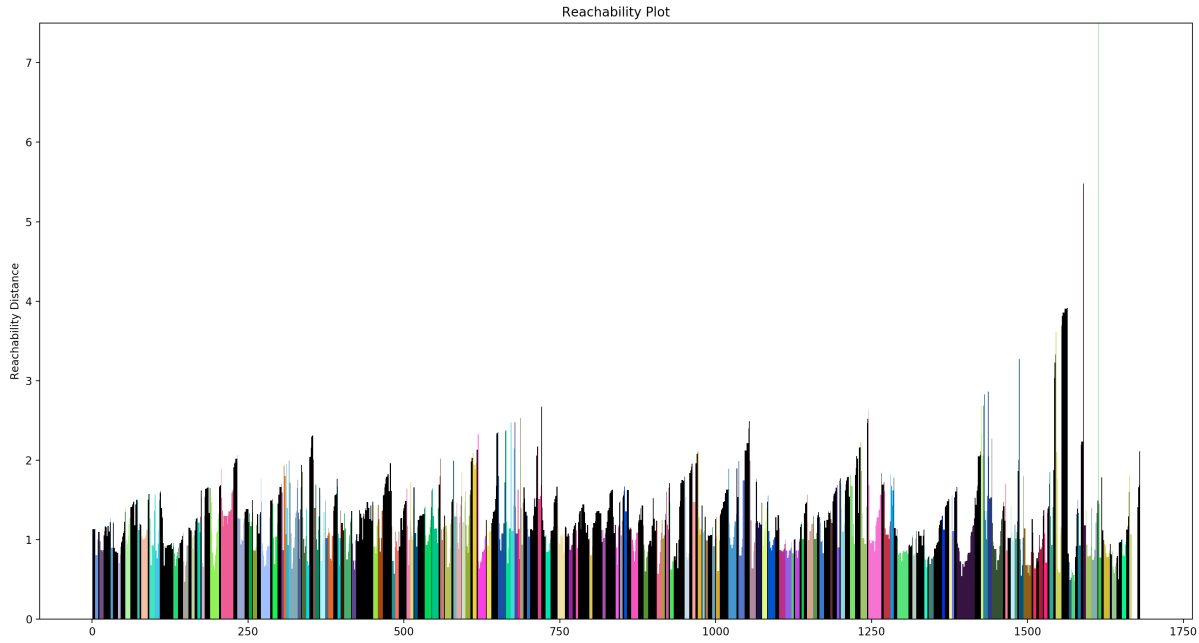

Figure 64: **1h dataset** (first column - 15 min) OPTICS reachability plot using OPTICS automatic cluster extraction (**xi**). The coloured bars highlight clusters, whilst the black ones indicate noise.

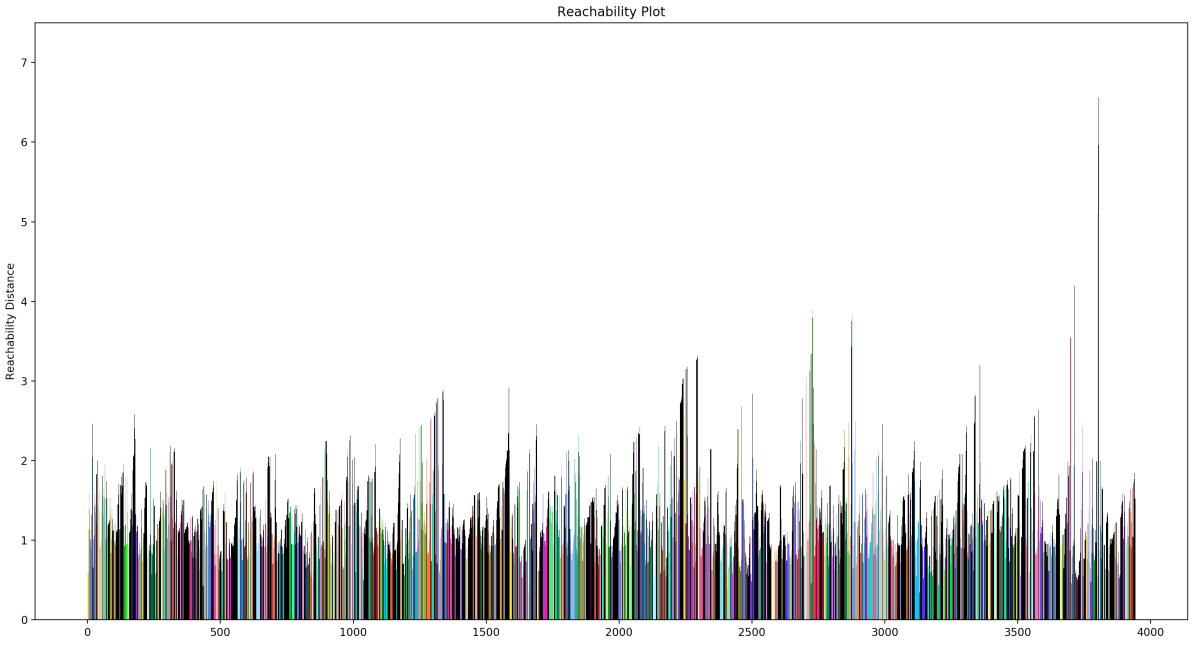

Figure 65: **3h dataset** (first column - 30 min) OPTICS reachability plot using OPTICS automatic cluster extraction (**xi**). The coloured bars highlight clusters, whilst the black ones indicate noise.

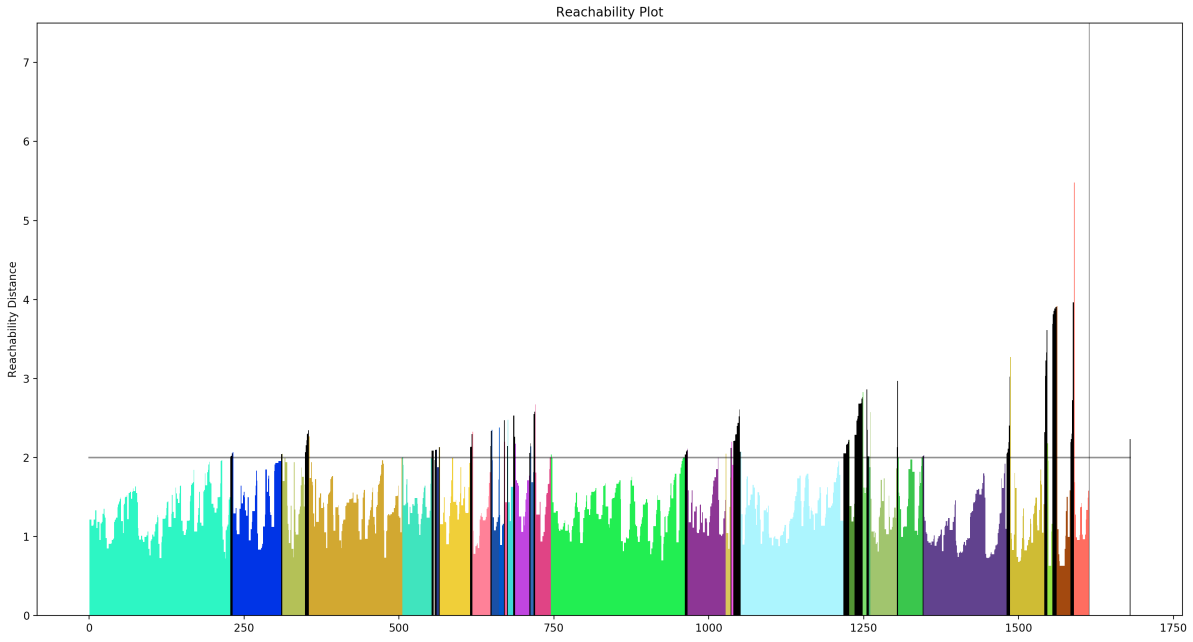

Figure 66: **1h dataset** (first column - 15 min) OPTICS reachability plot using **DBSCAN** clustering. The coloured bars highlight clusters, whilst the black ones indicate noise. The eps parameter, set at 2, his highlighted with a horizontal line.

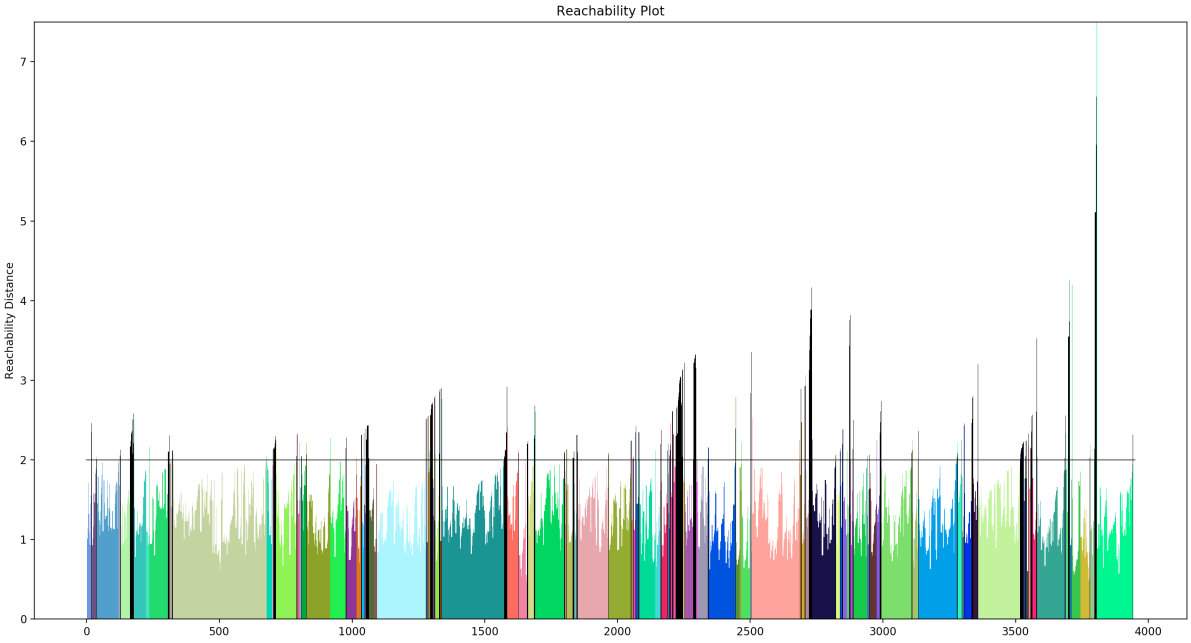

Figure 67: **3h dataset** (first column - 30 min) OPTICS reachability plot using **DBSCAN** clustering. The coloured bars highlight clusters, whilst the black ones indicate noise. The eps parameter, set at 2, his highlighted with a horizontal line.

C Clustering results

C.1 Clustering scatter plots

In the following scatter plots, data points coloured black are indicated as noise. Data points with other colours highlight clusters.

C.1.1 1h aggregated data files

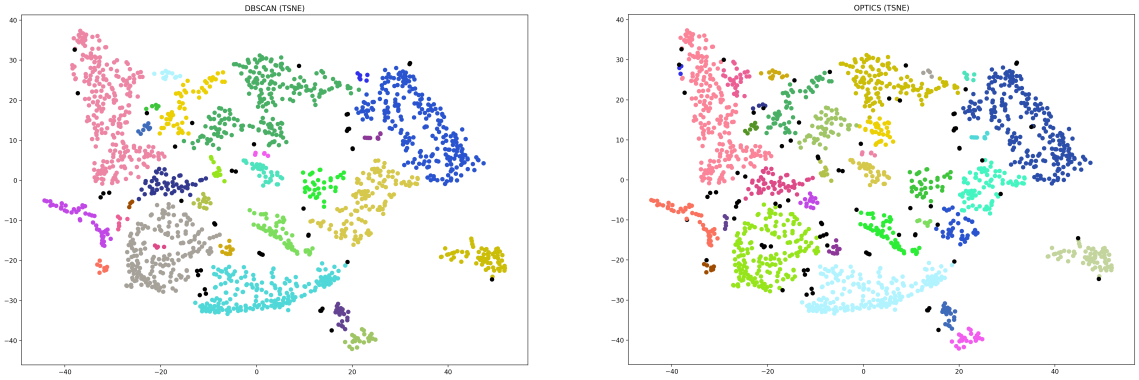

Figure 68: Comparison of the scatter plots from the DBSCAN (a) and OPTICS (b) clusterings of the 1st column, so the first **15 minutes** (1h data files: first 15 minutes).

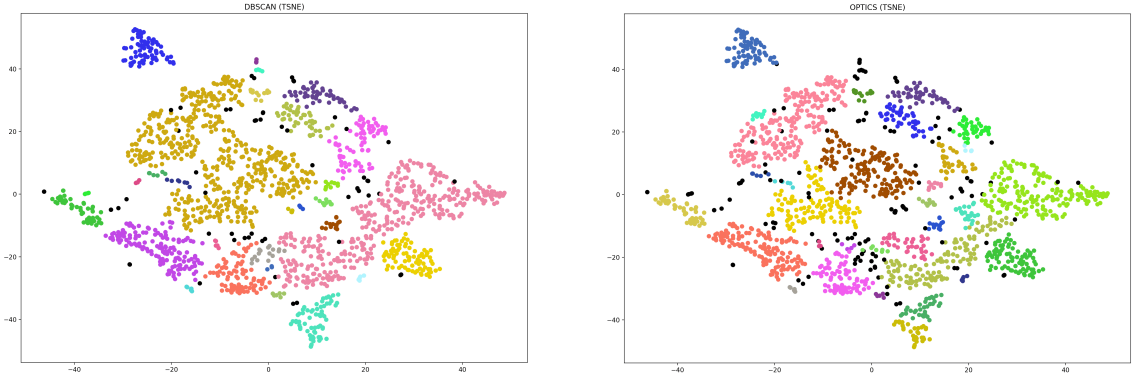

Figure 69: Comparison of the scatter plots from the DBSCAN (a) and OPTICS (b) clusterings of the average of the 1st column and 2nd column, so the first **30 minutes** (1h data files: 15 minutes & 30 minutes).

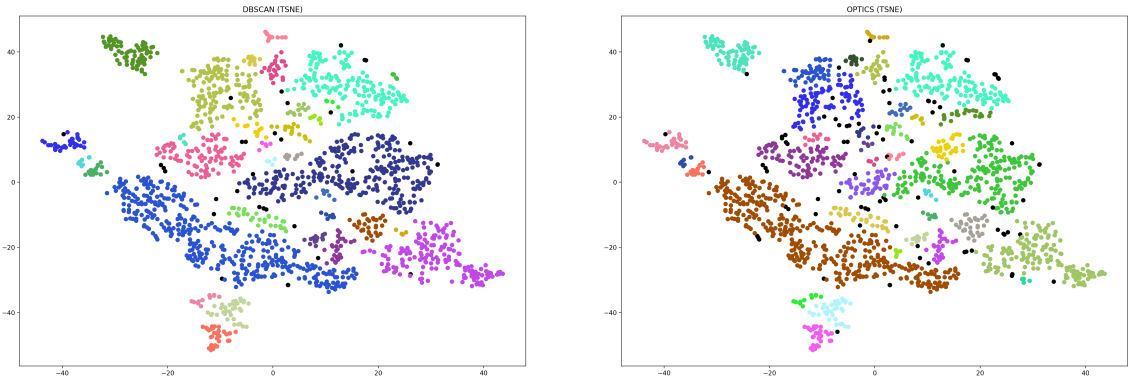

Figure 70: Comparison of the scatter plots from the DBSCAN (a) and OPTICS (b) clusterings of the average of the 1st column to the 3rd column, so the first **45 minutes** (1h data files: 15 minutes, 30 minutes & 45 minutes).

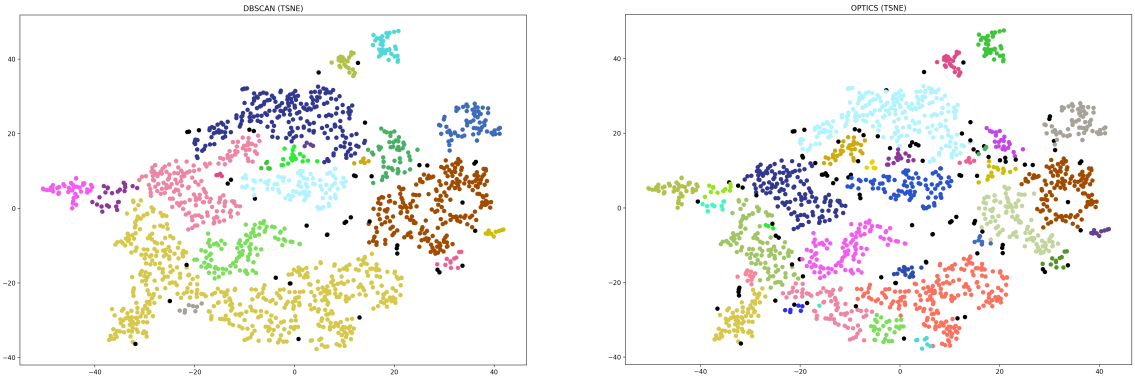

Figure 71: Comparison of the scatter plots from the DBSCAN (a) and OPTICS (b) clusterings of the average of the 1st column to the 4th column, so the whole **1 hour** (1h data files: 15 minutes, 30 minutes, 45 minutes & 1 hour).

C.1.2 3h aggregated data files

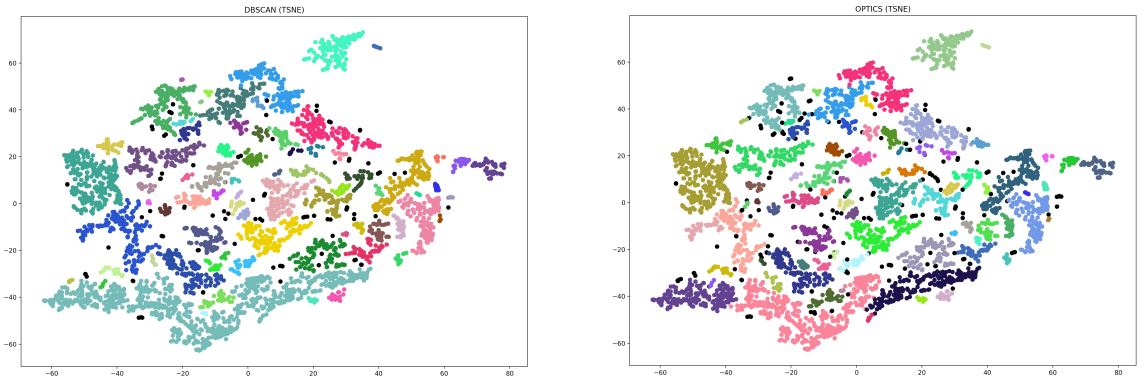

Figure 72: Comparison of the scatter plots from the DBSCAN (a) and OPTICS (b) clusterings of the 1st column, so the first **30 minutes** (3h data files: first 30 minutes).

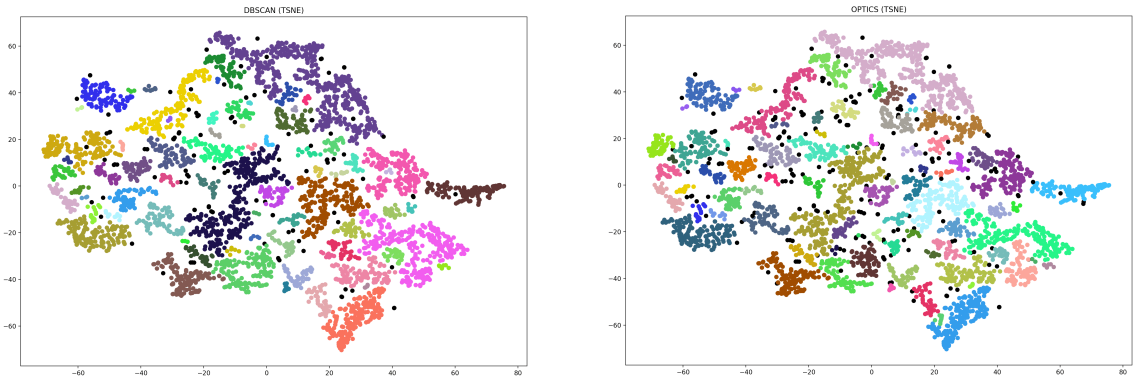

Figure 73: Comparison of the scatter plots from the DBSCAN (a) and OPTICS (b) clusterings of the average of the 1st column and 2nd column, so the first **1 hour** (3h data files: 30 minutes & 1 hour).

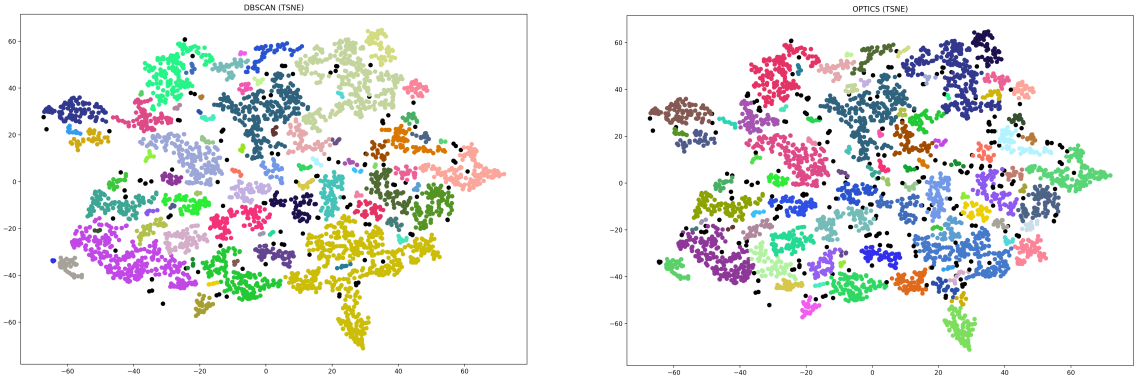

Figure 74: Comparison of the scatter plots from the DBSCAN (a) and OPTICS (b) clusterings of the average of the 1st column to the 3rd column, so the first **1.5 hours** (3h data files: 30 minutes, 1 hour & 1 hour 30 minutes).

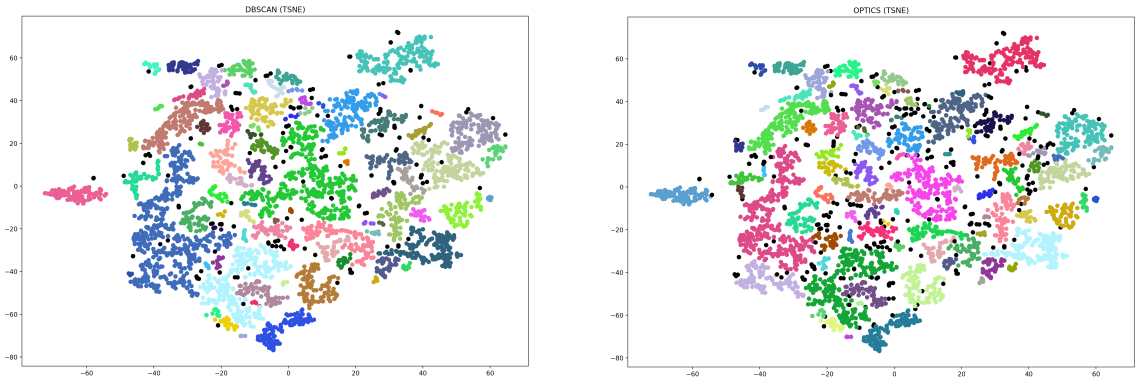

Figure 75: Comparison of the scatter plots from the DBSCAN (a) and OPTICS (b) clusterings of the average of the 1st column to the 4th column, so the first **2 hours** (3h data files: 30 minutes, 1 hour, 1 hour 30 minutes & 2 hours).

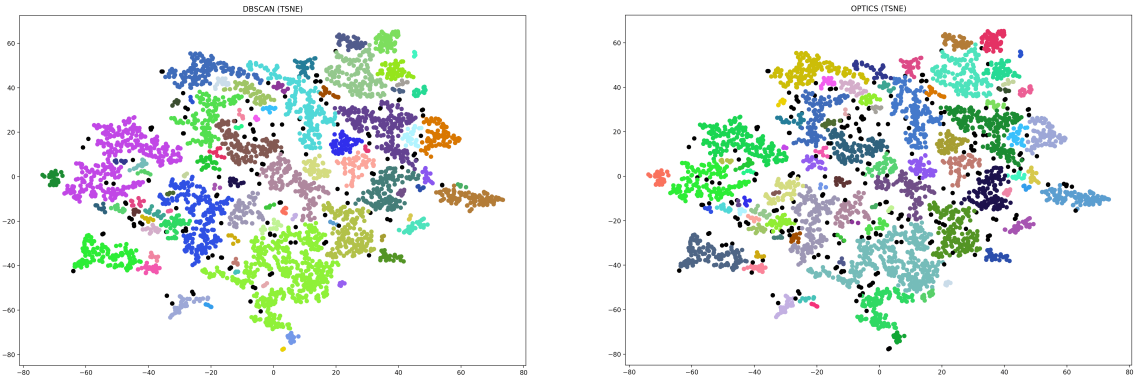

Figure 76: Comparison of the scatter plots from the DBSCAN (a) and OPTICS (b) clusterings of the average of the 1st column to the 5th column, so the first **2.5 hours** (3h data files: 30 minutes, 1 hour, 1 hour 30 minutes, 2 hours & 2 hours 30 minutes).

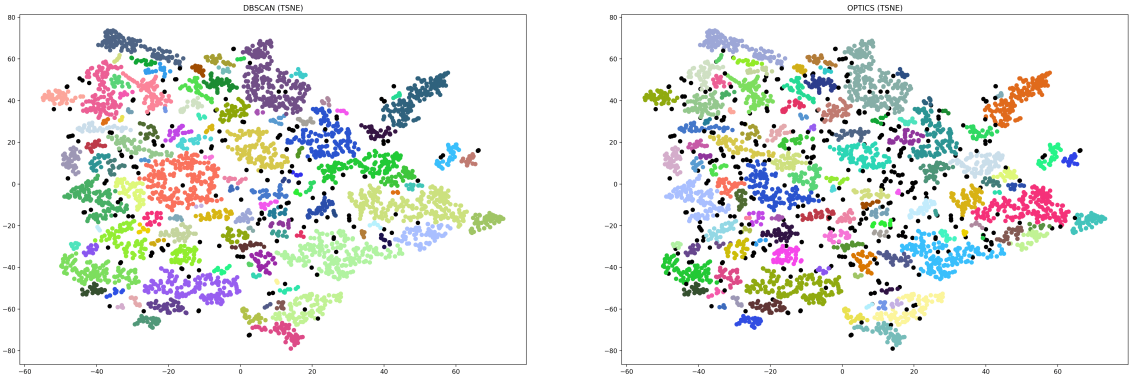

Figure 77: Comparison of the scatter plots from the DBSCAN (a) and OPTICS (b) clusterings of the average of the 1st column to the 6th column, so all **3 hours** (3h data files: 30 minutes, 1 hour, 1 hour 30 minutes, 2 hours, 2 hours 30 minutes & 3 hours).

C.2 Clustering evaluation results

In the following figures, the green highlighted values indicate the best achieving evaluation score values (1h or 3h files), for the corresponding clustering method. Furthermore, the dark green highlighted values also accentuate the overall best scoring values over all datasets (1h and 3h files).

1h Files						
	15 min	30 min	45 min	1h		
DBSCAN (TSNE)						
Silhouette	0.04409917	-0.09849845	-0.0932329	-0.23330191		
Davies Bouldin	1.965553013	1.408535372	1.549759164	2.03076771		
Calinski Harabasz	379.250218	237.2311173	313.5420497	151.2110635		
OPTICS						
Silhouette	0.0790162	0.15246919	-0.05314931	0.042187728		
Davies Bouldin	1.909221804	1.432838844	1.604143722	1.487652613		
Calinski Harabasz	341.9348451	439.4869733	248.8970787	295.5351996		

3h Files						
	30 min	1h	1h 30 min	2h	2h 30 min	3h
DBSCAN (TSNE)						
Silhouette	0.03163854	0.025676515	-0.02877813	0.063989125	-0.006347847	0.039090224
Davies Bouldin	1.595225606	1.386905334	1.831308621	1.565283337	1.685115208	1.765928396
Calinski Harabasz	660.300021	912.1243489	665.2710749	644.7382201	781.7245551	633.2488309
OPTICS						
Silhouette	0.05099258	0.06202586	0.07631619	0.11866711	0.08885	0.09892428
Davies Bouldin	1.640303918	1.719579308	1.708319079	1.722106779	1.419781716	1.47188292
Calinski Harabasz	700.3707789	523.0438423	504.3994953	418.4628186	506.8636832	340.4418048

	best values in files (1h or 3h)
	best values total (1h and 3h)

Figure 78: Evaluation scores comparison from the **first run** of t-SNE and clustering with a **learning rate of 20**.

1h Files						
	15 min	30 min	45 min	1h		
DBSCAN (TSNE)						
Silhouette	0.061859984	0.049978126	0.007422133	-0.01603307		
Davies Bouldin	1.721318764	1.477412627	2.293371608	1.556510771		
Calinski Harabasz	587.3448151	314.7345941	363.751391	434.4817134		
OPTICS						
Silhouette	0.10139497	0.14339069	-0.000247999	0.091312036		
Davies Bouldin	1.851297487	1.21728504	2.107907761	1.483656401		
Calinski Harabasz	488.1085954	356.6377613	291.1266469	371.4243781		
3h Files						
	30 min	1h	1h 30 min	2h	2h 30 min	3h
DBSCAN (TSNE)						
Silhouette	-0.002485462	0.02854126	-0.016798861	0.027074102	0.03494797	0.046173148
Davies Bouldin	1.938083017	1.452023108	1.878183603	1.401770691	1.643617425	1.593027178
Calinski Harabasz	467.7627938	881.5570846	507.1314968	579.5123589	627.0284348	724.8436508
OPTICS						
Silhouette	0.07204221	0.094111204	0.077061266	0.028278682	0.11853256	0.07739853
Davies Bouldin	2.196047237	1.783584125	1.876588633	1.401717031	1.486444695	2.063883814
Calinski Harabasz	707.6414399	586.3869193	353.3416269	336.8332351	406.5664744	433.4674822
	best values in files (1h or 3h)					
	best values total (1h and 3h)					

Figure 79: Evaluation scores comparison from the **second run** of t-SNE and clustering with a **learning rate of 20**.

1h Files						
	15 min	30 min	45 min	1h		
DBSCAN (TSNE)						
Silhouette	0.052979577	-0.024260162	-0.042905383	-0.12466749		
Davies Bouldin	1.843435889	1.442973999	1.921565386	1.79363924		
Calinski Harabasz	483.2975165	275.9828557	338.6467203	292.8463885		
OPTICS						
Silhouette	0.090205585	0.14792994	-0.026698655	0.066749882		
Davies Bouldin	1.880259645	1.325061942	1.856025741	1.485654507		
Calinski Harabasz	415.0217203	398.0623673	270.0118628	333.4797888		
3h Files						
	30 min	1h	1h 30 min	2h	2h 30 min	3h
DBSCAN (TSNE)						
Silhouette	0.014576539	0.027108888	-0.022788496	0.045531614	0.014300062	0.042631686
Davies Bouldin	1.766654312	1.419464221	1.854746112	1.483527014	1.664366317	1.679477787
Calinski Harabasz	564.0314074	896.8407168	586.2012859	612.1252895	704.3764949	679.0462408
OPTICS						
Silhouette	0.061517395	0.078068532	0.076688728	0.073472896	0.10369128	0.088161405
Davies Bouldin	1.918175578	1.751581717	1.792453856	1.561911905	1.453113206	1.767883367
Calinski Harabasz	704.0061094	554.7153808	428.8705611	377.6480269	456.7150788	386.9546435
	best values in files (1h or 3h)					
	best values total (1h and 3h)					

Figure 80: Evaluation scores comparison averaged from **figures 78 and 79**.

1h Files						
	15 min	30 min	45 min	1h		
DBSCAN (TSNE)						
Silhouette	0.045056932	-0.043946639	-0.068129525	0.034058403		
Davies Bouldin	1.974228023	1.623043713	1.561681712	1.330793149		
Calinski Harabasz	559.9454484	231.1185974	314.9127009	518.1632965		
OPTICS						
Silhouette	0.087323241	0.078877471	-0.044939384	0.050577533		
Davies Bouldin	1.647662855	1.714452117	1.548555372	1.354076657		
Calinski Harabasz	455.8046908	306.9855407	268.0225278	378.5922696		
3h Files						
	30 min	1h	1h 30 min	2h	2h 30 min	3h
DBSCAN (TSNE)						
Silhouette	-0.03370953	-0.028693724	-0.014684342	0.035463296	0.018177651	0.024473445
Davies Bouldin	1.843484805	1.914727542	1.881877562	1.578954586	1.668429671	1.776349426
Calinski Harabasz	627.1549248	725.4648494	627.0653245	756.8045021	680.7680095	692.6218533
OPTICS						
Silhouette	0.011725605	0.057709865	0.112025782	0.111947685	0.081173912	0.076792531
Davies Bouldin	1.871782347	1.728019021	1.670963152	1.39067254	1.537877073	1.928194677
Calinski Harabasz	480.0815334	567.1386341	445.5336128	501.6112069	454.7315535	437.6176714
	best values in files (1h or 3h)					
	best values total (1h and 3h)					

Figure 81: Evaluation scores comparison **averaged** from **2 runs** of t-SNE and clustering with a **learning rate of 20**.

1h Files						
	15 min	30 min	45 min	1h		
DBSCAN (TSNE)						
Silhouette	0.062392585	0.109573543	-0.004795788	-0.068260521		
Davies Bouldin	2.309679877	1.725495953	1.782488054	1.608990382		
Calinski Harabasz	440.260006	540.8427817	380.9053749	281.6679029		
OPTICS						
Silhouette	0.057782359	0.135444269	0.017859722	0.036272764		
Davies Bouldin	2.004440686	1.750887229	2.079905994	1.546211321		
Calinski Harabasz	324.1682685	336.6839227	267.442482	199.8783014		
3h Files						
	30 min	1h	1h 30 min	2h	2h 30 min	3h
DBSCAN (TSNE)						
Silhouette	0.054977857	0.136667132	0.125094607	0.172261804	0.142229527	0.131898537
Davies Bouldin	1.497732311	1.409259524	1.403925898	1.50888884	1.439275292	1.368191426
Calinski Harabasz	348.4941339	296.3657299	275.6990944	207.365258	190.8214068	197.7513201
OPTICS						
Silhouette	0.085169926	0.095759317	0.127076074	0.080362737	0.047243498	0.084326543
Davies Bouldin	1.532057234	1.468021265	1.400929179	1.518005655	1.37525721	1.264660171
Calinski Harabasz	144.7781324	104.1385105	102.4009152	83.40832451	65.84819665	69.71735313
	best values in files (1h or 3h)					
	best values total (1h and 3h)					

Figure 82: Evaluation scores comparison **averaged** from **2 runs** of t-SNE and clustering with a **learning rate of 800**.

Final comparisons	2nd Place				
	15 min (1h)	30 min (1h)	1h (1h)	30 min (3h)	1h (3h)
DBSCAN (TSNE)					
Silhouette	0.053476365	0.013788914	-0.052956536	0.011948289	0.045027432
Davies Bouldin	2.04244793	1.597171222	1.577807591	1.702623809	1.581150429
Calinski Harabasz	494.5009903	349.3147449	364.2258626	513.226822	639.5570987
OPTICS					
Silhouette	0.078437062	0.12075056	0.05120006	0.052804309	0.077179238
Davies Bouldin	1.844121062	1.596800429	1.461980828	1.774005053	1.649207334
Calinski Harabasz	398.3315599	347.2439435	303.9834533	442.9552584	408.6641751

Final comparisons	3rd Place				
	15 min (1h)	30 min (1h)	30 min (3h)	1h (3h)	
DBSCAN (TSNE)					
Silhouette	0.053476365	0.013788914	0.011948289	0.045027432	
Davies Bouldin	2.04244793	1.597171222	1.702623809	1.581150429	
Calinski Harabasz	494.5009903	349.3147449	513.226822	639.5570987	
OPTICS					
Silhouette	0.078437062	0.12075056	0.052804309	0.077179238	
Davies Bouldin	1.844121062	1.596800429	1.774005053	1.649207334	
Calinski Harabasz	398.3315599	347.2439435	442.9552584	408.6641751	

Final comparisons	3rd Place				
	30 min (1h)	1h (3h)			
DBSCAN (TSNE)					
Silhouette	0.013788914	0.045027432			
Davies Bouldin	1.597171222	1.581150429			
Calinski Harabasz	349.3147449	639.5570987			
OPTICS					
Silhouette	0.12075056	0.077179238			
Davies Bouldin	1.596800429	1.649207334			
Calinski Harabasz	347.2439435	408.6641751			

Final comparisons	5th Place				
	15 min (1h)	30 min (3h)			
DBSCAN (TSNE)					
Silhouette	0.053476365	0.011948289			
Davies Bouldin	2.04244793	1.702623809			
Calinski Harabasz	494.5009903	513.226822			
OPTICS					
Silhouette	0.078437062	0.052804309			
Davies Bouldin	1.844121062	1.774005053			
Calinski Harabasz	398.3315599	442.9552584			

Figure 83: Evaluation scores comparison to determine **2nd, 3rd, 4th, 5th, and 6th place**.

Final comparisons	**30 min (1h), 1h (1h), 1h (3h)**		
	30 min (1h)	**1h (1h)**	**1h (3h)**
DBSCAN (TSNE)			
Silhouette	0.013788914	-0.052956536	0.045027432
Davies Bouldin	1.597171222	1.577807591	1.581150429
Calinski Harabasz	349.3147449	364.2258626	639.5570987
OPTICS			
Silhouette	0.12075056	0.05120006	0.077179238
Davies Bouldin	1.596800429	1.461980828	1.649207334
Calinski Harabasz	347.2439435	303.9834533	408.6641751

Figure 84: Evaluation scores of direct comparison of **30 min (1h), 1h (1h), and 1h (3h)**.

D git-Repository

Link to the GitLab Repository on `gitlab.mediacube.at`:
`https://gitlab.mediacube.at/fhs41216/BacThesis`

Git repository contents:

- **Experiment:** Source code of the experiment
- **Thesis:** LaTeX code of the thesis
- **Literature:** Reference papers available as PDF
- **Websites:** Referenced websites as PDF
- **EvaluationResults:** Excel spreadsheets of cluster evaluation score results

E Archived Websites

`https://web.archive.org/web/20200624031033/https://www.anaconda.com/`, snapshot 24.06.2020, 03:10:33

`https://web.archive.org/web/20200624072345/https://scikit-learn.org/stable/`, snapshot 24.06.2020, 07:23:45

`https://web.archive.org/web/20200626201341/https://matplotlib.org/`, snapshot 26.06.2020, 20:13:41

`https://web.archive.org/web/20200624221340/https://developer.android.com/guide/topics/sensors/sensors_motion`, snapshot 24.06.2020, 22:13:40

`https://web.archive.org/web/20200620043347/https://tools.ietf.org/html/rfc4180`, snapshot 25.06.2020, 05:29:41

`https://web.archive.org/web/20200626201347/https://pandas.pydata.org/`, snapshot 26.06.2020, 20:13:47

`https://web.archive.org/web/20200506182431/https://pandas.pydata.org/about/`, snapshot 06.05.2020, 18:24:31

`https://web.archive.org/web/20200614223428/https://pandas.pydata.org/pandas-docs/stable/reference/api/pandas.read_csv.html`, snapshot 14.06.2020, 22:34:28

`https://web.archive.org/web/20200616004253/https://pandas.pydata.org/pandas-docs/stable/reference/api/pandas.concat.html`, snapshot 16.06.2020, 00:42:53

https://web.archive.org/web/20200608042012/https://pandas.pydata.org/pandas-docs/stable/reference/api/pandas.DataFrame.dropna.html, snapshot 08.06.2020, 04:20:12

https://web.archive.org/web/20200605104434/https://scikit-learn.org/stable/modules/generated/sklearn.preprocessing.StandardScaler.html, snapshot 05.06.2020, 10:44:34

https://web.archive.org/web/20200623125839/https://scikit-learn.org/stable/modules/generated/sklearn.decomposition.PCA.html, snapshot 23.06.2020, 12:58:39

https://web.archive.org/web/20200609055322/https://scikit-learn.org/stable/modules/generated/sklearn.manifold.TSNE.html, snapshot 09.06.2020, 05:53:22

https://web.archive.org/web/20200623170602/https://distill.pub/2016/misread-tsne/, snapshot 23.06.2020, 17:06:02

https://web.archive.org/web/20200610080206/https://scikit-learn.org/stable/modules/generated/sklearn.cluster.DBSCAN.html, snapshot 10.06.2020, 09:17:34

https://web.archive.org/web/20200520193202/https://scikit-learn.org/stable/modules/generated/sklearn.cluster.OPTICS.html, snapshot 01.06.2020, 07:53:43

https://web.archive.org/web/20200512220200/https://humanstress.ca/stress/understand-your-stress/acute-vs-chronic-stress/, snapshot 12.05.2020, 22:02:00